

University of Nevada

Reno

✓ Interaction of Gold Cyanide, Thiocyanate, Thiosulfate,
and Thiourea Complexes with Carbon Matrices

A thesis submitted in partial fulfillment of the requirements
for the degree of Master of Science in Metallurgical Engineering

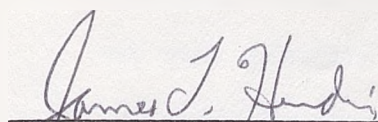
by

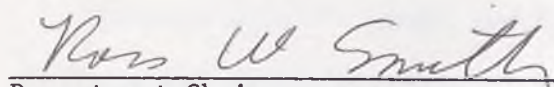
Neil Paul Gallagher

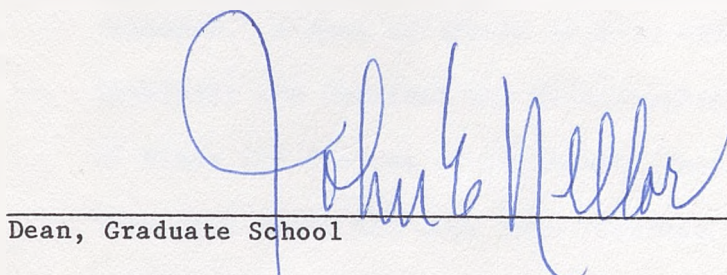
May 1987

Thesis
2209

The thesis of Neil Paul Gallagher is approved:


Thesis Advisor


Department Chair


Dean, Graduate School

University of Nevada

Reno

May 1987

ACKNOWLEDGMENTS

The author wishes to gratefully acknowledge the invaluable advice and assistance of Emil Milosavljevic' through whom the fruit of this labor was made possible. Ljiljana Solujic' is also gratefully acknowledged for meticulously preparing the gold complexes and sharing her knowledge of their chemistry. Dr. John Nelson is gratefully acknowledged for his illuminating discussions and advice during the course of this work. A special note of thanks and acknowledgement is given to Dr. Jim Hendrix for the financial support, guidance, and opportunity to perform this research. A note of thanks is also extended to the Departments of Chemistry and Chemical and Metallurgical Engineering and the U.S. Bureau of Mines for the use of equipment, facilities, and for sample analysis. This work would not have been possible without the unselfish dedication and sacrifice of the author's family to obtain its completion, and it is to them that he extends his greatest thanks and love.

ABSTRACT

Anodic dissolution of particulate gold in a flow-through electrode was investigated under controlled potential conditions with electrolyte solutions containing complexing ligands. The resulting gold complexes were examined in column adsorption experiments to observe their affinity for adsorption on activated carbon. Observations of the effect of applied potential on the activated carbon adsorption of gold complexes were also made. Elemental gold mechanically mixed with spectroscopic or activated carbon was anodically dissolved in 0.1 M solutions of the complexing ligands, cyanide, thiosulfate, thiourea, and thiocyanate. Column adsorption experiments were conducted with the gold complexes of the respective solution ligands with on-line solution analysis via coupled flow-injection atomic absorption. The observed rate of anodic dissolution in a nonadsorbing matrix decreased for the various ligands in the order: $\text{CN}^- > \text{SC}(\text{NH}_2)_2 > \text{SCN}^- > \text{S}_2\text{O}_3^{2-}$. The rate of adsorption of the gold complexes decreased in the ligand order: $\text{SCN}^- > \text{SC}(\text{NH}_2)_2 > \text{CN}^- > \text{S}_2\text{O}_3^{2-}$; the application of negative potentials to activated carbon decreases its adsorption capacity for aurocyanide.

TABLE OF CONTENTS

I	INTRODUCTION	1
II	LITERATURE REVIEW AND THEORY	4
	A. Electrochemical Cell Design	4
	B. Anodic Behavior of Gold	5
	1. General Overview	5
	2. Anodic Behavior in Chloride Media	7
	3. Anodic Behavior in Thiocyanate Media	10
	4. Anodic Behavior in Thiourea Media	11
	5. Anodic Behavior in Cyanide Media	13
	6. Anodic Behavior in Thiosulfate Media	17
	C. Activated Carbon	18
	1. General Properties	18
	2. Physical Properties/Experimental Observations	19
	3. Historical Relationship of Activated Carbon to Gold ..	21
	4. Behavior of Activated Carbon in Electrolyte Solutions	22
	5. Irreversible Adsorption of Oxygen	23
	6. Adsorption/Precipitation of Gold from Solution	23
	D. Modelling of Column Processes	34
III	MATERIALS AND EQUIPMENT	37
	A. Materials and Reagents	37
	B. Equipment	39
	1. Flow Cell and Pump System	39
	2. Electrochemistry Equipment and Electrodes	45
	3. Flow Injection Analysis	46
IV	ANALYTICAL PROCEDURE	46
	A. Anodic Dissolutions Using a Stock Gold/Carbon Mixture	46
	B. On-line Flow-injection Analysis	49
V	EXPERIMENTAL PROCEDURE	50
	A. Working Electrode Preparation	50
	B. Solution Preparation	51

C.	Assembly of Electrochemical Cell	52
D.	Adsorption Cell/Tube Assembly	52
E.	General Operating Procedures	53
	1. Recycling Electrodisolutions and Electroelutions	53
	2. Column Adsorption Experiments	53
VI	RESULTS	54
A.	Premixed Gold/Carbon Electrodisolutions	54
B.	Specific Gold/Carbon Electrodisolutions	56
C.	Recycle and Non-recycle Electroelutions	57
D.	Flow Cell and Small Tube Adsorption Experiments	60
F.	Equilibrium Adsorption Experiments	63
VII	DISCUSSION	64
A.	Anodic Dissolutions in Spectroscopic Carbon	64
B.	Anodic Dissolutions in Activated Carbon	76
C.	Electroelution of Gold from Aurocyanide-Loaded Activated Carbon	83
D.	Flow Cell Adsorption Experiments	98
E.	Small Tube Adsorption Experiments	107
F.	Equilibrium Adsorption Experiments	125
VIII	CONCLUSIONS	131
IX	RECOMMENDATIONS	137
X	BIBLIOGRAPHY	139
XI	APPENDIX	146
A.	Atomic Absorption Data for Premixed Gold/Carbon Electrodisolutions	146
B.	Fire Assay and Initial Gold Determination Results for Premixed Gold/Carbon Electrodisolutions	149

C. Concentration Data for Specifically-Mixed Gold/Carbon Dissolutions	150
D. Concentration Data for the Electroelution of Aurocyanide from Activated Carbon	160
E. Concentration Data for Recycling Flow Cell Adsorption Experiments	164
F. Concentration Data for the Adsorption of Aurocyanide on the Freeport Gold Ore	171
G. Concentration Data for the Small Column Adsorption of Gold Complexes on Activated Carbon	173

LIST OF FIGURES

Figure 1.	Electrochemical Flow Regimes	6
Figure 2.	Experiment Solution Flow Regimes.....	36
Figure 3.	Cross Section of Electrochemical Cell	41
Figure 4.	Tygon-tube Adsorption Cell	44
Figure 5.	Modes of FIA-AAS Operation	47
Figure 6.	Anodic Dissolution of Gold from Spectroscopic Carbon in Cyanide Solution	65
Figure 7.	Anodic Dissolution of Gold from Spectroscopic Carbon in Thiourea, Thiosulfate, and Thiocyanate Solution ..	67
Figure 8.	Anodic Dissolution of Gold from Spectroscopic Carbon in Acidic and Alkaline Thiourea Solutions	70
Figure 9.	Anodic Dissolution of Gold from Spectroscopic Carbon in Neutral and Alkaline Thiocyanate Solutions	72
Figure 10.	Chemical and Anodic Dissolution of Gold from Spectroscopic Carbon in Cyanide Solution	74
Figure 11.	Anodic Dissolution of Gold from Activated Carbon in Acidic Thiourea Solution	78
Figure 12.	Anodic Dissolution of Gold from Activated Carbon in Thiosulfate Solution	80
Figure 13.	Chemical and Anodic Dissolution of Gold from Activated Carbon in Cyanide Solution	82
Figure 14.	Electroelution of Gold from Aurocyanide Loaded Activated Carbon with Caustic Cyanide Solution	85
Figure 15.	Gold Concentration Profile for Two-solution Electroelution with Caustic Cyanide	87
Figure 16.	Cathodic Current as a Function of Time for Two- Solution Electroelution with Caustic Cyanide	89
Figure 17.	Gold Concentration Profile for the Non-recirculating Electroelution with Caustic Cyanide Solution	91
Figure 18.	Proposed Gold Loading Gradient in an Activated Carbon Particle	92

Figure 19.	Effect of Eluent Composition on the Electroelution of Aurocyanide Loaded Activated Carbon	95
Figure 20.	Concentration Profile for the Electroelution of Aurocyanide Loaded Activated Carbon with Deionized Water	97
Figure 21.	Concentration Profiles for the Flow-Cell Adsorption of the Gold Thiourea, Thiocyanate, Chloride and Thiosulfate Complexes on Activated Carbon	100
Figure 22.	Concentration Profiles for the Flow-Cell Adsorption of Aurocyanide on Activated Carbon	102
Figure 23.	Recirculating Flow-Cell Adsorption of Aurocyanide on the Freeport Gold Ore	105
Figure 24.	Non-recirculating Flow-Cell Adsorption of Aurocyanide on the Freeport Gold Ore	106
Figure 25.	Concentration Profiles for the Small-Column Adsorption of Aurocyanide on Activated Carbon	108
Figure 26.	Concentration Profiles for the Small-Column Adsorption of Aurothiourea on Activated Carbon	109
Figure 27.	Concentration Profiles for the Small-Column Adsorption of Aurothiocyanate on Activated Carbon ...	110
Figure 28.	Concentration Profiles for the Small-Column Adsorption of Aurothiosulfate on Activated Carbon ...	111
Figure 29.	Average Gold Loading of Aurothiourea on Activated Carbon from the Small-Column Adsorptions	113
Figure 30.	Average Gold Loading of Aurocyanide on Activated Carbon from the Small-Column Adsorptions	114
Figure 31.	Deionized Water Elution Behavior of Gold Thiourea and Cyanide Complexes from the 0.0100 g Small-Column Adsorption Experiment	117
Figure 32.	Deionized Water Elution Behavior of Gold Thiourea and Cyanide Complexes from the 0.0500 g Small-Column Adsorption Experiment	118
Figure 33.	SEM Micrographs of Aurothiocyanate-Loaded Activated Carbon	120
Figure 34.	SEM Micrographs of Aurothiocyanate-Loaded Activated Carbon	121

Figure 35.	SEM Micrographs of Aurothiocyanate-Loaded Activated Carbon	122
Figure 36.	SEM Micrographs of Aurothiocyanate-Loaded Activated Carbon	123
Figure 37	Logarithmic Plot of Equilibrium Adsorption Data for Adsorption of Gold Complexes on Activated Carbon	127

LIST OF TABLES

Table 1.	ICP Analysis of Activated Carbon Sample	40
Table 2.	ICP Analysis of Freeport Gold Ore Samples	42
Table 3.	Equilibrium Aurocyanide Adsorption on the Freeport Gold Ore Sample	129
Table 4.	Equilibrium Aurothiourea Adsorption on the Freeport Gold Ore Sample	130
Table 5.	Equilibrium Aurothiocyanate Adsorption on the Activated Carbon Sample	130

INTRODUCTION

The poor recovery of gold from carbonaceous gold ores has long plagued the metallurgist's and engineer's attempts at gold beneficiation. The gold in these ores is intimately associated with the carbon components and is either passivated (occluded) by their presence or taken up as adsorbed or chelated species after dissolution; thus, besides posing problems in the recovery of the contained gold, they also have deleterious "preg robbing" effects when present in oxide-ore leaching circuits (1). The large, sometimes stockpiled supply of these ores coupled with the decreasing supply of high-grade oxide ores has promoted considerable research into the characterization and treatment of carbonaceous gold ores. For these ores, conventional cyanidation techniques have limited application with recoveries being consistently less than 60 percent; this leaves a "high-grade" tailings that in all probability will be uneconomical to treat should technology become available for carbonaceous ores. Two recent studies of carbonaceous gold ores have attempted to characterize the carbonaceous ore with respect to its carbon components and "preg robbing" capacity (1,2).

Three principal constituents have been identified in the carbonaceous material: hydrocarbon components, humic acid components, and elemental carbon components acting as activated carbon (2). The hydrocarbon component has little effect on gold recovery, but the humic acid fraction is suspected of chelating the gold cyanide complex. Due to the minute quantities of humic acid in the carbonaceous ore, it is difficult to extract portions sufficient to evaluate their adsorbing properties under controlled conditions; however, humic acid extracts

from lignite were shown to adsorb relatively large quantities of gold complex from an aurocyanide solution (2). Aurocyanide adsorption by the elemental carbon fraction of the carbonaceous ore has been compared to the adsorption of aurocyanide by the original ore. The results revealed similar behavior with respect to kinetics and changes in gold loading as a function of solution composition; however, the ore exhibited considerably higher gold loadings indicating that possibly the extraction procedure partially deactivated the elemental carbon fraction.

Aurocyanide adsorption by a carbonaceous gold ore has been compared to aurocyanide adsorption by activated carbon on an organic carbon basis (1). In this comparison of activated carbon to carbonaceous ore from Carlin, Nevada, it was found that the activated carbon sample investigated adsorbed an order of magnitude more gold from solution but at a rate four times slower than the carbonaceous ore based on active sites available for adsorption. This comparison cannot be completely generalized to other ores or activated carbons but gives a semiquantitative relationship of the adsorbing properties of carbonaceous ore and activated carbon.

There have been many attempts at processing carbonaceous ores, namely chlorination, oxidative acid leaching, pressure leaching, roasting, kerosene pretreatment, bioleaching, and chemical oxidation (2); although costly, some are economical enough to implement with suitable ores. (2,68). It has been proposed that electrostatic surface phenomena may influence the dissolution of gold from a carbonaceous matrix (2,3), and it is also widely known that the chloride complexes of

gold are reduced to the elemental state upon adsorption on activated carbon indicating that the carbon has a "redox" character. Thus, it was conceived that an investigation of the anodic dissolution of disseminated gold in a carbonaceous matrix would yield useful information that would be of value in the treatment of carbonaceous gold ores, recovery of gold from other conducting sources and could possibly be of value in the adsorption recovery of gold on activated carbon.

To investigate the anodic dissolution of gold, two things are needed initially: an electrochemical reactor and a conducting solution that will stabilize the oxidized gold atoms. There are many types of electrochemical cells with the choice depending on what information is to be gathered on the electrochemical system of interest. For the present work, a system was needed which would facilitate a small sample, give a nearly constant potential distribution, and be capable of possibly high current densities. A flow cell utilizing a porous packed bed electrode operated in the "flow by" configuration was selected to meet the above criteria. These cells have been used for analytical as well as industrial applications (13).

The second initial requirement to perform the anodic investigation is the selection of the complexing media to be used. A survey of the relevant gold chemistry and complexing agents of practical interest (4,5,6,7,8) revealed that the cyanide (CN^-), thiourea ($\text{CS}(\text{NH}_2)_2$), thiosulfate ($\text{S}_2\text{O}_3^{-2}$), and thiocyanate (SCN^-) ligands had potential for practical significance.

Thus, the present research was to approach four directions: The first was to investigate the anodic dissolution of disseminated gold

from a conducting nonadsorbing matrix (spectroscopic carbon) using different complexing solutions. The second was to examine the anodic dissolution of disseminated gold from a conducting adsorbing matrix (activated carbon) in different complexing media. The third objective was to examine the adsorption behavior of the different gold complexes on an activated carbon sample and if possible a carbonaceous ore sample. A fourth area to be examined, if possible, was the effects of applied potential on the affinity of activated carbon for gold complexes.

LITERATURE REVIEW AND THEORY

Electrochemical Cell Design

It was proposed in this research to examine the anodic dissolution of gold with the gold in a disseminated "ore-like" state. Thus, it was conceived to suspend particulate gold in a conducting matrix in a flow-through cell; this type of electrode is commonly known as a particulate electrode or porous electrode. Porous electrodes have received a considerable amount of interest in the recent past with many applications in galvanic cells, electrochemical synthesis, and analytical chemistry (9,10,11); the mathematical description and physical characteristics of porous electrodes has recently been discussed (12,13).

For the application of dissolving gold from a bed of particles under controlled potential conditions, it is desirable to have a high conductivity within the electrode with little ohmic voltage drop. Thus, the "flow-by" (12,13) configuration was used with a cylindrical porous vycor (inert) membrane partition used to separate the anolyte and

catholyte flows. The porous electrode configurations are shown in figure 1. The "flow-through" electrode is more amenable to mathematical description than the "flow-by" configuration due to the inherent two dimensional current distribution in the "flow-by" electrode; however, under high current or flow conditions, the "flow-through" configuration can lead to considerable ohmic voltage drop (14). To minimize electrode polarization, the counter electrode should have as high a surface area as possible.

With this design and expected low current densities, the potential distribution should be nearly constant throughout the bed; an unavoidable amount of potential drop in the bed is incurred with carbon particles due to their finite conductivity (12). To compensate for this and other sources of voltage drop, a three electrode system utilizing a platinum wire working and auxiliary electrodes and a saturated silver/silver chloride reference electrode can be used (14).

Anodic Behavior of Gold

1. General Overview

The bulk of aqueous gold electrochemistry has been conducted in noncomplexing, chloride, cyanide and thiourea media; a very limited amount of work has been done in thiocyanate and thiosulfate media. The general anodic behavior of gold in complexing and noncomplexing aqueous media was summarized by Nicol (7,8). In this work which did not discuss thiosulfate with respect to anodic gold dissolution, the author discussed under what conditions with respect to pH, ligand concentration, and potential, gold was actively dissolved or dissolved under passivating conditions. It was noted that both gold(I) and

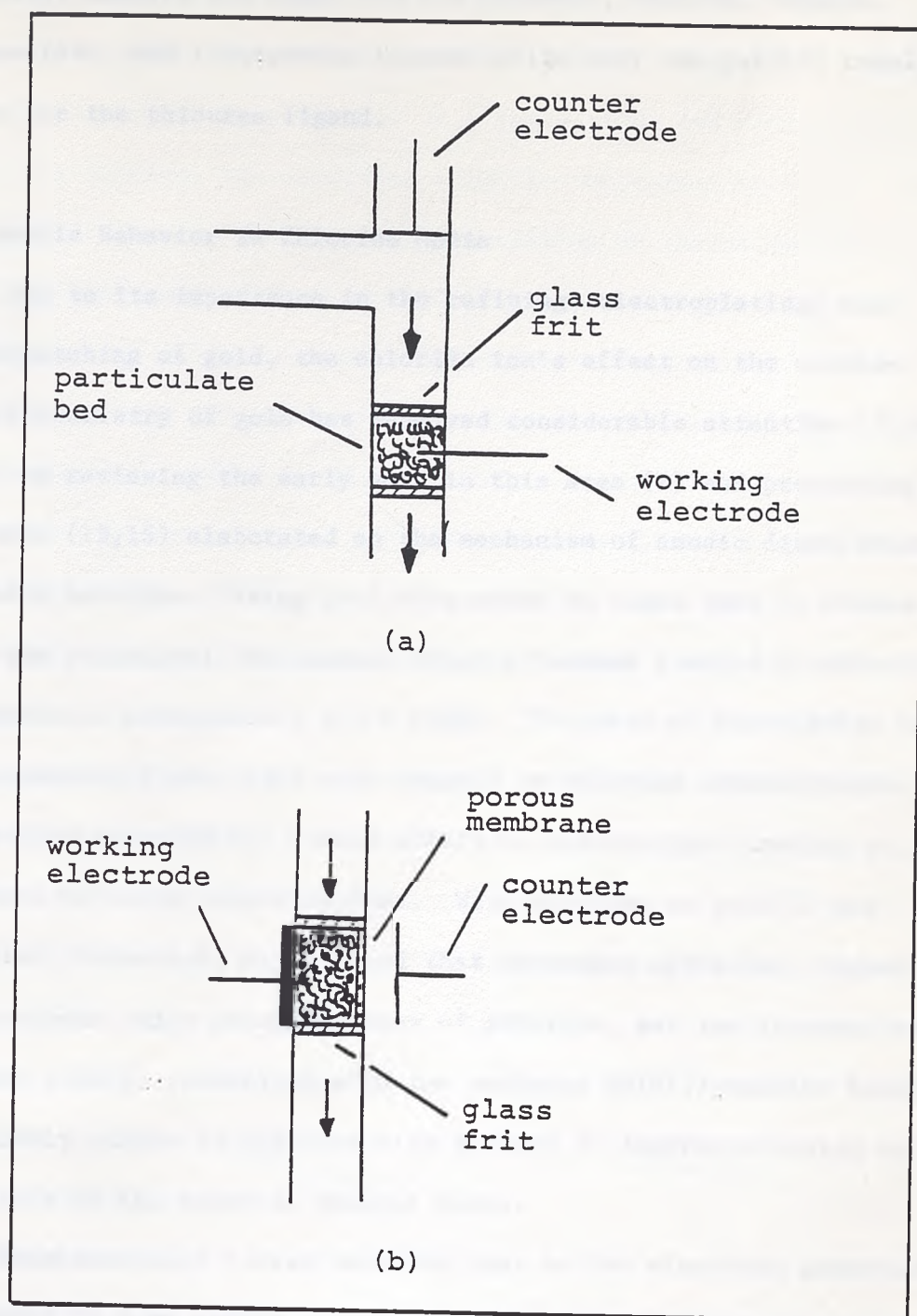


Figure 1. Electrode configurations for flow-through particulate electrodes: (a) "flow-through" regime with parallel solution and current flow, (b) "flow-by" regime with perpendicular solution and current flow.

gold(III) species are known for the chloride, cyanide, bromide, thiosulfate, and thiocyanate ligands while only the gold(I) complex is known for the thiourea ligand.

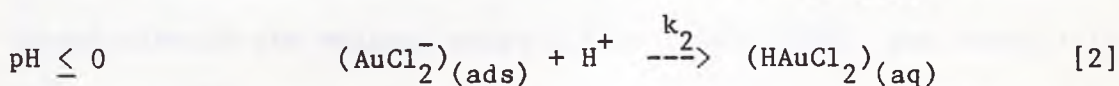
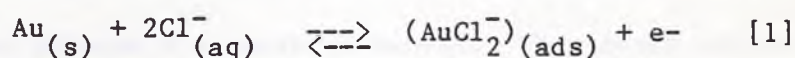
2. Anodic Behavior in Chloride Media

Due to its importance in the refining, electroplating, and electroetching of gold, the chloride ion's effect on the aqueous electrochemistry of gold has received considerable attention (7,15-21). Nicol in reviewing the early work in this area (7) and presenting his own work (15,16) elaborated on the mechanism of anodic dissolution in chloride solution. Using gold electrodes he found that in dilute chloride solutions: The current density becomes limited by chloride ion transport at potentials > 1.0 V (SHE). The rate of dissolution is approximately first order with respect to chloride concentration, and the proton activity has little effect on dissolution kinetics at constant chloride concentrations. With relation to gold(I) and gold(III) formation, Nicol found that increased agitation, higher temperatures, high concentrations of chloride, and low current densities favored gold(I) production with the produced gold(I) species being relatively stable in solution with respect to disproportioning and had a half-life on the order of several hours.

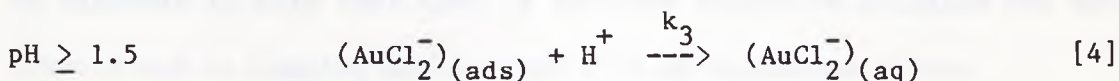
Experimentally it was observed that as the electrode potential is increased to more anodic values, a region of passivated dissolution is encountered. As was noted by Nicol (15) and Lovrecek (17) and further investigated by Podesta (18), a proposed mechanism for the anodic dissolution reaction under passivation conditions in chloride media is

the initial diffusion controlled dissolution of gold as AuCl_2^- , but with a low chloride-ion concentration at the gold-solution interface, an oxide layer begins to form. As this layer grows and dissolution as AuCl_2^- is limited, the interface chloride concentration begins to increase leading to the chemical dissolution of the oxide film. This exposes fresh gold surface for AuCl_2^- dissolution. The net effect of this mechanism is the production of current oscillations at a constant potential. With reference to this behavior, Benari (22) found that passivation was absent in concentrated chloride-dimethylsulfoxide solutions indicating either a decreased tendency for oxide formation or higher oxide dissolution kinetics.

Frankenthal and Siconolfi's (19) work with gold wire and foil in chloride solutions revealed the active, prepasive, passive and transpassive behavior of the anodic gold dissolution with pH, potential, chloride concentration, and stirring taken as variables. They derived mechanistic models and current expressions from their data for two pH ranges (≤ 0 and ≥ 1.5). The model developed was represented as follows,



$$i = k_2 [\text{Cl}^-]^2 [\text{H}^+] \exp(\eta F / RT) \quad [3]$$

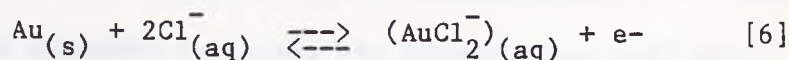


$$i = k_3 [\text{Cl}^-]^2 \exp(\eta F / RT) \quad [5]$$

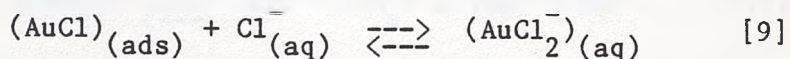
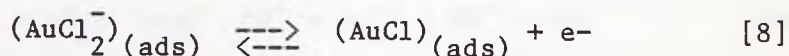
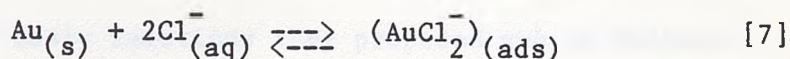
where the variables are defined as:

i = current density	R = gas constant
k_2, k_3 = rate constants	T = absolute temperature
η = overpotential ($E - E^0$)	F = Faraday's constant

This model differed from that of Horikoski et al. (20) who performed anodic gold dissolutions in 0.2 M H_2SO_4 and varying concentrations of chloride ions. His work resulted in an overall electrochemical process,



with the three elementary steps:

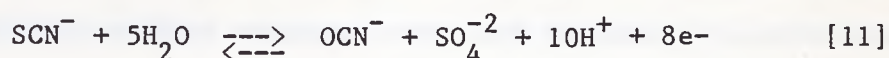
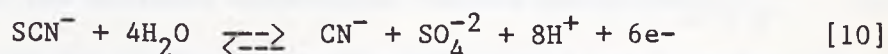


These processes resulted in current peaks in the voltammogram at 0.1 and 0.3 V (SCE). From the pH and chloride concentration behavior relative to these peaks, they deduced the above mechanism. They found active dissolution in the voltage range 0.8 to 1.05 V (SCE), and above 1.10 V (SCE) gold(III) was seen to form; they also determined that reaction nine was the rate limiting step in the active dissolution range. It is of interest to note that this is the same mechanism proposed for anodic dissolution in cyanide media which will be discussed later.

3. Anodic Behavior in Thiocyanate Media

The little anodic work done with thiocyanate ion prior to 1980 was reviewed by Nicol (7). The reported voltammetry work revealed very similar electrochemical behavior to that of the chloride ion with respect to active dissolution, passivation, and reactivation. The proposed major difference between the chloride and thiocyanate systems is the ease of oxidation of the respective ligands with thiocyanate the more readily oxidized. The standard state electrochemical potentials for thiocyanogen and chlorine formation are respectively 0.77 and 1.36 V.

Byerly and Enns (23) investigated the aqueous oxidation of SCN^- to CN^- and SO_4^{-2} . the basic reactions they proposed are as follows:



Their work which consisted of controlled current electrolysis resulted in complete conversion of the thiocyanate. Cyanide recoveries were dependent on whether the solutions were buffered or not; if the solution pH was allowed to decrease, CN^- was stabilized as HCN with respect to OCN^- formation.

In an earlier piece of literature Nicholson (24) investigated the electro-oxidation of SCN^- for analytical purposes. The observed voltametric behavior indicated the presence of multiple reaction steps involving thiocyanogen formation as had been reported

previously to give an overall reaction:



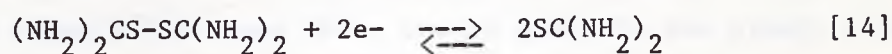
which is what Byerley and Enns assumed.

4. Anodic Behavior in Thiourea Media

In the past couple of decades, thiourea $[\text{SC}(\text{NH}_2)_2]$ has increasingly been studied as a lixiviant for gold (24,26 27,28); the chemical dissolution is normally carried out with ferric iron as a source of oxidant. The proposed process of chemical dissolution involves the rapid reaction of ferric iron with the thiourea ligand forming formididine disulfide which then oxidizes the gold with subsequent complexation to the cationic dithiourea complex $[\text{Au}(\text{SC}(\text{NH}_2)_2)_2]^+$. The general trends in the chemical dissolution process are reaction rate increases for higher oxidant concentrations and thiourea concentrations. The rate of dissolution decreased with aged solutions due to further oxidation products of thiourea (H_2NCN , S^0 , SO_4^{2-}) passivating the gold surface (25,26).

It has been proposed (29) that SO_2 can be used to increase precious metal recovery and lower reagent consumption by preventing excessive oxidation of thiourea; the theory is that the initial oxidation of thiourea to formididine disulfide is a reversible reaction and by the selective use of SO_2 which is selective in reducing formididine disulfide, the concentration of formididine disulfide may be adequately controlled. This prevents both passivation and excessive reagent consumption.

The anodic behavior of gold in thiourea has received minimal attention in the literature (7,30). In Groenewald's work (30), the anodic behavior of the gold/thiourea system was studied by coulometric and constant potential amperometric methods utilizing a gold-disk electrode. Solutions containing $[\text{Au}(\text{SC}(\text{NH}_2)_2)_2]^+$ were either made from synthesized $\text{Au}[\text{SC}(\text{NH}_2)_2]\text{ClO}_4$, or electrochemically generated in-situ; formamidine disulfide was produced by hydrogen peroxide addition. In this study, the anodic current was found to be independent of acid concentration over the range 0.01 to 0.1M and negligible effects were incurred changing from H_2SO_4 to HCl or HClO_4 ; the exchange current density of approximately $8 \times 10^{-6} \text{ A/cm}^2$ indicates that the gold-thiourea reaction is a reversible electrochemical process (30). The peak current density at 100 percent current efficiency was seen to increase dramatically upon going from a 0.01 M thiourea solution to 0.1M thiourea solution. 100% current efficiency was obtained at potentials up to approximately 0.4 V (SHE) with the gold surface appearing unaltered; at potentials higher than 0.4V, the current efficiency and rate of gold dissolution dropped and the gold was seen to form dark areas on its surface. The standard state potentials for the two reactions:



are 0.38 V and 0.42 V respectively explaining the drop in current efficiency due to excessive thiourea oxidation. It was determined through rotating disk experiments that the anodic reaction was largely

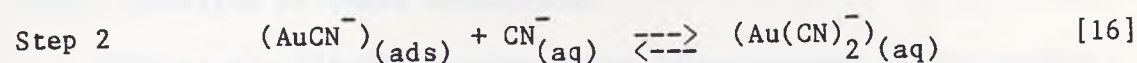
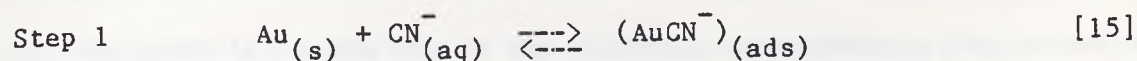
diffusion controlled at peak current densities. Cathodic polarization curves indicated diffusion controlled gold deposition at a potential of -0.2 V.

5. Anodic Behavior in Cyanide Media

Cyanide solution is the conventional lixiviant for gold in the chemical treatment of gold ores and is proposed to be the principal one for years to come (5). In the chemical leaching of gold with cyanide, the mechanism is one of corrosion with at least part of the gold surface acting as an anode and another portion as a cathode where oxygen is reduced to hydrogen peroxide and eventually to hydroxide ion; if the gold surface is in contact with a foreign conductive surface, it is possible for the cathodic reaction to occur separate from the gold surface. The oxidized gold atom is then complexed by adsorbed cyanide ligands to form the stable $\text{Au}(\text{CN})_2^-$ anion in solution. Many factors affect the kinetics of the chemical gold dissolution in cyanide media with the three most important being cyanide concentration, dissolved oxygen concentration, and the gold surface area (31).

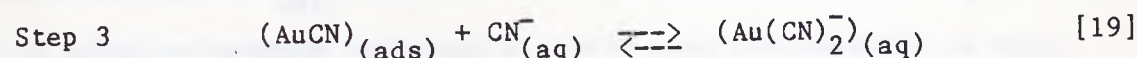
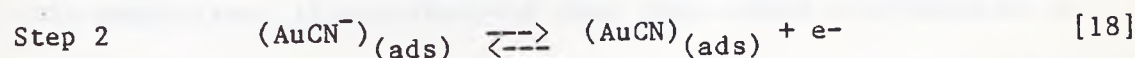
The literature on the anodic dissolution of gold in cyanide media up to 1979 has been reviewed by Nicol (8) with the latest research at that time done by Pan et al. (32) and Kirk et al. (33). The work up to that point had clearly indicated three anodic peaks in the steady state voltammograms for gold electrodes in alkaline cyanide; the potentials (SHE) of these peaks occurred at -0.41 V (peak No. 1), 0.28 V (peak No. 2), and 0.62 V (peak No. 3); the steady-state current at each peak increased in the order $0.62 > 0.28 > -0.41$ V. The reaction mechanisms

proposed to account for this behavior were of two similar types. The one proposed by Cathro and Kock (34) and supported by Pan et al. (32),



explained the cyanide concentration behavior and tafel slope of the first and second peaks while the third was not addressed in this respect; it was proposed that step 1 was rate determining at peak 2 and step 2 was rate determining at peak 3.

Kirk et al. (32) suggested the mechanism:



This mechanism explained the behavior of peak 2 and peak 3 with respect to the concentrations of cyanide and hydroxide ion (peak 2 was unaffected by the concentration of either species and peak 3 increased with cyanide concentration and decreased with increasing hydroxide concentrations) with step 2 rate determining for peak 2 and step 3 rate determining in the potential range of peak 3.

From experimental observations, it was proposed that Au_2O_3 formation was leading to surface passivation at the peak 3 potential, 0.62 V. The passivation occurring at the other two peaks was suspected

to be due to a layer of the AuCN polymer (8) on the gold surface or mixed ligand species such as $(\text{AuCNOH})_{\text{ads}}$. Initially it was not considered possible that lower oxides or hydroxides could be passivating at the lower two peaks due to the supposed thermodynamic limitation of their formation at these potentials.

Kirk et al. (34-36) continued the investigation of the anodic behavior of gold in alkaline cyanide solutions using information gained from cyclic voltammetry. This technique coupled with various experimental conditions yielded more detailed information on the passivating phenomena and the mechanism of dissolution at peak 1 (-0.41 V).

In this work the anodic behavior of gold in alkaline solution absent of cyanide was investigated to compare to that with cyanide. In this comparison, it was observed that three peaks attributable to monolayer $(\text{AuOH})_{\text{ads}}$ formation were observed cathodic to Au_2O_3 formation in alkaline aqueous solution; a fourth peak attributable to Au_2O_3 formation was observed anodic to these three. When these peaks were compared to those in cyanide solution, the correspondence to the passivation potentials was good (35).

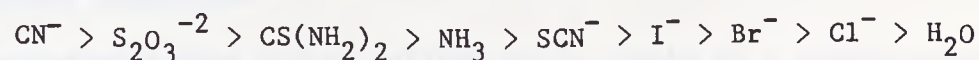
Cyclic potential sweeps in alkaline cyanide indicated that oxide reduction occurred just anodic to each anodic peak with the gold surface reactivated to dissolution by the proposed mechanism; thus, at the lower potentials, OH^- ions are competing with cyanide ions for adsorption sites with the resulting insoluble gold hydroxide passivating the surface. The investigation of the potential region of peak one revealed that step two in the proposed mechanism is rate determining under steady

state conditions; with increases in the potential scanning rate, peak one was seen to separate into two peaks. The initial peak initially decreased to zero while the new peak increased in magnitude. This phenomenon was explained in terms of the sweep rate relative to the rates of step 1 and step 2 in the reaction mechanism. As the sweep rate increases, the rate of step 2 is slow relative to the voltage scan rate resulting in a decreased extent of reaction. At the same time, the electrochemically influenced adsorption process which has a much greater rate relative to the voltage scan rate results in an increased current with scan rate (i.e. same charge passed in a shorter time interval). It was also found that stirring increased the peak height of this adsorption peak indicating that desorption of the product (step 3) was rate controlling.

It was concluded from these observations that the proposed adsorption step was essential to fully explain the experimental observations and that discrepancies in the literature (8) on the rate controlling step at peak 1 were due to changes with cyclic scan rates which do not fully reflect steady state phenomena. Thus, for steady-state conditions, step 2 is rate controlling for the anodic peaks at -0.41 V and 0.28 V while step 3 is rate controlling at 0.62 V; passivation is caused by monolayer AuOH formation at -0.41 V and 0.28 V and by Au_2O_3 formation at 0.62 V. Little is said in these references about the possible formation of $\text{Au}(\text{CN})_4^-$; this species is reported to have a limited stability in aqueous solution (37).

6. Anodic Behavior in Thiosulfate Media

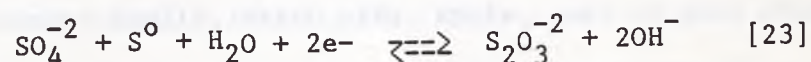
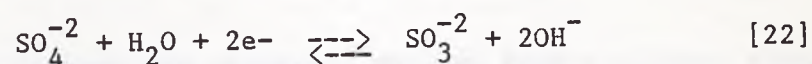
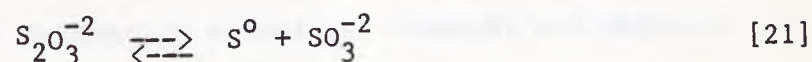
With respect to anodic behavior, thiosulfate is the least studied of the ligands forming stable gold complexes. This is surprising considering that of the common ligands for gold(I), the standard emf data indicate a stability order:



The standard-state emf for the reaction,

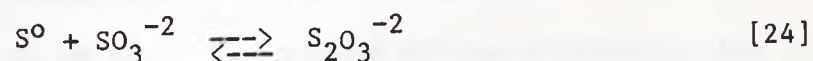


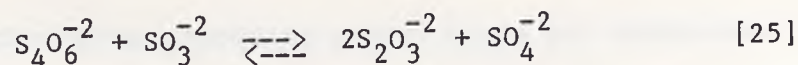
is 0.20 V. The probable complication with the anodic dissolution of gold in thiosulfate solutions is the oxidation of $\text{S}_2\text{O}_3^{-2}$ to sulfur, sulfite, and sulfate via the reactions:



The ease of thiosulfate oxidation by oxygen has been reported in the literature (38) to cause the formation of a passivating layer of colloidal sulfur on the gold surface (39).

In these studies, sulfite ion was advocated for colloidal sulfur control and tetrathionate control through the reactions:





The sulfite ion is reportedly a good nucleophile in attacking the sulfur-sulfur bond (40) which would explain its beneficial effect.

Activated carbon

1. General Properties

Activated carbon can be defined quite simply as a carbonaceous material capable of adsorbing adsorbate molecules. This definition is associated with a large amount of information not all of which is reconcilable within itself; thus a more explicit definition is that activated carbon is carbonaceous material that has been treated in some way to give it the capability of adsorbing adsorbate molecules. This now excludes unaltered natural materials, some of which behave like activated carbon; the similar behavior of some natural materials (such as coals) is likely to occur by coincident chemical and physical interactions.

Most activated carbons are materials derived from a natural source of carbon such as coconut shells, peach pits, coals, peat or wood which have been charred or calcined with coincident or separate activation.

Charring and calcining refer to the partial combustion of the source material driving off impurity elements and increasing the carbon content of the material. If this process is done in air, O_2 , H_2O , or CO_2 then coincident activation can occur, but in many instances, this process is done in vacuum or air with activation conducted in another step with H_2O , air, O_2 or CO_2 . The purpose of the activation step is to

oxidize the edge carbon atoms producing active sites for adsorption.

Activated carbons are classified into two types for categorizing purposes, even though most commercial carbons will exhibit properties of both since they are readily interconvertable. The two designations are summarized below:

Type	Activation Conditions	Physical Properties
H	Temperature $>700^{\circ}\text{C}$, CO_2 , vacuum exposed to air, O_2 at R.T.	Hydrophobic Surface Positive Zeta Potential adsorbs acid
L	Temperature $<400^{\circ}\text{C}$, O_2 , Air	Hydrophillic Surface Negative Zeta Potential adsorbs base

It should be noted that heating an L carbon in vacuum at 700°C followed by cooling in vacuum and exposure to air at room temperature results in the formation of an H carbon while exposure of an H carbon to air while cooling after activation or to an oxidant in solution after activation (cooling in vacuum) results in the formation of an L carbon.

2. Physical Properties/Experimental Observations

Correlations of the products of outgassing to each carbon type indicates that decomposition of L-carbon sites results in CO_2 formation, whereas CO formation is associated with the H-carbon sites. This also correlates with the observed surface phenomena of hydrophobicity, zeta potential, and adsorption of protons or neutralization of OH^- .

If it is postulated that carboxylic acid and phenol functional groups are present on the L-carbon, the hydrophillic nature would be

explained in the ionic and hydrogen bonding interactions with H_2O , the neutralization of base is explained in carboxylate and phenolate formation which leads to a negatively charged surface and subsequently, a negative zeta potential.

If aromatic quinone-type groups are postulated to populate the edge carbon atoms in H-type carbons, the relative hydrophobicity is explained with decreased hydrogen bonding with H_2O , and the adsorption of protons leading to a positive zeta potential is explained in terms of the protonation of the carbonyl groups with possible incipient oxidation of water to peroxide resulting in the formation of a phenol group.

To give evidence to postulations such as the above, much indirect experimental evidence has been gathered about activated carbons with some direct, although limited, evidence gathered through infrared spectroscopy and electrochemical techniques. The amorphous and opaque nature of the carbon limits the application of direct spectroscopic and x-ray techniques. Some of the indirect methods are offgas analysis, multi-strength base titrations, bromination, reaction with diazomethane, and reactions with other organic reagents.

Correlations are then made such as the moles of base neutralized to the moles of CO_2 outgassed, moles of H_2O or alcohol adsorbed per mole of CO_2 outgassed, and the behavior of the carbon with respect to saponification after treatment with diazomethane (carboxylates give esters, aromatic carbonyles give ethers). Thus, from all these correlations and a limited amount of direct evidence such as IR spectra and aqueous redox behavior, it is postulated that commercial activated carbons will contain significant quantities of carboxylates and

carboxylic anhydrides, phenol/phenolates, hydroquinone/quinones, lactones, and peroxides (41).

3. Historical Relationship of Activated Carbon to Gold

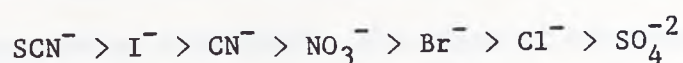
The relationship of gold to activated carbon has been under investigation since the latter portion of the 18th century (44). The early work was done when it was observed that activated charcoal caused the precipitation of metallic gold from AuCl_4^- solutions, and later, after the advent of the cyanidation process, that activated carbon could precipitate gold in some form from cyanide solution. Due to the poor loading characteristics of these early carbons which were burned and then smelted to recover the gold and the advances in the Merrill Crowe zinc precipitation process, activated carbon remained overlooked until approximately 1950. It was then that Zadra (42) developed a practical method of eluting adsorbed gold cyanide from activated carbon after adsorption in situ from the ore-pulp solution; this is commonly known as the carbon-in-pulp process (CIP).

The development of an efficient elution procedure led to other methods of contacting such as carbon-in-leach (CIL), and carbon-in-column (CIC) (sometimes called carbon-in-clear solution) (43).

The commercial application of CIP processing in the early seventies along with increased gold prices and better carbons gave rise to a multitude of chemical and engineering studies and reviews on the adsorption of gold and silver from solution by activated carbon and their subsequent elution (43-65,74,75).

4. Behavior of Activated Carbon in Electrolyte Solutions

The general behavior of activated carbon with respect to simple electrolyte adsorption as been discussed by Mattson and Mark (41). In work up to this time, it was found that appreciable specific anion adsorption occurred from aqueous solution depending on the solution pH (hydroxide adsorption). The softer anions were found to be preferentially adsorbed as is found in specific anion adsorption on electrode surfaces. The adsorption affinity is ordered:



The adsorption of monovalent cations is favored at higher pH values through cation exchange on carboxylate and phenolate groups as well as double layer adsorption to keep electrical neutrality in the diffuse double layer. Polyvalent cations are not specifically adsorbed to an appreciable extent due to their larger solvation spheres; however, adsorption in the diffuse layer can be considerable when a strongly adsorbing anion is present. At lower pH values cation adsorption is less due to competition with H^+ (41).

Polyvalent metal cations follow monovalent cations in not adsorbing at low pH but the pH for incipient adsorption compared to monovalent cations is lower reportedly due to the formation of hydroxylated species (66). A correlation of the pH for incipient adsorption and the pH for incipient hydrolysis to colloidal hydroxides (adsorption pH was always less than hydrolysis pH) was found with electrokinetic measurements indicating the carbon surface after adsorption to behave as that of the metal hydroxide.

5. Irreversible Adsorption of Oxygen

The properties of activated carbon with respect to acid and base adsorption has already been discussed, but it is also known from the early work on activated carbon (42) that an activated carbon that is degassed at high temperature ($>1000^{\circ}\text{C}$) under vacuum and then kept from exposure to air does not adsorb acid upon exposure to aqueous solution as does a normal H carbon. If oxygen or air is allowed to enter the solution, the acid is adsorbed and the active carbon behaves just like an H type with no degassing; also, at low concentrations of electrolyte (double layer adsorption minimized), the moles of adsorbed acid was equal to the moles of oxygen adsorbed (41). Thus, activated carbon is capable of irreversibly adsorbing oxygen.

6. Adsorption/Precipitation of Gold from Solution

With respect to gold adsorption, the mechanism of AuCl_4^- adsorption on activated carbon did not prove to be difficult to elucidate since metallic gold was easily discernable on the carbon surface even at low gold loadings (44,53,55,67). The gold chloride is reduced at the carbon surface with subsequent oxidation of a carbon functional group. The gold was observed by microscopy (67) to be deposited as small sperules ranging in size from 0.5 micrometers at low gold loadings to 30 micrometers at higher loadings. Multilayer formation was observed in some particles and increased surface coverage was associated with increased particle porosity; this is indicative of the higher number of edge carbons in a porous particle, and thus, activated sites capable of oxidation.

In reviewing the present state of knowledge with respect to the mechanism of $\text{Au}(\text{CN})_2^-$ adsorption, it is relevant to first state the theories proposed over the years (44,53-55). The theories of adsorption were summarized by McDougall (53-55) as:

1. $\text{Au}(\text{CN})_2^-$ is adsorbed as the anion or salt
e.g. $\text{Au}(\text{CN})_2^-$, $\text{Ca}[\text{Au}(\text{CN})_2]_2$
2. $\text{Au}(\text{CN})_2^-$ is adsorbed as a modified compound such as AuCN or a cluster compound
3. $\text{Au}(\text{CN})_2^-$ is reduced to elemental gold in the carbon pores.

The third theory has largely been discounted based on the fact that elemental gold has not been detected in cross-sectioned samples and the reduction potential of the carbon ($E > -0.13 \text{ V}$) is not sufficient to reduce $\text{Au}(\text{CN})_2^-$; however, the first two theories are still in dispute.

It is also instructive at this point to introduce the Freundlich isotherm expression (41) which correlates the adsorption of many neutral molecules on activated carbon. The theoretical basis of the isotherm is the adsorption site free energy is assumed to be exponentially related to the surface coverage and the adsorption is reversible. The isotherm is commonly written,

$$Q = BC^n \quad [26]$$

where: Q = the gold loading (mg/g, mmol/g, ...)

B = constant (mg/g, mmol/g, ...)

C = solution concentration (ppm, mmol/l, ...)

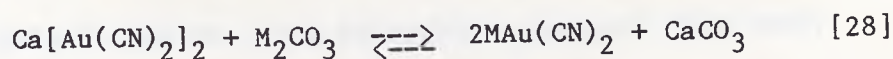
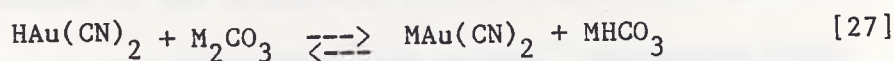
n = constant

The constants B and n will vary depending on the type of adsorption (physical, chemical) and on the adsorbate species. For physical adsorption of neutral molecules n will range from 0.5 to 1.0 (65).

Davidson (44) was one of the earliest of the modern researchers to gather information about the mechanism of $\text{Au}(\text{CN})_2^-$ adsorption by activated carbon. His first observations were the substantial effects that ionic strength, pH and the nature of the spectator cations had on the equilibrium gold capacity and loading kinetics. The effects of temperature on the equilibrium gold capacity were also addressed, but the general trends in this area were already known from the early work of Zadra.

Davidson found that increased ionic strength enhanced gold adsorption, and the gold loading was increased significantly by the presence of the calcium ion and lower pH's. These observations led to his discovery of using deionized water as an effective eluting solution. He also found that a carbon loaded in a calcium solution which was relatively inert to 90°C water elution could be made amenable to elution by pretreating the carbon with a carbonate solution at 50°C. The effectiveness of the pretreatment stage for different carbonates followed the order: $\text{K}^+ > \text{Na}^+ > \text{Li}^+ > \text{NH}_4^+$. In later work by Davidson (45,46), it was found beneficial to use a cyanide/hydroxide solution in the pretreatment which kept calcium carbonate from fouling the carbon. These results led Davidson to propose the mechanism that gold was adsorbed from plant solutions as the neutral complexes $\text{HAu}(\text{CN})_2$ (predominately at lower pH values) and $\text{Ca}(\text{Au}(\text{CN})_2)_2$ which when treated with the carbonate solution resulted in bicarbonate or calcium carbonate

formation and the corresponding alkali aurocyanide salt:



He postulated that these neutral complexes were adsorbed with the stability of the neutral complexes following the order (44): $\text{Ca}^{+2} > \text{Mg}^{+2} > \text{H}^+ > \text{Li}^+ > \text{Na}^+ > \text{K}^+$.

A few years later Dixon, Cho, and Pitt made a thorough study of the kinetics and characteristics of Au(CN)_2^- and Ag(CN)_2^- adsorption on activated charcoal (49-52). In their earliest work (49), it was found that the adsorption of gold and silver cyanide was a diffusion controlled rate process (activation energy of 2.1 kCal/mol) with the isotheric heat of adsorption having an exponential dependence on surface coverage. In later work (50) they determined that: Ca^{+2} gives higher Ag(CN)_2^- adsorptions than Na^+ , cyanide ion decreased Ag(CN)_2^- adsorption through competition for adsorption sites, calcium and sodium were adsorbed with the Ag(CN)_2^- but not in stoichiometric quantities, decreasing pH increased the silver loading, and the adsorption capacity of activated charcoal for Au(CN)_2^- was greater than for Ag(CN)_2^- .

In this work, they proposed an ion-solvation theory of adsorption where it was postulated that the larger more weakly hydrated anions were more strongly adsorbed through a specific adsorption mechanism on the surface active site. They also proposed that Ca^{+2} and Na^+ were then adsorbed in the diffuse double layer giving rise in the case of Ca^{+2} to

still further sites for adsorption. The rest of the work by Cho and Pitt (51,52) focused on the adsorption kinetics which were modelled quite well with the rate of $\text{Au}(\text{CN})_2^-$ and $\text{Ag}(\text{CN})_2^-$ adsorption being controlled by pore diffusion. One interesting note of this work, however, is the reported reversibility shown by the adsorption of $\text{Ag}(\text{CN})_2^-$ in 0.04 M sodium cyanide solution.

The next involved study of the adsorption of gold cyanide on activated carbon was done by McDougall et al. (53-55) who thoroughly reviewed the pertinent literature and presented results of their adsorption studies on steam activated coconut-shell carbon. Their work supported Davidson's conclusions on the effects of ionic strength, Ca^{+2} ion, and temperature on the loading of $\text{Au}(\text{CN})_2^-$; they additionally determined that it took months for the adsorption process to approach equilibrium.

In another phase of their work, they compared the loading of the activated carbon to that on IRA 400 anion exchange resin by observing the effect of the perchlorate and chloride ions on the equilibrium gold loading. It is known that the ClO_4^- ion is a large weakly hydrated ion as is $\text{Au}(\text{CN})_2^-$ and competes with it for sites on an ion exchange resin. They found that perchlorate and chloride ions had little effect on the equilibrium capacity of activated carbon for gold cyanide concluding that the adsorption was not akin to normal ion exchange where electrostatic interactions predominate. Further work where the loaded carbon was investigated by x-ray photoelectron spectroscopy (XPS) and nitrogen analysis revealed that the oxidation state of the gold on the

carbon was 0.3 and the nitrogen adsorbed was always significantly less than stoichiometric $\text{Au}(\text{CN})_2^-$ and approached a molar gold to nitrogen ratio of 1:1 at high gold loadings. The reduced oxidation state compared to $\text{Au}(\text{CN})_2^-$ was attributed to a cluster compound or AuCN polymer on the carbon surface.

In conjunction with the XPS study, the reduction potential of various carbons was correlated to the gold loading of the carbon. The correlation which was relatively good, revealed that the higher the reducing character of the carbon, the higher was the gold loading. It was also shown in this study that $\text{Hg}(\text{CN})_2$ competes with $\text{Au}(\text{CN})_2^-$ for adsorption sites; however, the adsorption of $\text{Hg}(\text{CN})_2$ was unaffected by pH or ionic strength. The obvious conclusion being that the process leading to adsorption of $\text{Hg}(\text{CN})_2$ on activated carbon was different than that for $\text{Au}(\text{CN})_2^-$ and $\text{Ag}(\text{CN})_2^-$.

Fleming and Nicol (68), in the culmination of a series of reports on the kinetic modelling of activated carbon adsorption of aurocyanide, presented results on factors affecting the equilibrium loading of gold on activated carbon. They found as did Davidson (47,48) that the dicyano-copper(I) complex competes with $\text{Au}(\text{CN})_2^-$ for adsorption sites in the neutral pH range. Their work showed that a maximum in copper adsorption was obtained at molar cyanide to copper ratios of 2:1. At this mole ratio the copper adsorption decreased with increasing pH consistent with the shift in stability from $\text{Cu}(\text{CN})_2^-$ to $\text{Cu}(\text{CN})_3^{-2}$ (37). Thus the affinity of the activated carbon for the copper cyanide complexes follows the order: $\text{Cu}(\text{CN})_2^- > \text{Cu}(\text{CN})_3^{-2} > \text{Cu}(\text{CN})_4^{-3}$.

To examine the reversibility of $\text{Au}(\text{CN})_2^-$ adsorption, Fleming and Nicol equilibrated loaded carbon with unloaded carbon and found that the equilibrium did shift to nearly equal loadings on the two carbons indicating that at least the bulk of the adsorbed gold was adsorbed in a reversible process.

In work on simulated and real plant solutions, Davidson (47) found that moderately low concentrations of SCN^- and $\text{S}_2\text{O}_3^{2-}$ had detrimental effects on the adsorption of $\text{Au}(\text{CN})_2^-$. He found that 90 ppm SCN^- slowed gold adsorption at high pH while 4 ppm $\text{S}_2\text{O}_3^{2-}$ had a detrimental effect on gold adsorption at low pH values; as noted above his work also demonstrated the effect of copper(I) cyanide complexes on the aurocyanide adsorption.

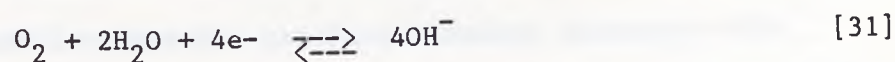
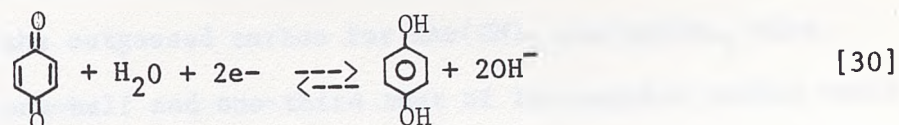
The effects of other solution species on the activated carbon adsorption of gold cyanide has also been reported on by Grabovskii and Ivanova (76). They concluded after examining the effect of $\text{Au}(\text{CN})_2^-$ solution concentration on the adsorption capacity of activated carbon for Ag, Cu, Zn, Fe, Ni, and Co, that higher valent anions are displaced from the activated carbon by lower valent anions. This is in agreement with the observations on the adsorption of copper cyanide complexes on activated carbon.

The most recent work done on the mechanism of aurocyanide adsorption is that of Tsuchida and Muir (64,65). Using a flow-through cell ("flow-through" regime) utilizing a bed of activated carbon in contact with a platinum wire as an electrode, the potential of the activated carbon was monitored during passage of solution through the bed; the pH of the exiting solution was also continuously monitored.

Their work showed that the potential of the carbon followed the expression (64),

$$E = E^0 - 0.059\text{pH} \quad [29]$$

which is consistent with the couples for the half reactions:



It was also observed that at low gold loadings from $\text{KAu}(\text{CN})_2$ solution, essentially zero potassium ion was adsorbed whereas at higher loadings potassium ion was adsorbed although in substoichiometric amounts. This amount increased with the equilibrium solution pH.

The carbon potential was lowered when adsorption of an anion occurred normally below that of the reversible redox pH of the carbon. The potential change upon passage of chloride solutions through the cell was found to follow the above redox expressions in a reversible manner. However, for I^- , CN^- , $\text{Au}(\text{CN})_2^-$, and $\text{Ag}(\text{CN})_2^-$, the lowering of the carbon potential was not reversible and significantly below that for the corresponding pH value for the reduction of O_2 ; thus, an electrochemically irreversible process had occurred. It was concluded that the reduction mechanism was more significant in $\text{Ag}(\text{CN})_2^-$ adsorption than $\text{Au}(\text{CN})_2^-$ adsorption.

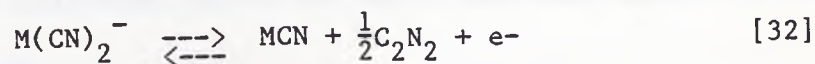
In another piece of work, Tsuchida and Muir (65) reported results from a study of the adsorption of $\text{Au}(\text{CN})_2^-$, $\text{Ag}(\text{CN})_2^-$, and $\text{Hg}(\text{CN})_2$ on normal activated carbon and activated carbon that had been outgassed at

950°C under a 10^{-5} torr vacuum. The carbon was then stored under nitrogen, and the solutions used for adsorption were kept free of oxygen. It was found that $\text{KAu}(\text{CN})_2$ and $\text{KAg}(\text{CN})_2$ adsorption on the outgassed carbon was similar to the adsorption of $\text{Hg}(\text{CN})_2$ with respect to the Freundlich isotherm giving n values of 0.6 to 0.8. The adsorption capacities of the outgassed carbon for $\text{KAu}(\text{CN})_2$ and $\text{Ag}(\text{CN})_2$ were approximately one-half and one-third that of the regular carbon while for $\text{Hg}(\text{CN})_2$, the loadings and isotherm remained unchanged with outgassing. The moles of potassium adsorbed on the deoxygenated carbon approximated a one to one molar ratio with respect to the moles gold or silver adsorbed. Upon exposure of the outgassed carbon to oxygen in solution, the adsorption capacity for gold and silver returned to the values found for the normal carbon except that the potassium ion adsorption was now much less than that in either adsorption on normal carbon or adsorption on deoxygenated carbon in an oxygen-free solution.

In experiments where the adsorption of $\text{KAu}(\text{CN})_2$ was conducted in the presence of acetonitrile, it was found that the adsorption could be suppressed completely with the deoxygenated carbon but not completely with the normal carbon. Thus, the organic solvent affected the ion exchange adsorption more than the reduction adsorption. In concluding their work, Tsuchida and Muir monitored the potentials of the deoxygenated carbon as $\text{KAg}(\text{CN})_2$ was adsorbed. The potential of the deoxygenated carbon was about 270 mV less than the normal carbon in H_2O and upon adsorption of $\text{KAg}(\text{CN})_2$ decreased similarly to normal carbon; however, it was found that upon flushing with H_2O , the carbon potential returned to its initial value. This indicated that the redox behavior

was reversible on the deoxygenated carbon; however, it was not stated whether the water washing eluted the silver complex from the carbon. It was also found that the potential behavior of the deoxygenated carbon upon exposure to oxygen containing $\text{KAg}(\text{CN})_2$ solutions approximated that found for the normal carbon in $\text{KAg}(\text{CN})_2$ solutions.

Thus, these authors proposed that the process of adsorption of $\text{Au}(\text{CN})_2^-$ and $\text{Ag}(\text{CN})_2^-$ by activated carbon is electrochemical in nature with reduction of adsorbed oxygen or functional groups and the coincident oxidation of $\text{Au}(\text{CN})_2^-$ or $\text{Ag}(\text{CN})_2^-$ according to the reaction (64):



This reaction sequence is proposed to originate through an ion-exchange mechanism with a surface functional group.

Further unpublished work by the same authors revealed that the oxidative mechanism is favored in the absence of free CN^- and at neutral pH; it was also concluded that the oxidative mechanism was less important relative to the ion-exchange mechanism on coconut carbons in comparison to peat carbons where the reverse is true.

The activated carbon adsorption of gold complexes other than the chloride and cyanide species has received minimal attention in the literature due to the lack of general commercial use of such complexes. The lixiviant nearest to commercial significance is acidic thiourea (29,69). The literature pertaining to the activated carbon adsorption

of $[\text{Au}(\text{SC}(\text{NH}_2)_2)_2]^+$ has been recently reviewed (69) and a couple of recent presentations have addressed the equilibrium and kinetic behavior of $[\text{Au}(\text{SC}(\text{NH}_2)_2)_2]^+$ adsorption on activated carbon (70,71). These two studies investigated parameters such as thiourea concentration, gold and silver complex concentration, stirring speed, and acid concentration. The maximum loading found approached 200mg Au/g carbon.

In Deschenes (69) review, the results of several Russian investigators were reported on with indications that gold loadings of 150 to 170 mg Au/g carbon were possible from a solution initially 0.85 ppm in gold. It was also found in these papers that thiourea was readily adsorbed by activated carbon but could be eluted easily with warm oxygen-free water.

An interesting topic covered in this review was the electroelution of $[\text{Au}(\text{SC}(\text{NH}_2)_2)_2]^+$ from cation exchange resins; this technique was studied by Russian scientists in the early 1970's (69). The cation-exchange resin, after being loaded with $[\text{Au}(\text{SC}(\text{NH}_2)_2)_2]^+$, is made the anode of an electrochemical cell. $[\text{Au}(\text{SC}(\text{NH}_2)_2)_2]^+$ is desorbed from the resin and is deposited on the cathode. Reported pilot plant work resulted in 30 percent current efficiencies with 95 to 98 percent precious metal recoveries from the resins. The electroelution technique is reported to accelerate the elution of the $[\text{Au}(\text{SC}(\text{NH}_2)_2)_2]^+$ complex.

A similar concept was proposed by Lie et al. (72) in a patent. This technique dealt with the one step electroelution/electrowinning of gold cyanide from activated carbon by making the activated carbon the anode in an electrochemical cell. By applying a potential across the cell, the gold could be desorbed and plated on the cathode; only the concept was demonstrated in this work.

There is but one notable reference to the activated carbon adsorption of gold complexes other than those of chloride, cyanide, and thiourea. Ivanova et al. (77) studied the activated carbon adsorption of Au, Ag, Cu, Zn, Fe, Ni, and Co from CN^- , SCN^- , CH_3COO^- , citrate, and thiourea solutions. It was found that Au and Ag were preferentially adsorbed over the other metals. They concluded that the nature of the ligand had little impact on the adsorption process, but it was the ability of the metal center to form donor-acceptor complexes with carbon atoms having unsaturated valences that led to the strong adsorption observed. It is of interest to note that his conclusion could possibly be applied to the observations on the adsorption of copper(I) cyano complexes. It was already noted that the affinity of activated carbon for copper(I) complexes follows the order: $\text{Cu}(\text{CN})_2^- > \text{Cu}(\text{CN})_3^{2-} > \text{Cu}(\text{CN})_4^{3-}$. The most obvious postulate would be that the adsorption is akin to ion exchange with the highly charged species more weakly held on a substrate with a low site density. But, if an interaction with the metal center is a prerequisite to adsorption, then changes in the coordination sphere of the metal center should affect the tendency for adsorption.

Modelling of Column Processes

To properly evaluate the results of concentration-time profiles or percent-recovery profiles for processes utilizing a column reactor, it is necessary to at least qualitatively relate the measured variables to

the transport processes occurring. Referring to figure 2, the basic mass transport model equation assuming plug flow behavior in the column and a perfectly mixed reservoir can be expressed (61,73):

$$\epsilon A \frac{dC(t,x)}{dt} = - \frac{WdC(t,x)}{dx} - r(1 - \epsilon)A \quad [33]$$

$$W(C_o - C_i) = V \frac{dC}{dt} \quad [34]$$

The variables are defined as follows:

W = solution flow rate	A = reactor cross-sectional area
ϵ = bed voidage	C = reactor solution concentration
C _i = reactor inlet concentration	C _o = reactor outlet concentration
r = reaction rate of species i	x = position in reactor
V = reservoir volume	t = time

For the case of dissolving solid material in the column and where the reactor can be assumed to be a well mixed system, i.e. the rate of reaction is independent of position, then the following can be written:

$$W(C_o - C_i) = \frac{dMg}{dt} \quad [35]$$

where Mg = mass solid Au in the reactor.

Equating expressions [34] and [35] reveals that the rate of change of concentration of the reservoir is proportional to the rate of gold dissolution in the reactor, and thus, the concentration behavior of the reservoir with respect to time reflects the gold recovery with respect to time and can be used to correlate the kinetic behavior of the different reaction conditions.

To model the adsorption of a species on activated carbon, the mass

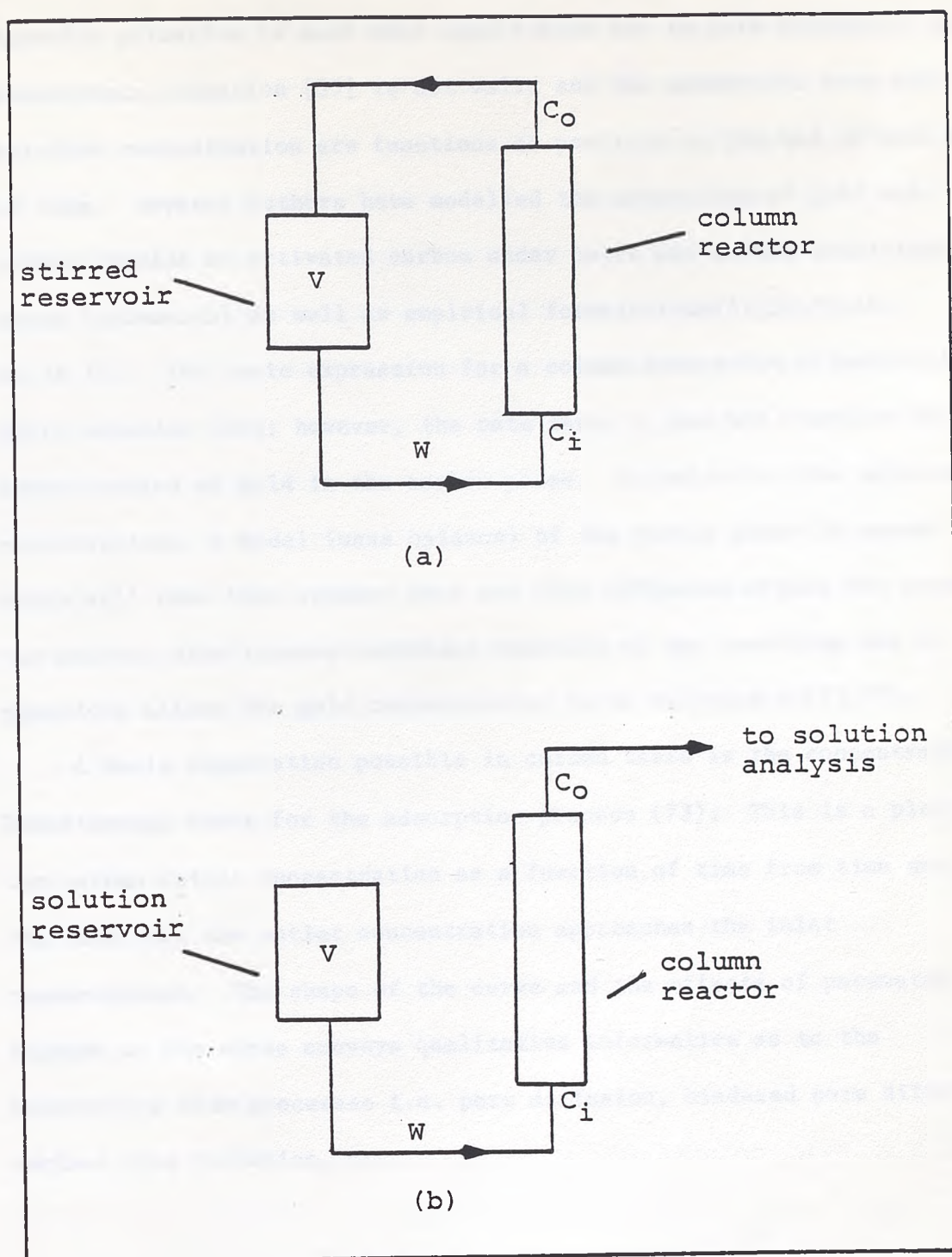


Figure 2. Flow regimes used in electrochemical and adsorption experiments: (a) recirculation mode with recycling working fluid, (b) nonrecirculating mode with a constant inlet composition - letter designations: V = reservoir volume, W = volumetric flowrate, C_i = column inlet concentration, C_o = column outlet concentration.

transfer situation is much more complicated due to pore diffusion; as a consequence, equation [35] is not valid and the adsorption rate and solution concentration are functions of position in the bed as well as of time. Several authors have modelled the adsorption of gold and silver cyanide on activated carbon under batch and column conditions using fundamental as well as empirical formulations (51,52,58,60, 61,74,75). The basic expression for a column adsorption situation is still equation [34]; however, the rate term, r , now will involve the concentration of gold in the carbon phase. To solve for the solution concentration, a model (mass balance) of the carbon phase is needed which will take into account pore and film diffusion within the pores of the carbon; simultaneous numerical solution of the resulting set of equations allows the gold concentration to be calculated (73,75).

A basic observation possible in column tests is the concentration breakthrough curve for the adsorption process (73). This is a plot of the column outlet concentration as a function of time from time zero to the time when the outlet concentration approaches the inlet concentration. The shape of the curve and the effects of parameter changes on the curve conveys qualitative information as to the controlling rate processes i.e. pore diffusion, hindered pore diffusion, surface film diffusion, etc.

MATERIALS AND EQUIPMENT

Materials and Reagents

The spectroscopic carbon used in the electrochemical cell was

originally obtained in the form of spectroscopic-grade graphite rods. These rods were crushed in a mortar and pestle and wet-screened to give a size distribution in the range of 180 to 425 micrometers; this approximate size distribution was shown previously to give sufficient electrical contact without undue backpressure (78). After screening, the sample was washed with deionized water followed by acetone and then dried at 100°C for one hour. The activated carbon material was obtained in the form of eight to sixteen mesh granules made from coconut shells and was supplied by Fisher Scientific. The eight to sixteen mesh activated carbon was prepared for use in the same manner as the spectroscopic carbon.

The surface areas of the activated carbon before and after preparation was determined by the B.E.T method using a Micromertics model 1200 Acusorb surface area analyzer. The outgassing step in the B.E.T. procedure which involved subjecting approximately 0.05 grams of sample to a temperature of 135°C to 140°C while under a vacuum of 10^{-4} torr resulted in a weight loss of 56.3 percent and 56.5 percent respectively for the prepared and unprepared material. The specific surface areas expressed in m^2/g based on the outgassed mass and initial mass for the 8 to 16 mesh carbon were $1514 \pm 73 \text{ m}^2/\text{g}$ and $852 \pm 41 \text{ m}^2/\text{g}$ respectively, and the same quantities for the prepared material (180 to 450 μm) were $1613 \pm 68 \text{ m}^2/\text{g}$ and $910.7 \pm 38 \text{ m}^2/\text{g}$ respectively. Average specific areas were computed based on the specific areas obtained from the adsorption and desorption isotherms.

Analysis of the activated carbon for impurities by subjecting the carbon to ashing, digestion, and finally inductively coupled plasma

analysis resulted in the composition shown in Table 1. The only notable impurity is potassium which apparently was not washed from the carbon.

The carbonaceous gold ore used in the experimental work was obtained from the Freeport Gold Mining Company (Battle Mountain, Nevada) in the form of minus 4 inch material. After crushing and grinding, the material was wet-screened to give a size fraction of 180 to 450 micrometers. After screening, the material was washed with deionized water and acetone and dried at 100°C for one hour. The U.S. Bureau of Mines inductively coupled plasma analysis is displayed in Table 2. The gold content of this ore was 0.25 oz/ton and the carbon content was 5.319 percent organic carbon and 6.060 percent total carbon.

The elemental gold used in dissolution experiments was obtained in semi-powder form and ground to give a powder consistency. All the atomic absorption standards were matrix matched and prepared from the gold complex under investigation. Anolyte, catholyte, adsorbate, and other miscellaneous solutions were generally made up from stock solutions of the appropriate species which were prepared using distilled, deionized, filtered, and deoxygenated water.

The reagents used in all solution preparations were ACS reagent grade and used as obtained from the manufacturer. The gold complexes of thiourea, thiocyanate, and thiosulfate were synthesized from HAuCl_4 according to procedures found in the literature (79-81). The cyanide complex was obtained from Johnson Matthey Co. as KAu(CN)_2 .

Equipment

1. Flow Cell and Pump System

The flow cell used in the electrochemical experiments and some of

Table 1. Inductively coupled plasma analysis of activated carbon

Element	ppm*	Element	ppm*
Al	370	Ba	5.6
Ca	520	Cr	6.9
Cu	27	Fe	600
K	0.59%	Mg	400
Mn	27	Na	730
Ni	4.6	Sn	21
Sr	5.0	Zn	110

* unless otherwise noted

the adsorption experiments is shown in Figure 3, while the flow regimes used are shown in Figure 2. The cell features a central cylindrical porous glass membrane (Vycor "thirsty" glass, Corning Glass Works) through which the anolyte flows and also contains the carbon working electrode (anode in all experiments except those involving electroelution) mixture. The volume exterior to the membrane and bounded by the outer lucite cylinder contains the catholyte solution which is continuously regenerated by pump lines entering through the top polyvinylchloride (pvc) cap. The membrane has a 0.7 centimeter outside diameter, a 0.5 centimeter inside diameter, and a length of 10. centimeters. The lucite shell has 3.8 centimeter outside diameter, a 3.1 centimeter inside diameter, and an internal volume of 73.5 cm³.

The membrane is held in place by a machined teflon plug threaded into the top pvc cap with a rubber O-ring seal made at the membrane-plug joint; the bottom seal is made directly into the bottom cap via a rubber

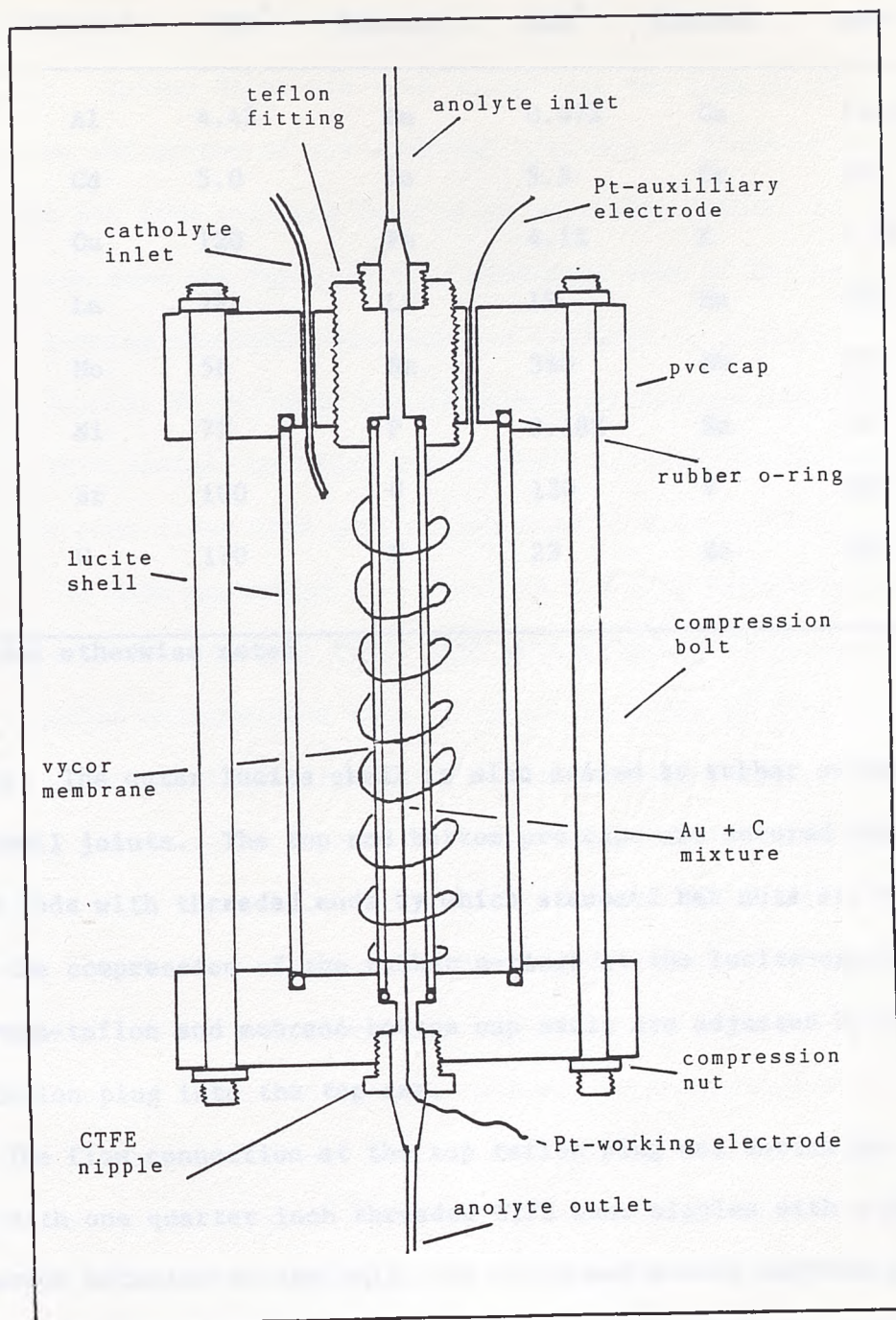


Figure 3. Cross-sectional view of electrochemical cell.

Table 2. Inductively coupled plasma analysis of Freeport gold ore

Element	ppm*	Element	ppm*	Element	ppm*
Al	4.4%	Ba	0.47%	Ca	13.2%
Cd	5.0	Co	5.5	Cr	170
Cu	120	Fe	4.1%	K	1.7%
La	28	Li	19	Mn	430
Mo	56	Na	360	Nb	85
Ni	77	P	0.18%	Sn	16
Sr	100	U	130	V	260
W	170	Y	23	Zn	190

* unless otherwise noted

o-ring. The outer lucite shell is also sealed by rubber o-rings at the cap-shell joints. The top and bottom pvc caps are secured together by brass rods with threaded ends by which standard hex nuts are used to vary the compression of the rubber o-rings at the lucite-cap joint. The membrane-teflon and mebrane-bottom cap seals are adjusted by advancing the teflon plug into the top cap.

The flow connection at the top teflon plug and bottom pvc cap is made with one quarter inch threaded CTFE Luer nipples with a male tube connector exterior to the cell; the inlet and outlet tubings are connected as the female fitting and sealed by heat-shrink tubing. The catholyte and anolyte inlet and outlet lines consisted of 0.5 millimeter inside diameter teflon tubing (Microline, Inc.) with the inlet lines adding solutions at the top of the cell, and the outlets removing fluids

from the bottom of the cell; thus, the cell was operated in the down-flow or "packed" mode as opposed to an "expanded" or "fluidized" mode (12). Cotton fiber was used to prevent any loss of the carbon bed at the top and bottom of the membrane tube due to fluid motion.

When the flow cell was used as an adsorbing column, the porous Vycor-glass tube was replaced by a nonporous tube of the same dimensions and the working electrode assembly was replaced by a simple Luer nipple.

An Ismatec 8-roller/40 rpm miniature peristaltic pump (Cole Parmer Company 7615 series) produced simultaneous anolyte and or catholyte flow; the pump lines used gave a flow rate of 4.5 or 2.8 milliliters per minute. In some experiments, a standard 3-roller Masterflex pump was used to deliver catholyte flow. All system tubing (less pump tubing) was of teflon construction with an inside diameter of 0.51 millimeters.

Flow-through (non-circulating) gold adsorption experiments involving small masses of carbon were performed using small pieces of tygon tubing as the column material. The small cell is depicted in figure 4. The adsorbing column consisted of a piece of Tygon No. R-3603 (0.4 mm I.D., 0.65 mm O.D.) tubing approximately 2 to 4 centimeters long which contained the given mass of carbon. At the outlet end of the tube, a filter assembly was made up of a piece of cotton fiber or teflon membrane situated between two pieces of silicon tubing (Masterflex No. 6424-13) with a 0.45 millimeter outside diameter which was compressed to fit inside the tygon tubing. Into the outer piece of silicon tubing protruded a section of 0.51 mm I.D. teflon tubing which was connected to the pump and flow-injection analysis system. The inlet end of the column simply had the Masterflex-teflon connection; the end joints were sealed with silicon sealant.

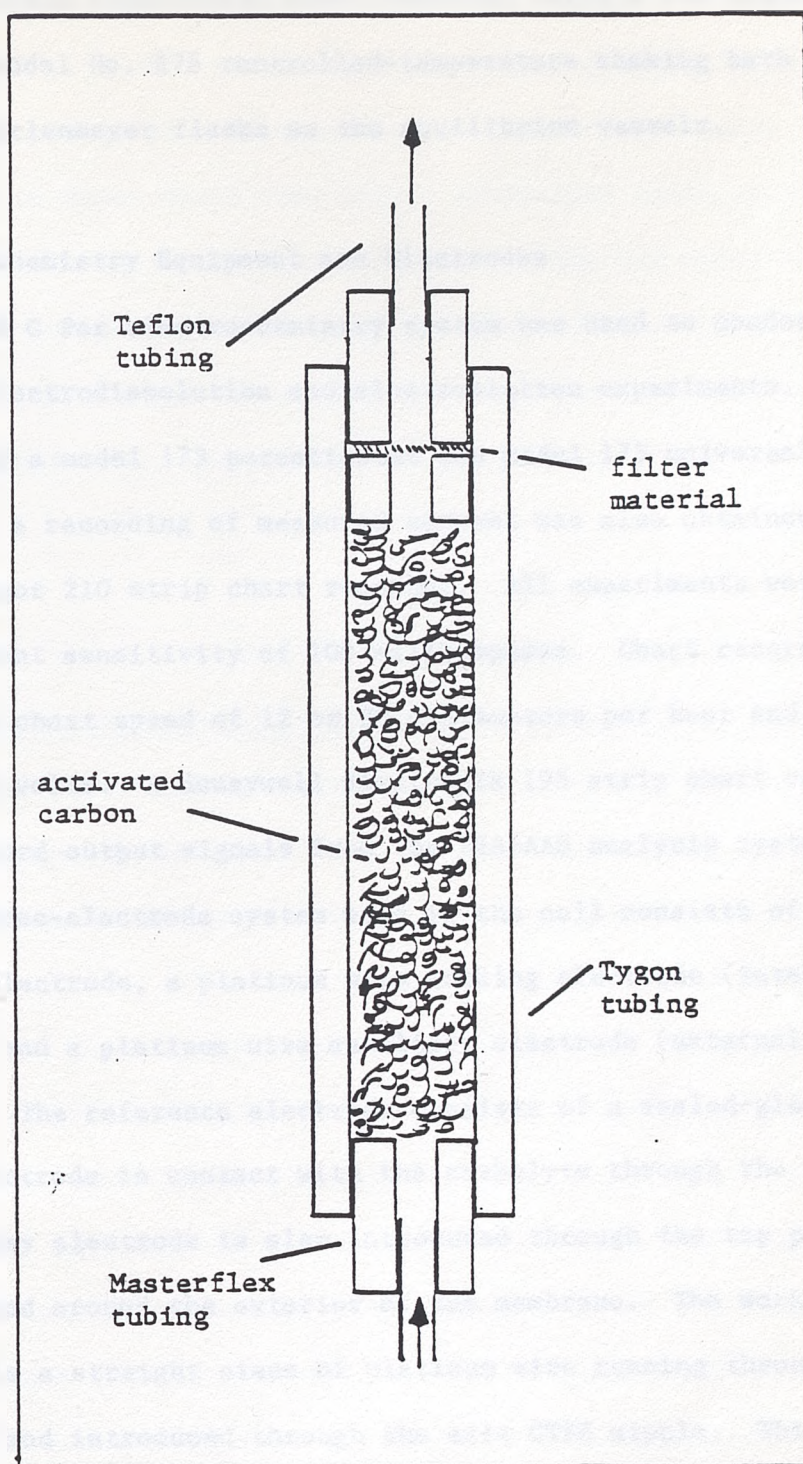


Figure 4. Cross-sectional view of small-tube flow-adsorption cell.

Equilibrium experiments were conducted using a New Brunswick Scientific model No. R76 controlled-temperature shaking bath using 125 milliliter Erlenmeyer flasks as the equilibrium vessels.

2. Electrochemistry Equipment and Electrodes

An EG & G Par electrochemistry system was used to conduct the flow-cell electrodisolution and electroelution experiments. The system consisted of a model 173 potentiostat and model 175 universal programmer; a recording of measured current was also obtained via a BBC Goere Servogor 210 strip chart recorder. All experiments were conducted with a current sensitivity of 100 milliamperes. Chart recordings were made with a chart speed of 12 or 30 centimeters per hour and an input span of 2.0 volts. A Honeywell Electronik 195 strip chart recorder was used to record output signals from the FIA-AAS analysis system.

The three-electrode system used in the cell consists of a Ag/AgCl reference electrode, a platinum wire working electrode (internal to the membrane), and a platinum wire auxiliary electrode (external to the membrane). The reference electrode consists of a sealed-glass membrane Ag/AgCl electrode in contact with the catholyte through the top cap. The auxiliary electrode is also introduced through the top pvc cap and loosely wound around the exterior of the membrane. The working electrode is a straight piece of platinum wire running through the carbon bed and introduced through the exit CTFE nipple. This is accomplished by precisely drilling a 2 millimeter hole through the side of the nipple and threading the platinum wire (1 millimeter diameter) through the hole; the hole then being sealed with liquid silicone sealant.

3. Flow-Injection Analysis Apparatus

The flow injection atomic absorption spectroscopy analysis system (FIA-AAS) consisted of a Tecator FIASTAR 5030 analyzer with the detector being a Perkin-Elmer Model 2280 atomic absorption spectrophotometer; the specifics of this unit are described below. The two modes of analysis are depicted in block diagram form in figure 5. The carrier fluid flow rate was 4.5 ml/min and the sample flow rate was 3 ml/min in regime (a) while for regime (b), the sample flow rate was either 4.5 ml/min or 2.8 ml/min.

ANALYTICAL PROCEDURE

Anodic Dissolution Experiments Using a Stock Gold/Carbon Mixture

In these experiments, where a stock supply of a mechanical gold/carbon mixture was used, both the solid and liquid phases were analyzed for gold content due to the inhomogeneity of the mechanical gold/carbon mixture. The liquid solutions (1ml aliquot diluted to 5 ml) taken from the flow system reservoir were analyzed using a Perkin-Elmer Model 2280 atomic absorption spectrophotometer utilizing a Perkin-Elmer hollow-cathode lamp (Intensitron No. 303-6031) operated at a continuous current of 10 milliamperes. All measurements were conducted at the 242.8 nanometer resonance line with a slit width of 0.7 nanometers; the aspiration rate was approximately 4.5 milliliters per minute. Matrix matching of standard solutions to sample solutions was instituted where possible, but no interferences were observed in the solutions used.

The procedure for sample measurement was as follows: After lamp and burner optimization, the standard solution (always 10 micrograms per

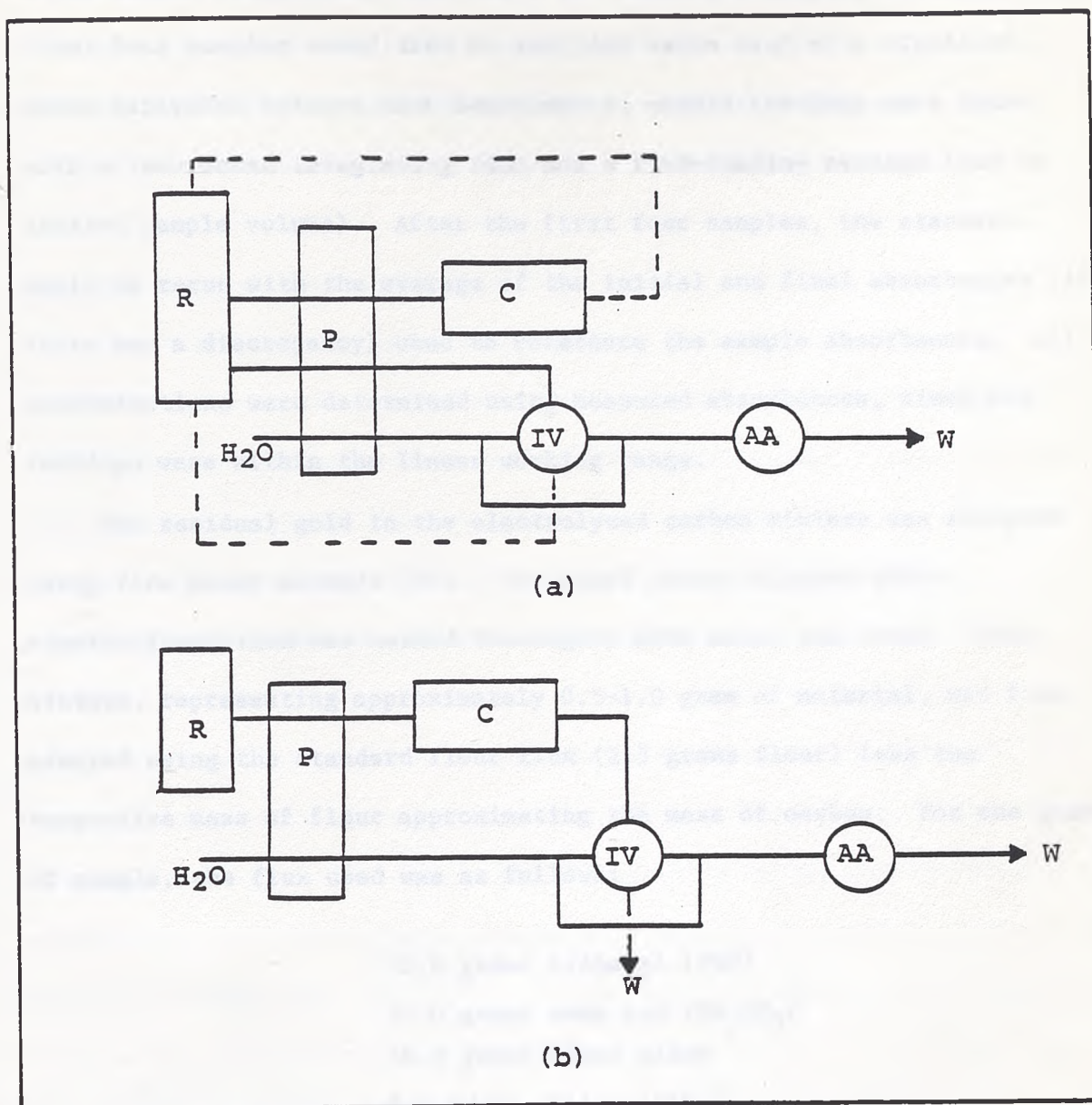


Figure 5. Electrolysis and adsorption flow regimes: (a) recycling working electrolyte or adsorbate solution, (b) nonrecycling fluid - letter designations: R = reservoir, P = pump, C = electrolysis or adsorption column, IV = injection valve, AA = atomic absorption, W = waste - dashed lines designate reservoir return lines.

milliliter) and a blank solution were aspirated to calibrate the spectrophotometer. The standard and blank solutions were measured with a two second integrating time and a ten reading-averaging sequence. The first four samples would then be analyzed twice each with distilled water aspirated between each measurement; sample readings were taken with a two-second integrating time and a five-reading average (due to limited sample volume). After the first four samples, the standard would be rerun with the average of the initial and final absorbances (if there was a discrepancy) used to reference the sample absorbances. All concentrations were determined using measured absorbances, since all readings were within the linear working range.

The residual gold in the electrolyzed carbon mixture was analyzed using fire assay methods (82). The final carbon mixture after electrodisolution was washed thoroughly with water and dried. This mixture, representing approximately 0.5-1.0 gram of material, was fire assayed using the standard flour flux (2.5 grams flour) less the respective mass of flour approximating the mass of carbon. For one gram of sample, the flux used was as follows:

- 70.0 grams litharge (PbO)
- 30.0 grams soda ash (Na_2CO_3)
- 10.0 grams borax glass
- 5.0 grams silica (SiO_2)
- 1.5 grams flour

The sample was thoroughly mixed with the flux and one Herman's inquart of silver (approximately 1.92 milligrams) in a fire clay crucible and

then covered with a layer of borax glass. The mixture was fused for one hour at 1050°C after which cupellation of the resulting lead button was conducted for one hour also at 1050°C . After cupellation, the dore bead was parted in concentrated nitric acid to leave a gold-black which after washing and annealing left the gold button. This button was then weighed to the nearest 0.01 milligram.

On-Line Flow-Injection Analysis

The liquid phases alone were analyzed in experiments using specifically prepared gold/carbon electrodes since accurate initial and final quantities of gold were known without final solid analysis. In all experiments except the premixed-gold electrodisolutions, the gold content of liquid samples was determined by flow injection-atomic absorption spectroscopic analysis (FFA-AAS).

The aqueous gold concentration in experiments with a recycling solution was monitored with respect to gold concentration with the FIA system continuously circulating sample solution through its sample loop (regime (a), figure 5). The gold concentration in the non-recirculating experiments was monitored by continuously passing the outlet column solution through the FIA system with the solution continuing on to waste (regime (b), figure 5).

In all experiments involving the FIA-AAS system of analysis, standard solutions in concentrations from five to fifty ppm were initially analyzed and generally reanalyzed every one-half hour of operation to reference the sample peaks; if drift in the gold-standard signals with respect to time was observed, these were compensated for by

linearizing the changes with time and incorporating the linearized time dependence into the concentration expressions. The measured signal from the FIA-AAS system was the peak height recorded by the Honeywell strip-chart recorder of the continuous output voltage from the atomic absorber. The output from the atomic absorber (0-10 mV) could be amplified or attenuated by adjusting the recorder span (1 mv to 5 V); for most experiments, a span of 1, 5, or 10 mV was used.

The sample concentrations were computed by assuming a linear absorptance dependence on concentration between standard solutions with the concentration differences in standard solutions generally 10 ppm; in cases where only one standard was available, linear behavior was assumed up to that particular standard concentration. Generally it was found that the FIA system of analysis broadened the linear absorbance range for gold to 50 ppm.

Solutions from equilibrium experiments were analyzed using the FIA-AAS system as described for the non-equilibrium experiments.

EXPERIMENTAL PROCEDURE

Working Electrode Preparation

The working electrode material was either a stock mechanical mixture of elemental gold and carbon, a specific mass of gold and carbon that was mechanically mixed, or a sample of activated carbon with a known concentration of adsorbed gold (from cyanide solution).

The stock mixture of gold and spectroscopic carbon was made to give a 1 percent (w/w) gold concentration and was made by mixing, in a container, 0.1000 grams gold with 9.900 grams spectroscopic carbon.

The specific mass mixture of gold and carbon (spectroscopic or activated carbon) consisted of individually measured masses of gold and carbon prepared for each experiment (generally 11.0 mg Au and 0.72 to 1.1 g carbon).

The activated-carbon with adsorbed gold was prepared by equilibrating a known mass of activated carbon and a known mass of KAu(CN)_2 in an appropriate volume of 0.1 M NaCN, 10^{-4} M KOH solution. The equilibration period was approximately four days after which the mixture was filtered and washed with H_2O . The filtrate volume was then recorded, the concentration of gold in the solution determined by FIA-AAS, the loaded carbon dried in air and finally stored in a glass container. The concentration of adsorbed gold was determined by difference between the initial gold present and the final gold in solution.

Solution Preparation

The anolyte and catholyte solutions were made from stock solutions of electrolyte and the solid ligand salt to be used. These solutions were generally made the day of use except for cyanide and thiourea solutions which were made up as stock ligand/electrolyte solutions. The initial series of premixed gold/carbon dissolutions used NaClO_4 as the supporting electrolyte in both the anolyte and catholyte. All other electrochemical experiments used NaCl as the supporting electrolyte for anolyte and catholyte solutions. All adsorbate solutions were prepared within 48 hours of use.

Assembly of Electrochemical Cell

The first requirement for operation of the electrochemical cell is the preconditioning of the porous glass membrane. This was accomplished by soaking the membrane in supporting electrolyte two days prior to first use and thereafter storing the membrane in supporting electrolyte.

After preconditioning, the flow cell was assembled except for the top cap; thus, with the working electrode and bottom o-ring in place, a small piece of wetted cotton was placed at the bottom of the membrane. Using a small funnel adapted to the membrane's inner diameter, the carbon mixture was fed to the top of the membrane. After filling to approximately 4 mm below the top of the membrane, a small piece of wetted cotton was placed on top of the bed. The prewound auxiliary electrode was then placed around the membrane and the external lead-end threaded through the top cap. The top cap was then set into place with the compression rods in place and the lucite-pvc joint made; finally the top of the membrane was guided into the bottom slot of the top teflon plug which was then advanced into the pvc cap. Before tightening the teflon plug onto the membrane, the lucite-pvc seal was made by tightening the compression rods to their final position-the teflon plug then being advanced to give a solution-tight seal at the membrane-teflon joint. The cell was then connected to the rest of the flow system and the pump tubes for catholyte flow inserted into the cell.

Adsorption cell/tube assembly

The experimental procedure for all packed-column adsorption experiments was essentially the same whether the electrochemical cell

(less electrodes and porous membrane) or tygon tube assemblies were used. The first step entailed loading the electrochemical cell column or small tygon-tubing column with the activated carbon and assembling the cell or sealing the tygon tube with connecting-tubing in place. The column arrangement was then connected to the flow configuration to be used (recycling, non-recycling).

General Operating Procedures

1. Recycling Electrodissolutions and Electroelutions.

After system assembly, the working electrode solution was circulated for two to five minutes prior to applying the selected voltage to the electrode system; the instant of potential application was time-zero on the experiment-time scale. At selected intervals, reservoir sampling was conducted either by the manual method of 1 ml aliquots into 5 ml volumetric flasks or the automatic (push button) FIA method where 200 microliters of reservoir solution was sent to the atomic absorption unit. Accumulated charge passed by the working electrode was recorded at selected times. At the conclusion of the experiment, the carbon residue was removed from the column, washed with water and dried; in experiments using the fire assay procedure, fire assaying of the final dried carbon was performed.

2. Column Adsorption Experiments

After the system was prepared for operation, the adsorbate solution was passed through the column either to the reservoir (recycling) or the FIA-AAS system (non-recycling); zero on the experiment time scale was taken as when the solution entered the column. At specified times,

adsorbate concentration was monitored via the FIA-AAS system. In certain experiments, distilled water was passed through the columns at the conclusion of the adsorption experiments to observe the water-eluting behavior of the adsorbate.

RESULTS

Premixed Gold/Carbon Electrodissolutions

The gold compositions of the liquid samples and final solid residues were used to determine first the initial gold present and then the percent extraction of gold from the carbon bed with respect to time. To accomplish this the final mass fraction of gold determined by fire assay data were used in conjunction with the solution analysis to calculate the initial gold present. The mathematical formulation required follows:

From a gold mass balance on the carbon bed, reservoir solution, and liquid samples, the following results,

$$Mg_t = Mg_i = Mg_b + Mg_r + Mg_a \quad [36]$$

where: Mg_t = total gold in the system at any time

Mg_i = initial mass of gold present

Mg_b = mass of solid gold in the bed at time, t

Mg_r = mass of gold in the reservoir at time, t

Mg_a = accumulated mass of gold in the liquid samples removed

It also follows that,

$$Mg_b = M_b X_g \quad [37]$$

$$Mg_r = C_r V_r \quad [38]$$

$$Mg_a = V_a \sum_{n=1}^j C_n \quad [39]$$

where: M_b = total mass of bed at time, t

X_g = mass fraction of gold in the bed at time, t

C_r = gold concentration in reservoir solution at time, t

V_r = reservoir solution volume at time, t

C_n = gold concentration in n^{th} analysis sample

V_a = analysis sample volume

j = sequential number of sample taken at time t ($j = 1, 2, \dots$)

Substituting these expressions into equation [36] results in the following:

$$Mg_i = M_b X_g + C_r V_r + V_a \sum_{n=1}^j C_n \quad [40]$$

An overall mass balance gives,

$$M_b = M_i - Mg_r - Mg_a \quad [41]$$

with M_i being the total initial bed mass. Substituting equation [41] into equation [40] along with equations [38] and [39] yields:

$$Mg_i = M_i - C_r V_r - X_g V_a \sum_{n=1}^j C_n + C_r V_r + V_a \sum_{n=1}^j C_n \quad [42]$$

or

$$Mg_i = X_{gf} M_i + V_{rf} C_{rf} + (X_{gf} V_a \sum_{n=1}^j C_n)(1 - X_{gf}) \quad [43]$$

where the subscript f designates final conditions.

The results of using equation [43] in conjunction with the experimental data are displayed in table II located in appendix B.

The percent dissolution versus time was calculated by using concentration data, solution volume data, and total initial gold data in the expression:

$$D_j = \frac{(C_j(V_{ro} - j) + v_a \sum_{n=1}^j C_n)100}{Mg_i} \quad [44]$$

where: D_j = percent dissolution at the j^{th} sample

V_{ro} = initial reservoir solution volume

The graphical results of the percent dissolution data are presented in figures 6 and 7; the atomic absorption data are given in appendix A, while the fire assay data and results are given in Tables 1 and 2 in appendix B.

Specific Gold/Carbon Electrodissolutions

These electrodissolution experiments involved a known initial mass of gold and known mass of spectroscopic or activated carbon, and all sample analysis was done via the FIA-AAS system of analysis. Thus, the percent dissolution is given by,

$$D_j = \frac{(C_j V_{ro} + v_a \sum_{n=1}^j C_n)100}{Mg_i} \quad [45]$$

where the variables are as designated earlier with the aliquot volume

now that of the FIA sample loop (always 200 microliters). It should be noted that using the FIA-AAS system in the recirculating mode does not decrease the solution volume since an equal volume of carrier solution is carried to the solution reservoir in place of the sample volume.

The results for percent dissolution or solution concentration versus time for specifically mixed carbon/gold dissolutions are depicted graphically in Figures 8 through 13. In some of these figures, data from the previously mentioned dissolutions are presented as well for comparative purposes. The raw data, calculated concentrations, and calculated percent dissolution are given in Tables 1 through 9 in appendix C.

Recycle and Non-Recycle Electroelutions

In these four experiments, a mass of gold-loaded activated carbon (gold adsorbed from CN^- media) was used as the working electrode in the electrochemical cell and the gold eluted by applying a negative potential to the carbon while passing a solution through the cell. At the time of these experiments, problems in loading the working electrode part of the cell resulted in only final electrolyzed masses being determined. Thus, it was necessary to again calculate the initial gold present. For the recycling experiments, the following relation was used:

$$Mg_1 = Xg_1 M_1 \quad [46]$$

The initial mass was calculated from the final mass plus the mass of the gold eluted assuming it was present as $\text{KAu}(\text{CN})_2$. Thus,

$$M_i = M_f + SMg_e \quad [47]$$

where: M_f = final total mass

S = stoichiometric conversion factor (mg gold to mg $\text{KAu}(\text{CN})_2$)

Mg_e = mass of gold eluted

A mass balance for the eluted gold yields,

$$Mg_e = (V_r C_j + V_a \sum_{n=1}^j C_n) 100 \quad [48]$$

Thus, the following results for the initial gold present:

$$Mg_i = X_{gi} (M_f + V_a C_{jf}) + V_a \sum_{n=1}^j C_n) 100 \quad [49]$$

The correction for the eluted gold mass to the final mass measured was less than 2.5 percent, but since it was readily estimated, the correction was made.

The calculation of percent recovery is similar to the calculation of percent dissolution in recycling dissolution experiments:

$$R_j = \frac{(V_r C_j + V_a \sum_{n=1}^j C_n) 100}{Mg_i} \quad [50]$$

The gold loading in mg Au/g carbon is given by,

$$Q(t) = Q(t=0) - \frac{Mg_e(t)}{M_c} \quad [51]$$

where M_c is the mass of activated carbon and the expression " (t) "

designates a functional time dependence.

For non-recycling electroelution experiments, a similar development applies except the total mass eluted at any given time is the integral of the column outlet solution concentration as a function of time. A gold mass balance on the carbon column yields,

$$W(C_o - C_i) = \frac{dMg_e}{dt} \quad [52]$$

where : W = volumetric flow rate

C_o = column outlet concentration

C_i = column inlet concentration

With an inlet concentration of zero and a zero initial condition for Mg_e , the following results:

$$Mg_e(t) = W \int_0^t C_o dt \quad [53]$$

Thus, integration from time zero to the final time gives the total mass eluted:

$$Mg_e(t=f) = W \int_0^{t=f} C_o dt \quad [54]$$

The total mass of eluted gold to correct the final measured mass is given by,

$$Mg_i = X_{gi}(M_f + SW \int_0^{t=f} C_o dt) \quad [55]$$

The percent recovery at any given time readily follows:

$$R(t) = \frac{Mg_e(t)100}{Mg_i} = \frac{100W \int_0^t C_o dt}{Mg_i} \quad [56]$$

The gold loading as a function of time is given by,

$$Q(t) = Q(t=0) - \frac{W \int_0^t C_o dt}{M_c} \quad [57]$$

The integration of concentration is readily accomplished by the use of the trapazoidal rule of integration, namely:

$$\int_a^b f(x) dx = \frac{\Delta x}{2} \sum_{k=1}^n C_o + 2C_k + \dots + 2C_{n-1} + C_n \quad [58]$$

Applying this to the gold concentration integral the following results:

$$Mg_e(t_j) = \frac{W\Delta t}{2} \sum_{k=1}^j C_o + 2C_k + \dots + 2C_{j-1} + C_j \quad [59]$$

The graphical results for the four electroelution experiments conducted are displayed in Figure 14 through 20 while the raw data, calculated concentrations, percent recovery results, and gold loading results are displayed in Tables 1 through 4 in appendix D.

Flow Cell and Small Tube Adsorption Experiments

It was determined through experiment that the outlet concentration of $AuCl_4^-$, $Au(SCN)_2^-$, $[Au(SC(NH_2)_2)_2]^+$, and $Au(CN)_2^-$ adsorption experiments utilizing the electrochemical cell was very nearly zero for

the greater part of the experiment, and since these experiments were to compare the adsorption of the different gold complexes, only the final portions of the experiments would possibly be of any value. Thus, the graphical displays of the concentration time behavior for these experiments is referenced to a model of the recycling experiments with a zero column outlet concentration. The mass balance on the well-mixed reservoir already presented (equation [34]) yields,

$$W(C_o - C_i) = -V \frac{dC_i}{dt} \quad [34]$$

Integrating this expression with $C_o = 0$ and $C_i(t=0) = C_{i0}$ gives,

$$C_i(t) = C_{i0} \exp^{-(t/\tau)} \quad [60]$$

where $\tau = V/W$ is the reservoir residence time. Using calculated residence times in this expression, the predicted concentration has been plotted with the experimental concentration results which are displayed in figures 21 through 22; the raw data for these experiments is tabulated in appendix E.

Two experiments were conducted with the flow cell in the recycling mode with the Freeport carbonaceous ore sample as the adsorbent and $\text{Au}(\text{CN})_2^-$ as the adsorbate. The graphical representation of the reservoir concentration as a function of time is displayed in figure 23. The two concentrations of Au were 37.5 and 10.0 ppm with respective ore masses of 2.1213 grams and 2.1964 grams. The experimental data with calculated results are tabulated in tables 1 and 2 in appendix F.

The results of two non-recirculating adsorption experiments involving the adsorption of $\text{Au}(\text{CN})_2^-$ on the Freeport carbonaceous sample in the presence of sodium chloride and calcium chloride are displayed in figure 27; the inlet gold concentration for each experiment was 10.0 ppm; the respective masses of carbonaceous ore for the NaCl and CaCl_2 experiments were 1.9592 and 1.8932 grams; the raw data and calculated results are tabulated in tables 3 and 4 in appendix F.

Figures 25 to 28 display the outlet concentration as a function of time for the non-recirculating adsorption experiments using 0.1000, 0.0500, and 0.0100 grams of activated carbon for $[\text{Au}(\text{SC}(\text{NH}_2)_2)_2]^+$, $\text{Au}(\text{SCN})_2^-$, and $\text{Au}(\text{CN})_2^-$, and 0.1000 grams for the single experiment involving $\text{Au}(\text{S}_2\text{O}_3)_2^{-3}$; these experiments were conducted in the small tygon columns. Plotted in figures 29 and 30 are the calculated average gold loadings as a function of time for the small-column adsorptions of $[\text{Au}(\text{SC}(\text{NH}_2)_2)_2]^+$ and $\text{Au}(\text{CN})_2^-$ on activated carbon. The computation of the gold loading is similar to the calculation of the mass gold eluted for the non-recirculating electroelution (equation [53]). A mass balance on the small column yields:

$$W(C_i - C_o) = M \frac{dQ}{cdt} \quad [61]$$

Integrating this expression with an initial gold loading of zero and a constant inlet composition of C_i gives,

$$Q(t) = \frac{W}{M} \int_0^t (C_i - C_o) dt \quad [62]$$

Using the trapazoidal rule of integration (equation (58)) yields:

$$Q(t) = \frac{W\Delta t}{2M_c} \sum_{k=1}^j C_0 + 2C_k + \dots + 2C_{j-1} + C_j \quad [63]$$

Plotted in figures 31 and 32 are the concentration versus time profiles for the deionized water elution of gold following adsorption for the above mentioned experiments involving adsorption of $[\text{Au}(\text{SC}(\text{NH}_2)_2)_2]^+$ and $\text{Au}(\text{CN})_2^-$ on activated carbon in the small columns; the percent recovery of $\text{Au}(\text{CN})_2^-$ is also plotted in these figures. The two plots of the eluting behavior of the gold complexes on 0.0100 g (figure 31) and 0.0500 g (figure 32) of activated carbon represent the column-outlet gold concentration where the water-eluting solution was passed through the column immediately after stoppage of adsorbate delivery. The experimental data is presented in appendix G.

Equilibrium Adsorption Experiments

Figure 37 contains the results of the equilibrium experiments for $\text{Au}(\text{CN})_2^-$, $\text{Au}(\text{SCN})_2^-$, and $[\text{Au}(\text{SC}(\text{NH}_2)_2)_2]^+$ adsorption on the activated carbon sample at a 0.1 M concentration of the respective ligand and 0.1 M HCl for the thiourea data; the correlation parameters to the Freundlich equation are displayed in this figure. Tables 3 and 4 give the equilibrium adsorption results for adsorption of $[\text{Au}(\text{SC}(\text{NH}_2)_2)_2]^+$ and $\text{Au}(\text{CN})_2^-$ on the Freeport gold-ore sample under the same solution conditions as the equilibrium experiments with activated carbon. Table 5 contains the results of $\text{Au}(\text{SCN})_2^-$ adsorption on activated carbon with respect to pH.

DISCUSSION

Anodic Dissolutions in Spectroscopic Carbon

The initial set of results for anodically dissolving elemental gold from the porous electrode of spectroscopic carbon indicated that the rate of dissolution closely followed the order of the respective gold-complex stability except for the thiosulfate ligand $S_2O_3^{2-}$. The initial conditions of these experiments were kept constant with respect to initial pH (pH=11), ligand concentration (0.1M) and applied potential (1.2 V vs Ag/AgCl). The pH dropped in all of these experiments except for the cyanide dissolution (figure 6) using NaCl as the supporting electrolyte; the pH increased slightly in this experiment due to oxidation of Cl^- to Cl_2 and subsequent hydrolysis to HClO.

The cyanide media (figure 6) exhibited the most rapid anodic dissolution kinetics with nearly complete dissolution in 30 to 40 minutes. The switch from perchlorate to chloride ion in the supporting electrolyte should have had little effect under these conditions, since the chloride or perchlorate complex is not nearly as stable as the cyanide species. The results indicate a slight kinetic increase with the change and the overall higher recovery with the chloride solution as will be seen later could be due to errors in the overall gold mass balance; one hundred percent dissolution should have been achieved.

In these two experiments, the initial current was approximately 170 milliamperes which decayed linearly with time. The slope of this decay was greater in the chloride media than the perchlorate media which is possibly due to the differences in the fluxes of chloride ions, hydroxide ions, and protons through the porous membrane; the net effect

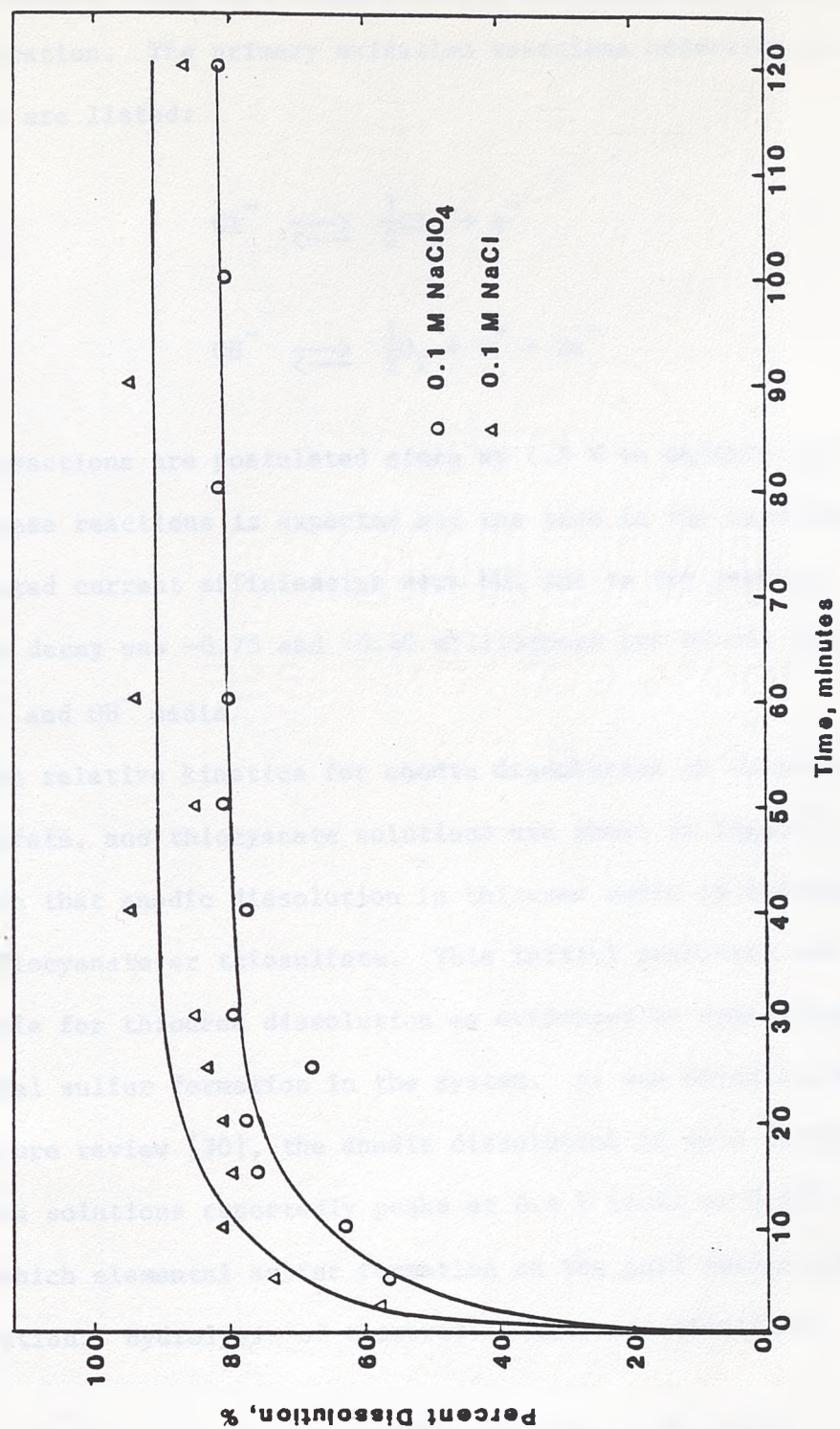
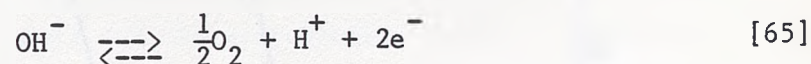
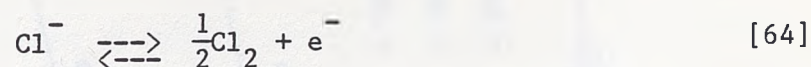


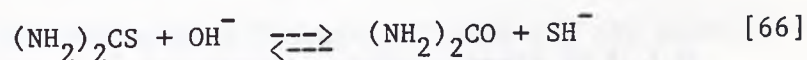
Figure 6. Percent dissolution as a function of time for the anodic dissolution of gold from a spectroscopic carbon matrix in 0.1 M KCN solution at an applied potential of 1.2 V.

concentration drops more rapidly in the anolyte than the hydroxide concentration. The primary oxidation reactions occurring at 1.2 V vs Ag/AgCl are listed:



These reactions are postulated since at 1.2 V vs Ag/AgCl gas evolution from these reactions is expected and was seen in the experiments and the calculated current efficiencies were but one to two percent. The current decay was -0.75 and -0.40 milliamperes per minute respectively for Cl^- and OH^- media.

The relative kinetics for anodic dissolution in thiourea, thiosulfate, and thiocyanate solutions are shown in figure 7 and indicate that anodic dissolution in thiourea media is moderately faster than thiocyanate or thiosulfate. This initial condition was not favorable for thiourea dissolution as evidenced by considerable colloidal sulfur formation in the system. As was noted in the literature review [30], the anodic dissolution of gold in acidic thiourea solutions reportedly peaks at 0.4 V (SHE) or 0.205 vs Ag/AgCl after which elemental sulfur formation on the gold surface inhibits dissolution. Hydrolysis of thiourea to urea and bisulfide,



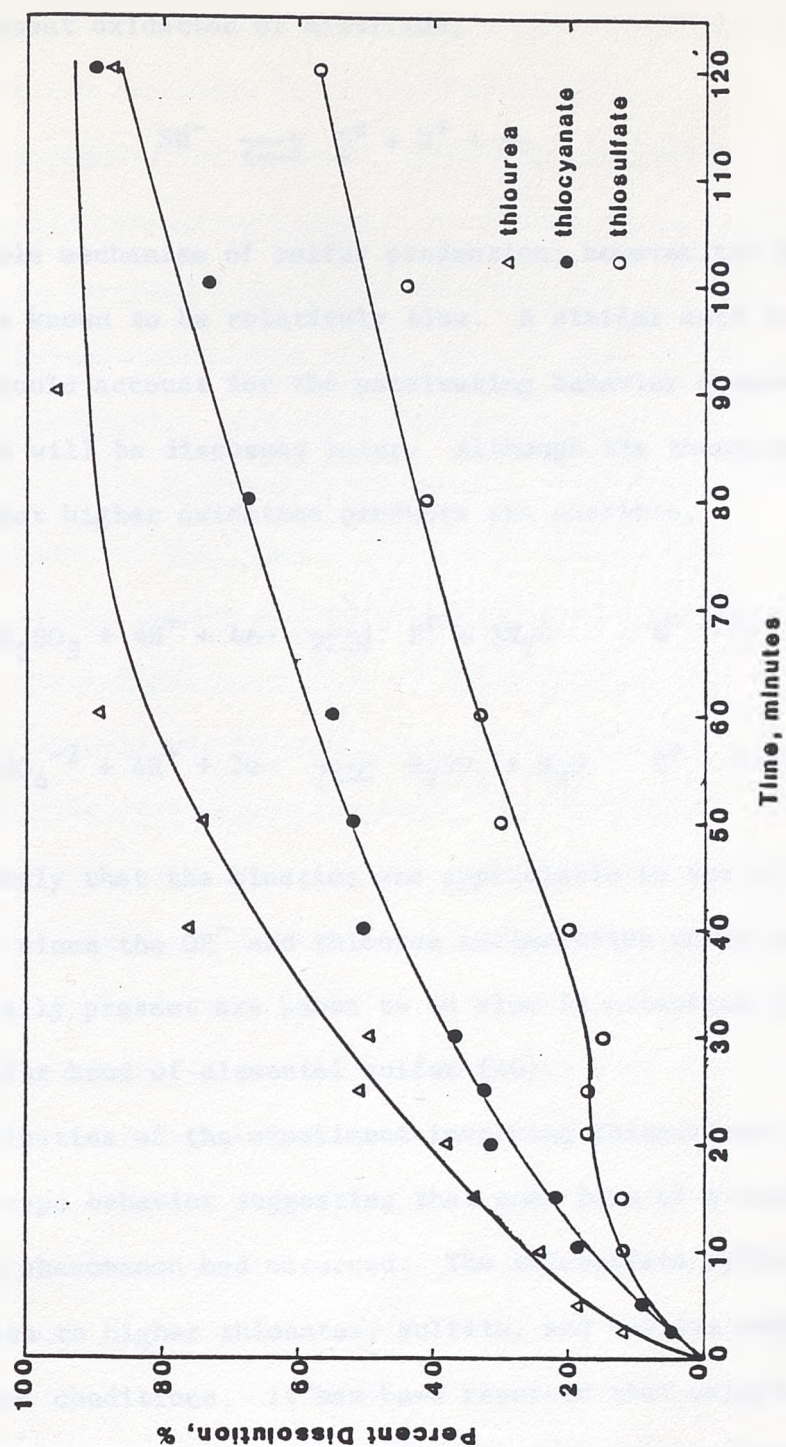
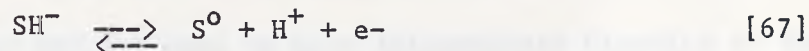
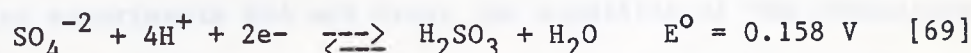
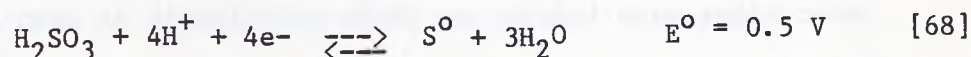


Figure 7. Percent dissolution as a function of time for the anodic dissolution of gold from a spectroscopic carbon matrix in 0.1 M thiourea, thiosulfate, and thiocyanate solutions at an applied potential of 1.2 V.

with subsequent oxidation of bisulfide,



is a possible mechanism of sulfur production; however, the hydrolysis reaction is known to be relatively slow. A similar acid catalyzed mechanism could account for the passivating behavior observed in acidic media which will be discussed later. Although the thermodynamics indicate that higher oxidation products are possible,



It is unlikely that the kinetics are appreciable in the present solutions, since the OH^- and thiourea nucleophiles which are the only ones initially present are known to be slow in attacking the sulfur-sulfur bond of elemental sulfur (40).

The kinetics of the experiment involving thiosulfate ion exhibited a plateau-type behavior suggesting that some form of a reaction inhibiting phenomenon had occurred. The thiosulfate system lends itself to oxidation to higher thionates, sulfite, and sulfate under the experimental conditions. It has been reported that oxidation of thiosulfate on the gold surface under chemical dissolution leads to passivation by elemental sulfur (39) and is a possible explanation for the slow and multimodal kinetics found here. The current behavior for the thiosulfate ligand was different from other electrodisolutions in

that it was nearly constant at 160 milliamperes which may be attributable to the oxidation reactions involving thiosulfate.

The thiocyanate ion was seen to give intermediate kinetics to that of thiourea and thiosulfate (figure 7). Following approximately fifty minutes of an apparent logarithmic behavior, the kinetics for this experiment became near-linear with a rate of approximately 65 micrograms per minute. The anodic oxidation of SCN to CN^- is probable from reports in the literature on its ease of anodic oxidation (7,23). This could lead, if the kinetics of SCN^- oxidation were rapid enough, to a reduced rate of dissolution after an initial more rapid rate.

Since the initial conditions of dissolution in the thiourea and thiocyanate experiments did not favor the stability of the respective solution species, experiments in acidic and neutral solutions respectively were conducted. In the case of thiourea, the electrodisolution was conducted under the conditions of 0.1 M thiourea, 0.1 M HCl, and a potential of 0.5 V vs Ag/AgCl; it was undesirable at this point using the flow-injection system to have colloidal sulfur formation so the lower potential was used. The percent recovery is plotted in comparison to the initial experiment in figure 8.

This figure indicates a similar kinetic behavior in the two experiments and considering the differences in the experimental conditions with respect to pH and potential, two rate limiting processes are evident. Firstly, the rate of dissolution at potentials above 0.5 V vs Ag/AgCl is controlled by diffusion of thiourea to the surface or diffusion of $[\text{Au}(\text{SC}(\text{NH}_2)_2)_2]^+$ from the surface, and secondly, the rate of dissolution is controlled by the rate of diffusion of reactants or

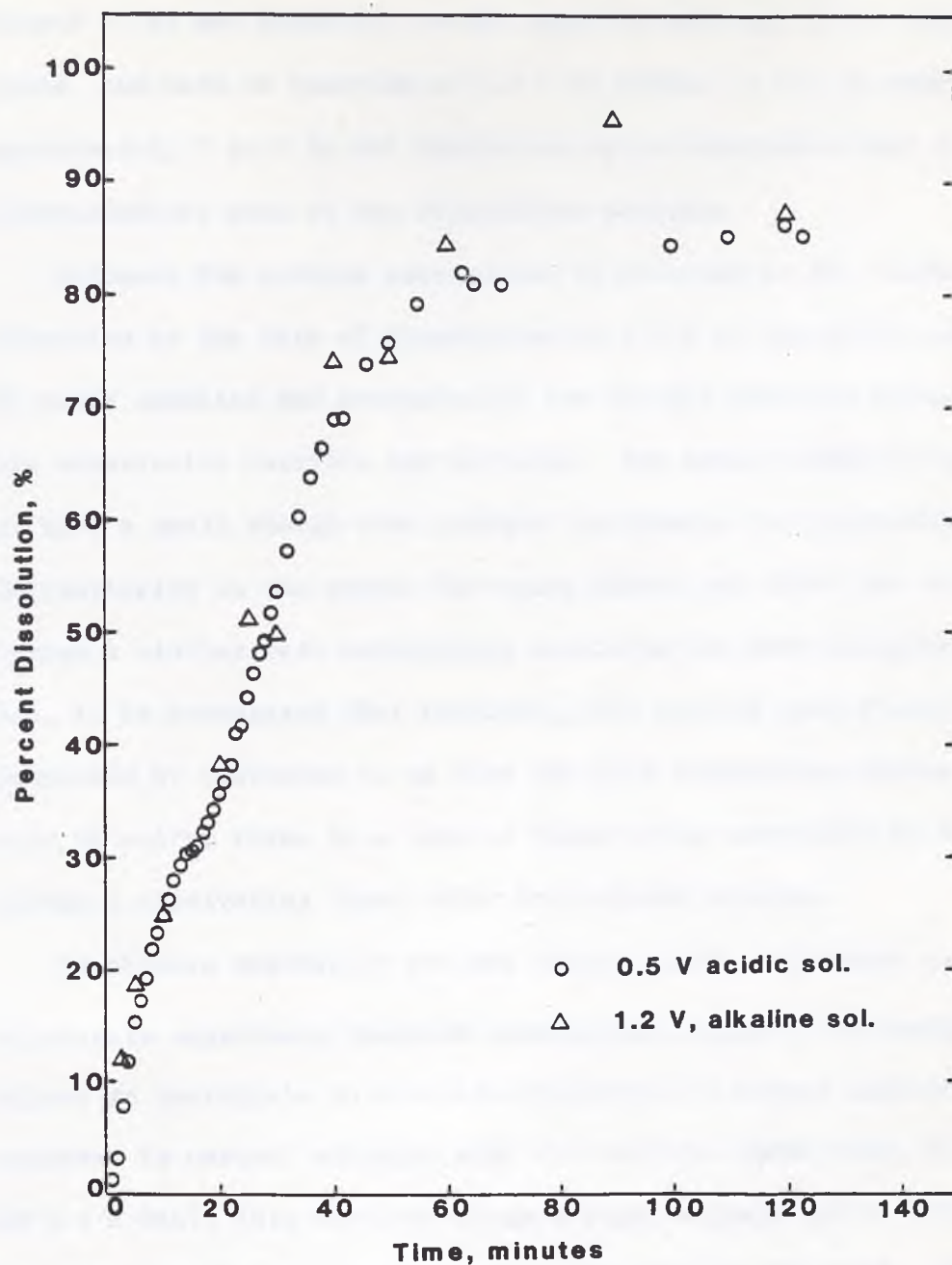


Figure 8. Percent dissolution as a function of time for the anodic dissolution of gold from a spectroscopic carbon matrix in acidic and alkaline 0.1 M thiourea solutions at 0.5 and 1.2 V respectively.

products through a passivating layer of sulfur at the gold surface.

These conclusions are based on the supposition that unless the effects of pH and potential on the reaction rate are of an inverse nature, the rate of reaction at 0.5 V or higher in the pH range of approximately 1 to 7 is not controlled by an adsorption step or an electrochemical step in the dissolution process.

Evidence for surface passivation is observed in the slight inflection in the rate of dissolution at 0.5 V in the acidic solution. The rapid sampling and precision of the FIA-AAS analysis system makes this observation possible and reliable. The manual sampling method does not have a small enough time interval to observe the passivation, but the similarity in the curves for times before and after the inflection implies a similar rate controlling mechanism for each dissolution. Thus, it is postulated that initially, the rate of gold dissolution is controlled by diffusion to or from the gold surface but shifts as a layer of sulfur forms to a rate of dissolution controlled by diffusion through a passivating layer which is a slower process.

To observe whether or not the initial basic conditions in the first thiocyanate experiment hindered dissolution ($\text{Au}(\text{SCN})_2^-$ is unstable with respect to hydrolysis in alkaline solutions), a second experiment was conducted in neutral solution with the solution conditions, 0.1 M KSCN, and 0.1 M NaCl; this resulted in an initial solution pH of 6.38. The comparison of the two experiments is displayed in figure 9. The results of this comparison are somewhat unexpected in that the initial lower pH did not improve the kinetics but showed an opposite effect. The similarity in the curves suggests similar rate determining processes and

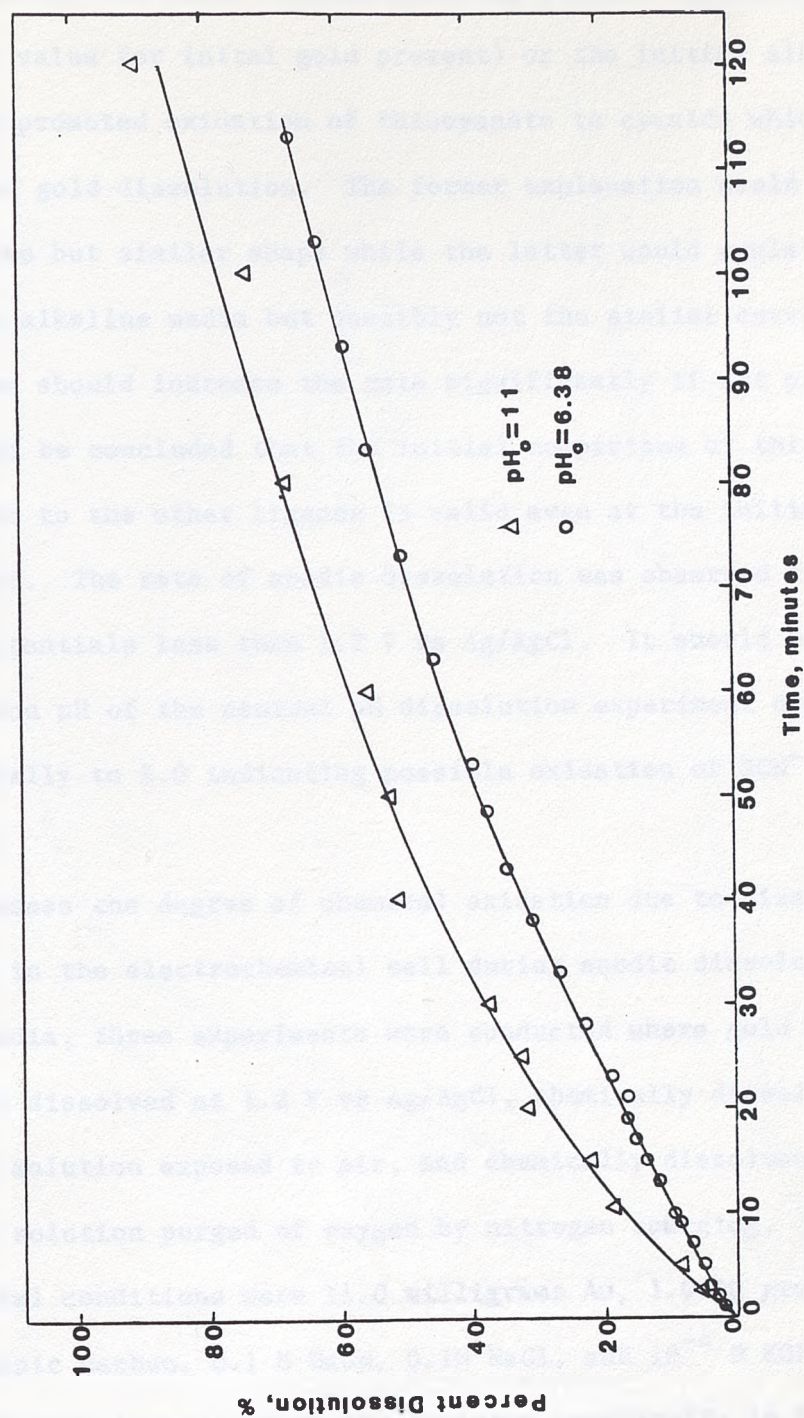


Figure 9. Percent dissolution as a function of time for the anodic dissolution of gold from a spectroscopic carbon matrix in neutral and alkaline thiocyanate solutions at an applied potential of 1.2 V.

two possible explanations for these results can be formulated: The fire assay result of the final residue from the initial experiment is in error (low value for initial gold present) or the initial alkaline conditions promoted oxidation of thiocyanate to cyanide which accelerated gold dissolution. The former explanation would explain the higher curve but similar shape while the latter would explain the higher results in alkaline media but possibly not the similar curve shapes as cyanide ion should increase the rate significantly if not protonated. But, it can be concluded that the initial comparison of thiocyanate dissolution to the other ligands is valid even at the initially high solution pH. The rate of anodic dissolution was observed to be very slow at potentials less than 1.2 V vs Ag/AgCl. It should be noted that the solution pH of the neutral pH dissolution experiment dropped from 6.38 initially to 2.0 indicating possible oxidation of SCN^- as discussed earlier.

To assess the degree of chemical oxidation due to dissolved oxygen occurring in the electrochemical cell during anodic dissolution in cyanide media, three experiments were conducted where gold was anodically dissolved at 1.2 V vs Ag/AgCl, chemically dissolved with the reservoir solution exposed to air, and chemically dissolved with the reservoir solution purged of oxygen by nitrogen sparging. The experimental conditions were 11.0 milligrams Au, 1.0990 grams spectroscopic carbon, 0.1 M NaCN, 0.1M NaCl, and 10^{-4} M KOH. The results of this investigation are depicted graphically in figure 10. The obvious conclusions from these experiments is that at 1.2 V vs Ag/AgCl, the anodic dissolution is slightly faster than the air

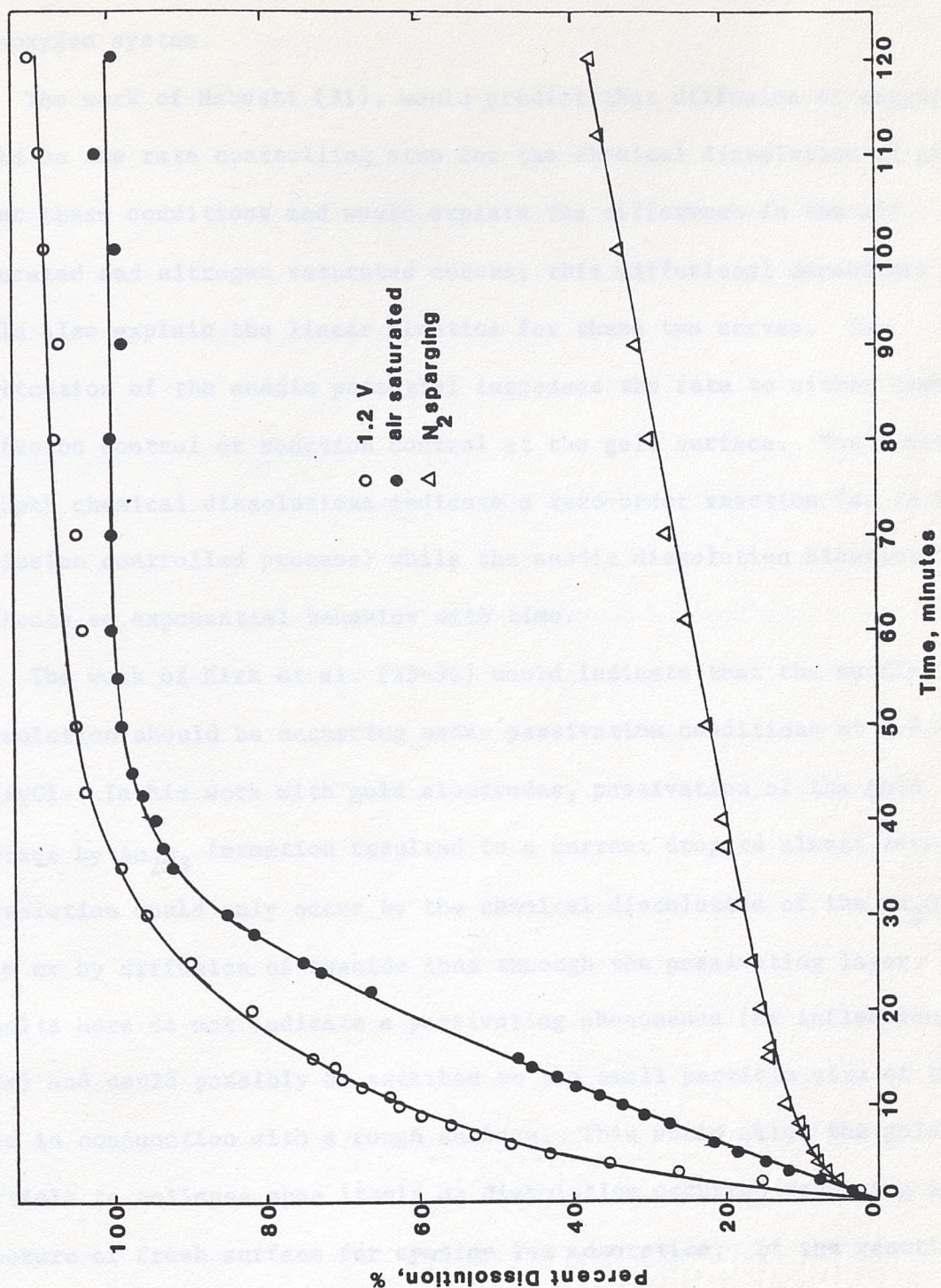


Figure 10. Percent dissolution profiles for the anodic and chemical dissolution of gold from a spectroscopic matrix in 0.1 M KCN solutions.

saturated cyanide dissolution which is considerably faster than the low-oxygen system.

The work of Habashi (31), would predict that diffusion of oxygen would be the rate controlling step for the chemical dissolution of gold under these conditions and would explain the difference in the air saturated and nitrogen saturated curves; this diffusional dependence would also explain the linear kinetics for these two curves. The application of the anodic potential increases the rate to either cyanide diffusion control or reaction control at the gold surface. The kinetics of both chemical dissolutions indicate a zero-order reaction (as in a diffusion controlled process) while the anodic dissolution kinetics indicate an exponential behavior with time.

The work of Kirk et al. (33-36) would indicate that the anodic dissolution should be occurring under passivation conditions at 1.2 V vs Ag/AgCl. In his work with gold electrodes, passivation of the gold surface by Au_2O_3 formation resulted in a current drop to almost zero; dissolution could only occur by the chemical dissolution of the Au_2O_3 film or by diffusion of cyanide ions through the passivating layer. The results here do not indicate a passivating phenomenon (no inflections in rate) and could possibly be ascribed to the small particle size of the gold in conjunction with a rough surface. This would allow the gold particle to collapse upon itself as dissolution occurred resulting in exposure of fresh surface for cyanide ion adsorption. If the reaction rate had not reached control by cyanide ion diffusion, then it is possible that the cyanide ion concentration at the gold surface was sufficient to inhibit oxide formation by the rapid formation of

$(\text{AuCN})_{\text{ads}}$. Dissolution as metastable $\text{Au}(\text{CN})_4^-$ cannot be ruled out either.

Obviously there is little kinetic advantage to be gained by applying a potential to the solid matrix in cyanide solutions in the presence of air. The final extraction value in excess of 100 percent in the anodic dissolution experiment is the result of a small leak in the system throughout the experiment.

Anodic Dissolutions in Activated Carbon

To relate the anodic dissolution of gold in spectroscopic carbon to that in an adsorbing carbon matrix, anodic dissolution experiments were performed with the porous carbon matrix made of coconut shell activated carbon. Experiments were performed in cyanide, thiourea, thiosulfate and chloride media. The poor results of the chloride experiment along with the slow anodic dissolution and strong adsorbing character of $\text{Au}(\text{SCN})_2^-$ indicated that little would be gained by investigating thiocyanate which is chemically similar to the chloride ion. The conditions of each experiment were the same as those in the spectroscopic carbon dissolutions except for the anodic dissolution in chloride media which was not performed on spectroscopic carbon; the solution composition in this experiment was 0.4 M NaCl, 0.1 M HCl.

The attempt at anodically dissolving gold from the activated carbon matrix in 0.1M HCl, 0.4 M NaCl solution at potentials up to 2.0 V vs Ag/AgCl failed completely with no detectable gold in solution after ten minutes. These conditions, although not investigated for spectroscopic carbon, should be conducive to gold dissolution as indicated in the

literature. The explanation for zero dissolution can not be simply based on the known adsorption behavior of AuCl_4^- since this species was noted earlier to adsorb by a reduction mechanism to metallic gold on the outer carbon surface. With the carbon potential maintained at +2.0 V reduction-adsorption of dissolved AuCl_4^- or AuCl_2^- should not be possible. Thus, the dissolution process was influenced in some way by the presence of the activated carbon possibly through the selective adsorption of chloride ions under the influence of the positive potential. Another possible explanation is the adsorption of AuCl_4^- or AuCl_2^- by a non-reductive mechanism more akin to the adsorption of $\text{Au}(\text{CN})_2^-$; this in combination with slow dissolution kinetics could account for a zero outlet gold concentration.

The attempt at anodically dissolving gold from the activated carbon matrix with acidic thiourea proved little better in overall results. The conditions for dissolution were an anolyte solution of 0.1 M HCl and 0.1 M thiourea and an applied potential ranging up to 0.8 V vs Ag/AgCl. Again, the adsorption of any dissolved material is nearly complete as evidenced by the graphical display of gold concentration in solution versus time in figure 11; at the peak gold concentration of 3.6 ppm, the percent dissolution was 8.3 percent. This result when compared to the zero percent dissolution in chloride media shows that faster dissolution kinetics prevail in $[\text{Au}(\text{SC}(\text{NH}_2)_2)_2]^+$ formation but that the adsorption is also very fast. It is of interest to note that at the positive potentials, the cationic complex is still adsorbed indicating that adsorption has taken place by a non-electrostatic process.

As reported in the literature, it was observed in adsorption

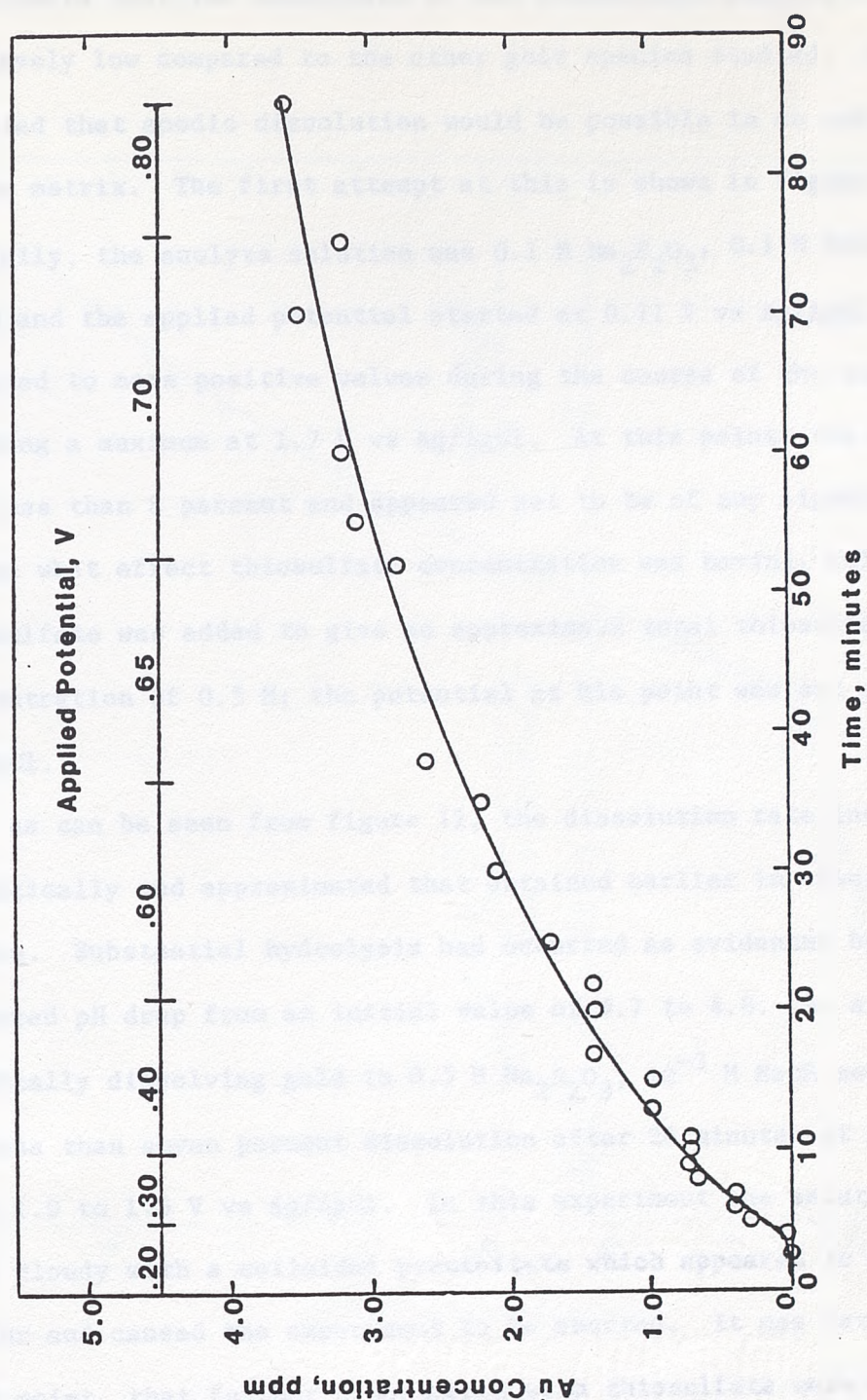


Figure 11. Reservoir gold concentration as a function of time for the anodic dissolution of gold from an activated carbon matrix in 0.1 M thiourea, 0.1 M HCl solution.

experiments that the adsorption of the thiosulfate complex of gold was relatively low compared to the other gold species studied. Thus, it was expected that anodic dissolution would be possible in an activated carbon matrix. The first attempt at this is shown in figure 12.

Initially, the anolyte solution was 0.1 M $\text{Na}_2\text{S}_2\text{O}_3$, 0.1 M NaCl, and 10^{-4} M KOH and the applied potential started at 0.11 V vs Ag/AgCl and was adjusted to more positive values during the course of the experiment reaching a maximum at 1.7 V vs Ag/AgCl. At this point, the dissolution was less than 8 percent and appeared not to be of any significance, but to see what effect thiosulfate concentration was having, solid sodium thiosulfate was added to give an approximate total thiosulfate concentration of 0.5 M; the potential at this point was set at 1.2 V vs Ag/AgCl.

As can be seen from figure 12, the dissolution rate increased dramatically and approximated that obtained earlier in spectroscopic carbon. Substantial hydrolysis had occurred as evidenced by the measured pH drop from an initial value of 9.7 to 4.8. An attempt at anodically dissolving gold in 0.5 M $\text{Na}_2\text{S}_2\text{O}_3$, 10^{-3} M NaOH media resulted in less than seven percent dissolution after 26 minutes at potentials from 1.0 to 1.5 V vs Ag/AgCl. In this experiment the solution became very cloudy with a colloidal precipitate which appeared to be elemental sulfur and caused the experiment to be aborted. It was determined at this point, that further experiments with thiosulfate were not practical.

The behavior of the rate of dissolution in the initial activated carbon/ $\text{S}_2\text{O}_3^{-2}$ experiment possibly indicates that the initial rate was

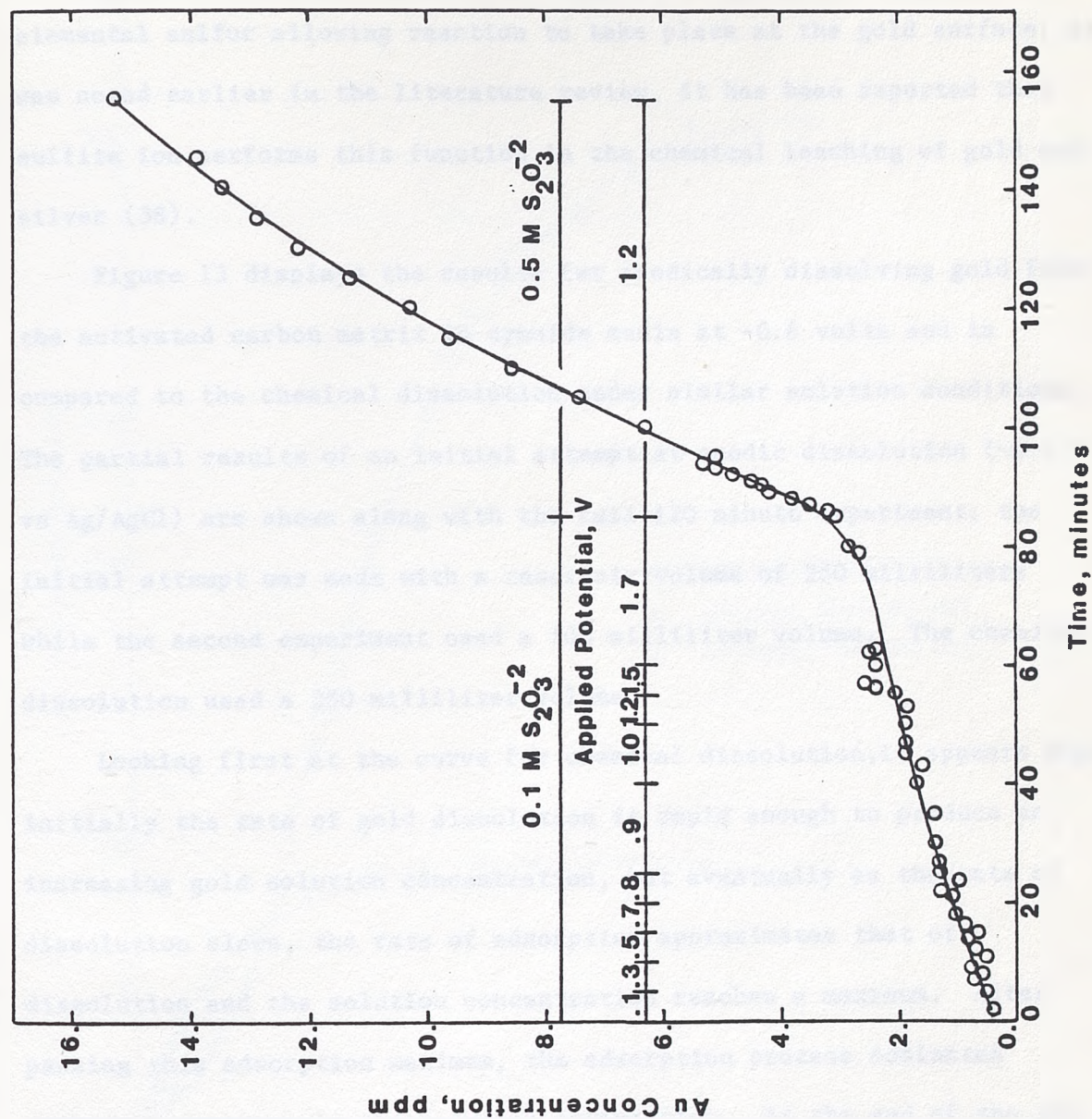


Figure 12. Gold-reservoir concentration as a function of time for the anodic dissolution of gold from an activated carbon matrix in thiosulfate solution.

under passivation control by elemental sulfur formation on the gold surface. As fresh $S_2O_3^{-2}$ was added, bisulfide from hydrolysis or sulfite from oxidation was available in sufficient quantities to react with the elemental sulfur allowing reaction to take place at the gold surface; as was noted earlier in the literature review, it has been reported that sulfite ion performs this function in the chemical leaching of gold and silver (38).

Figure 13 displays the results for anodically dissolving gold from the activated carbon matrix in cyanide media at -0.6 volts and is compared to the chemical dissolution under similar solution conditions. The partial results of an initial attempt at anodic dissolution (-0.6 V vs Ag/AgCl) are shown along with the full 120 minute experiment; the initial attempt was made with a reservoir volume of 250 milliliters while the second experiment used a 100 milliliter volume. The chemical dissolution used a 250 milliliter volume.

Looking first at the curve for chemical dissolution, it appears that initially the rate of gold dissolution is rapid enough to produce an increasing gold solution concentration, but eventually as the rate of dissolution slows, the rate of adsorption approximates that of dissolution and the solution concentration reaches a maximum. After passing this adsorption maximum, the adsorption process dominates causing a decrease in the solution composition. At the end of the 120 minute experiment, potentials ranging from -0.7 V to 2.0 V vs Ag/AgCl were applied in attempts to improve the gold recovery. Only at negative potentials approaching -0.6 V did the composition of gold in solution show an increase with time.

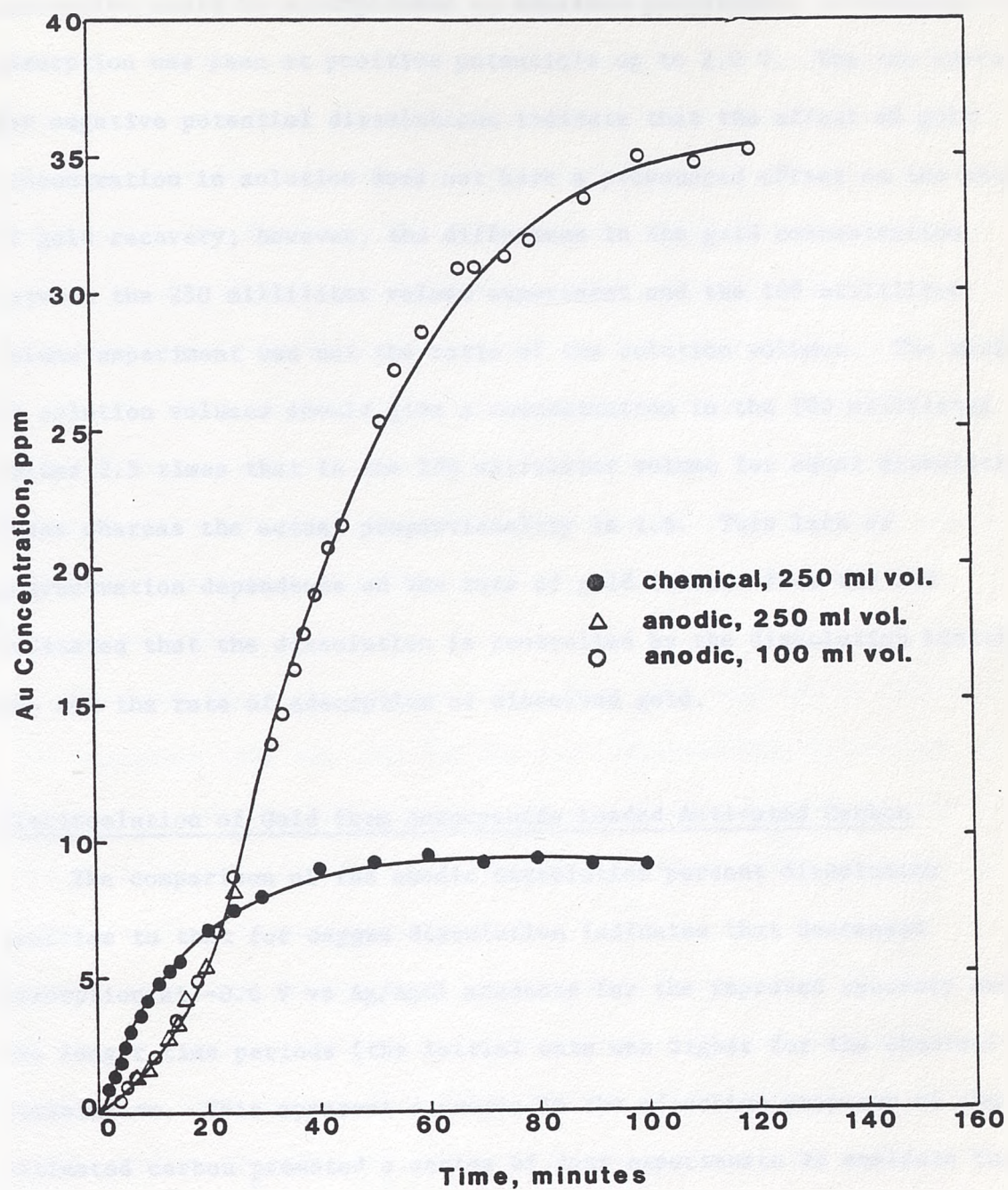


Figure 13. Concentration profiles for the anodic and chemical dissolution of gold from an activated carbon matrix in 0.1 M NaCN solution.

From observations on the effect of applied potential on the adsorption process, it was concluded that dissolution without complete adsorption could be accomplished at negative potentials; no decrease in adsorption was seen at positive potentials up to 2.0 V. The two curves for negative potential dissolutions indicate that the effect of gold concentration in solution does not have a pronounced effect on the rate of gold recovery; however, the difference in the gold concentration between the 250 milliliter volume experiment and the 100 milliliter volume experiment was not the ratio of the solution volumes. The ratio of solution volumes should give a concentration in the 100 milliliter volume 2.5 times that in the 250 milliliter volume for equal dissolution rates whereas the actual proportionality is 1.6. This lack of concentration dependence on the rate of gold release from the bed indicates that the dissolution is controlled by the dissolution kinetics and not the rate of adsorption of dissolved gold.

Electroelution of Gold from Aurocyanide Loaded Activated Carbon

The comparison of the anodic dissolution percent dissolution profiles to that for oxygen dissolution indicates that decreased adsorption at -0.6 V vs Ag/AgCl accounts for the improved recovery over the longer time periods (the initial rate was higher for the chemical dissolution. This apparent decrease in the adsorbing property of the activated carbon promoted a series of four experiments to evaluate the possibilities of desorbing gold from a previously loaded carbon.

To evaluate this potential application, four experiments were conducted to observe the negative potential desorption of $\text{Au}(\text{CN})_2^-$ as a function of time. In this investigation, the initial choice of the

desorbing solution (0.1 M NaCN, 0.1 M NaOH) was based on three criteria: Firstly, the effect of the aqueous cyanide concentration on the Au(CN)_2^- stability at negative potentials with decreased potentials possible at higher cyanide activities. Secondly, the tendency for hydrogen production at negative potentials is decreased with increased OH^- concentration. And thirdly, the known effect of caustic cyanide solutions in the developed stripping processes for removing the gold cyanide complex from activated carbon. Thus, from the above considerations, caustic cyanide solution should have been a good choice.

In the four experiments performed on this subject, two were recirculating electroelutions utilizing carbons of two different gold loadings while the third and fourth used the non-recirculating mode of operation; the fourth experiment also used deionized water as the eluting solution.

The time-dependent behavior of percent gold recovery as calculated from equations [50] and [56] for the two recirculating experiments and the caustic solution non-recirculating experiment respectively are plotted in figure 14. The two recirculating experiments contrast two substantially different gold loadings.

In comparing the two modes of operation (figure 14), it appears that in the recirculating system, the gold in solution approaches an equilibrium with that in the solid, and the gold loading is determined by the surface or solid potential which was set at -0.6 V vs Ag/AgCl. The non-recycling elution which shows a maximum in the rate of elution does not approach equilibrium on this time scale; thus, from the applications aspect, flow-through electroelution gives a higher but slower recovery. In comparing the two recirculating curves, the higher

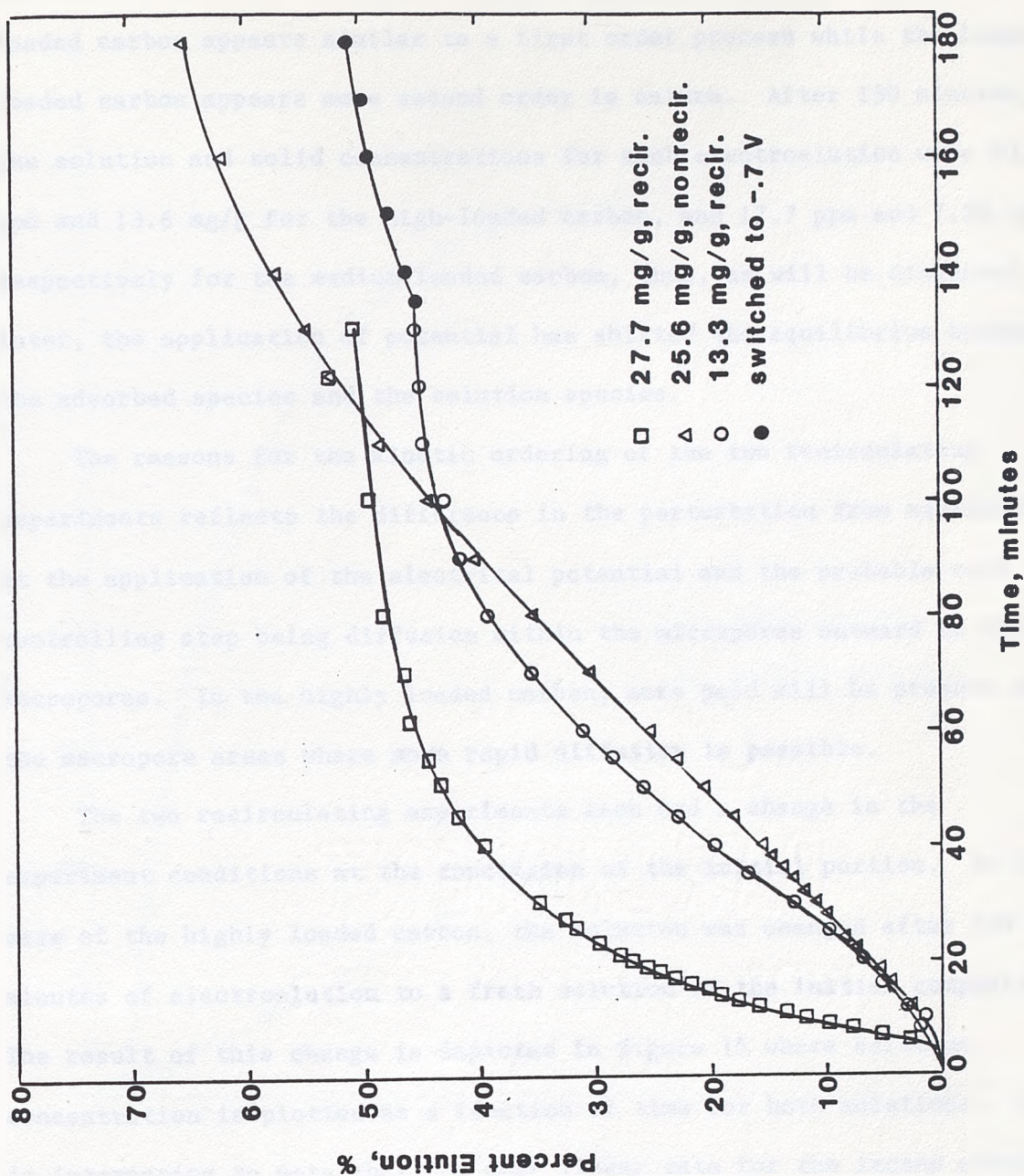


Figure 14. Percent elution as a function of time for the negative-potential electroelution of gold from an aurocyanide-loaded activated carbon with 0.1 M NaCN, 0.1 M NaOH solution.

gold loading (27.7 mg Au/g carbon) gave a faster approach to equilibrium and also a different shaped curve. The electroelution of the highly loaded carbon appears similar to a first order process while the lower loaded carbon appears more second order in nature. After 130 minutes, the solution and solid concentrations for each electroelution were 40.1 ppm and 13.6 mg/g for the high-loaded carbon, and 17.7 ppm and 7.26 mg/g respectively for the medium loaded carbon, thus, as will be discussed later, the application of potential has shifted the equilibrium between the adsorbed species and the solution species.

The reasons for the kinetic ordering of the two recirculating experiments reflects the difference in the perturbation from equilibrium at the application of the electrical potential and the probable rate controlling step being diffusion within the micropores outward to the macropores. In the highly loaded carbon, more gold will be present in the macropore areas where more rapid diffusion is possible.

The two recirculating experiments each had a change in the experiment conditions at the conclusion of the initial portion. In the case of the highly loaded carbon, the solution was changed after 130 minutes of electroelution to a fresh solution of the initial composition. The result of this change is depicted in figure 15 where solution concentration is plotted as a function of time for both solutions. It is interesting to note that the near linear rate for the second solution (0.14 ppm/min) is substantially greater than the final portion of the first solution curve (0.032 ppm/min). This again reflects the kinetic driving force being the difference between the solution concentration and the equilibrium concentration in the micropore/macropore areas.

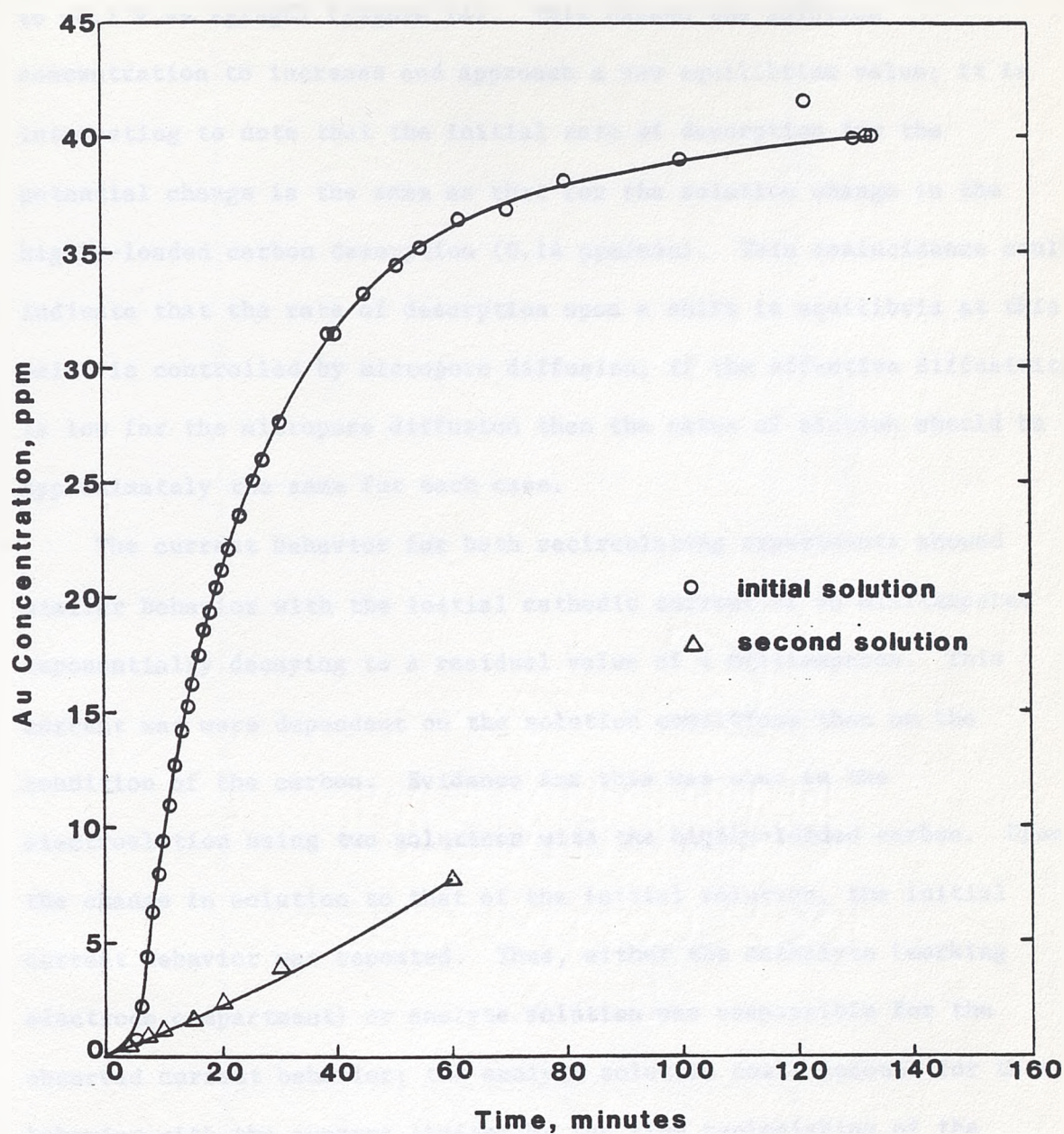


Figure 15. Gold concentration as a function of time for the caustic-cyanide (0.1 M NaCN, NaOH) electroelution (-0.6 V) of gold from an aurocyanide-loaded activated carbon having an initial loading of 27.7 mg/g.

The variable change at the end of the electroelution of the moderately loaded carbon (13.3 mg/g) was a decrease in applied potential to -0.7 V vs Ag/AgCl (figure 14). This caused the solution concentration to increase and approach a new equilibrium value; it is interesting to note that the initial rate of desorption for the potential change is the same as that for the solution change in the highly-loaded carbon desorption (0.14 ppm/min). This coincidence could indicate that the rate of desorption upon a shift in equilibria at this point is controlled by micropore diffusion; if the effective diffusivity is low for the micropore diffusion then the rates of elution should be approximately the same for each case.

The current behavior for both recirculating experiments showed similar behavior with the initial cathodic current of 40 milliamperes exponentially decaying to a residual value of 4 milliamperes. This current was more dependent on the solution conditions than on the condition of the carbon. Evidence for this was seen in the electroelution using two solutions with the highly-loaded carbon. Upon the change in solution to that of the initial solution, the initial current behavior was repeated. Thus, either the catholyte (working electrode compartment) or anolyte solution was responsible for the observed current behavior; the anolyte solution could account for this behavior with the current limited by the slow replenishing of the anolyte solution.

The initial current behavior for the medium-loaded carbon elution with subsequent potential change is displayed in figure 16; the current change upon switching from -0.6 V to -0.7 V represents the final

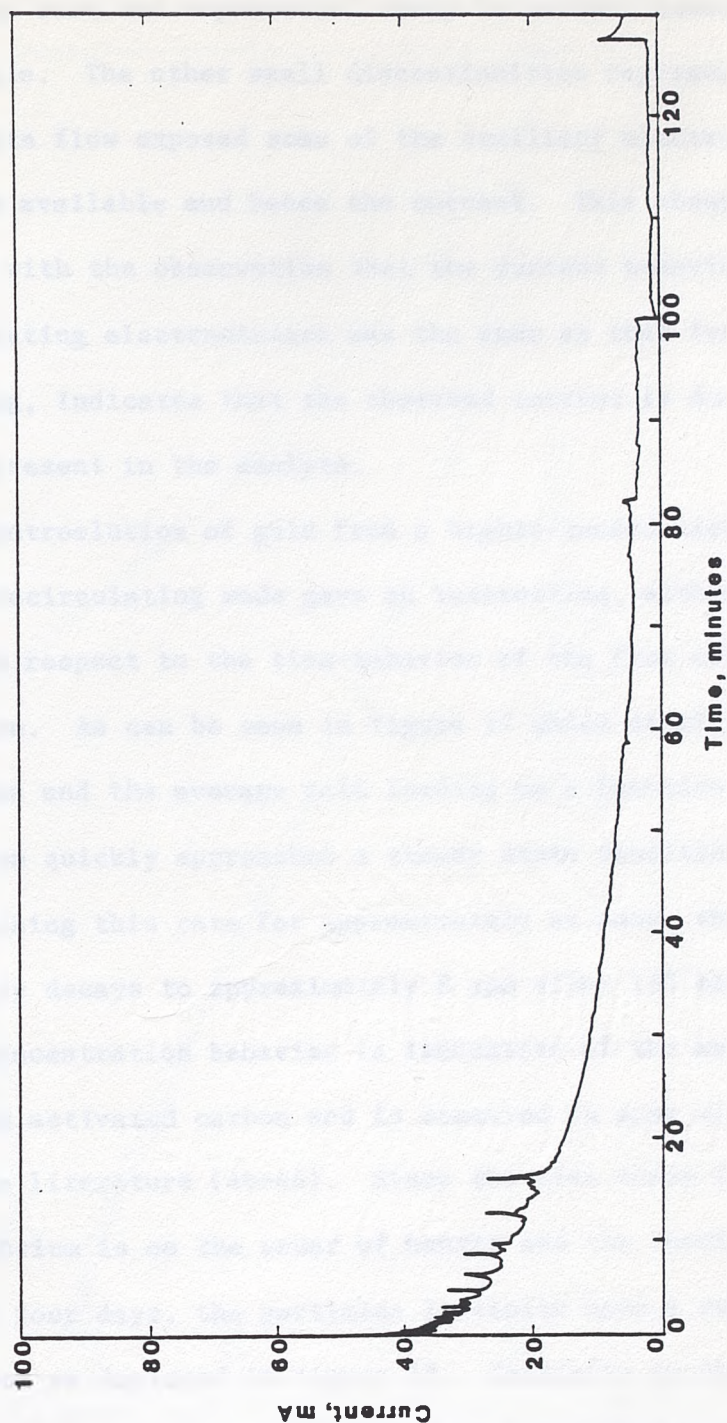


Figure 16. Cathodic current as a function of time for the recirculating electroelution (0.1 M NaCN, NaOH, -0.6 V) of gold from an aurocyanide loaded activated carbon having an initial loading of 13.3 mg/g.

discontinuous rise and exponential decay in current towards the end of the time scale. The other small discontinuities represent times where uneven anolyte flow exposed some of the auxiliary electrode limiting the surface area available and hence the current. This observation in conjunction with the observation that the current behavior for the non-recirculating electroelution was the same as that for the recirculating, indicates that the observed current is due to oxidation of species present in the anolyte.

The electroelution of gold from a highly-loaded carbon (25.6 mg/g) in the non-recirculating mode gave an interesting, although predictable, display with respect to the time-behavior of the flow cell outlet concentration. As can be seen in figure 17 which displays the outlet concentration and the average gold loading as a function of time, the concentration quickly approaches a steady state condition on elution. After sustaining this rate for approximately an hour, the concentration exponentially decays to approximately 8 ppm after 180 minutes.

This concentration behavior is indicative of the way gold cyanide is loaded on activated carbon and is observed in some elution profiles found in the literature (44-46). Since the time scale for approach to true equilibrium is on the order of months and the loading process here was but for four days, the particles initially have a concentration gradient such as depicted in figure 18. Initially in the electroelution, the rate of desorption is controlled by mass transfer at the solution-carbon interface. But as elution proceeds, the outer carbon surface becomes depleted of gold cyanide and the rate of elution becomes controlled by diffusion of gold cyanide species from the

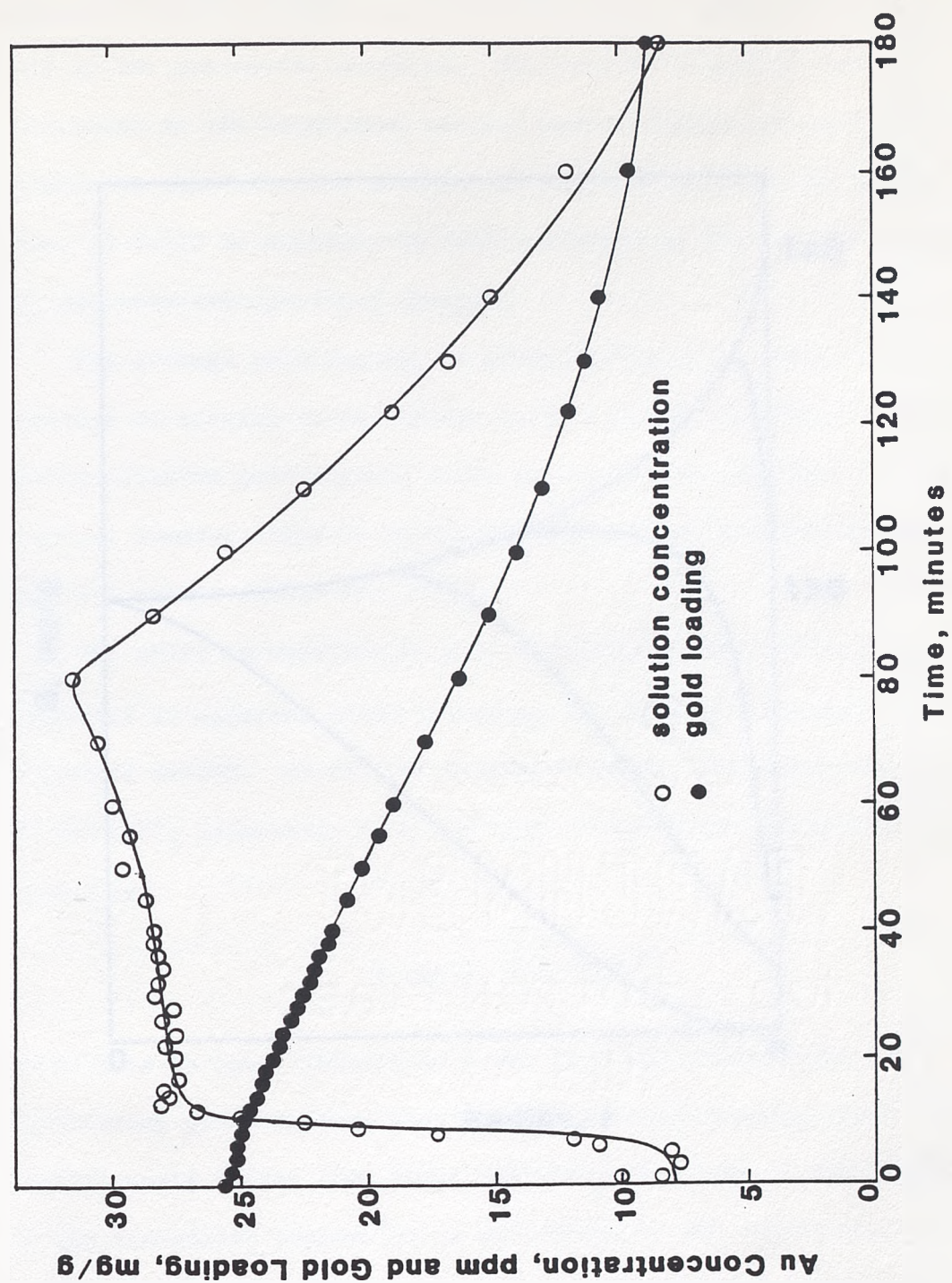


Figure 17. Concentration and gold loading profiles for the nonrecirculating electroelution (0.1 M NaCN, NaOH, -0.6 V) of gold from an aurocyanide-loaded activated carbon having an initial loading of 25.6 mg/g.

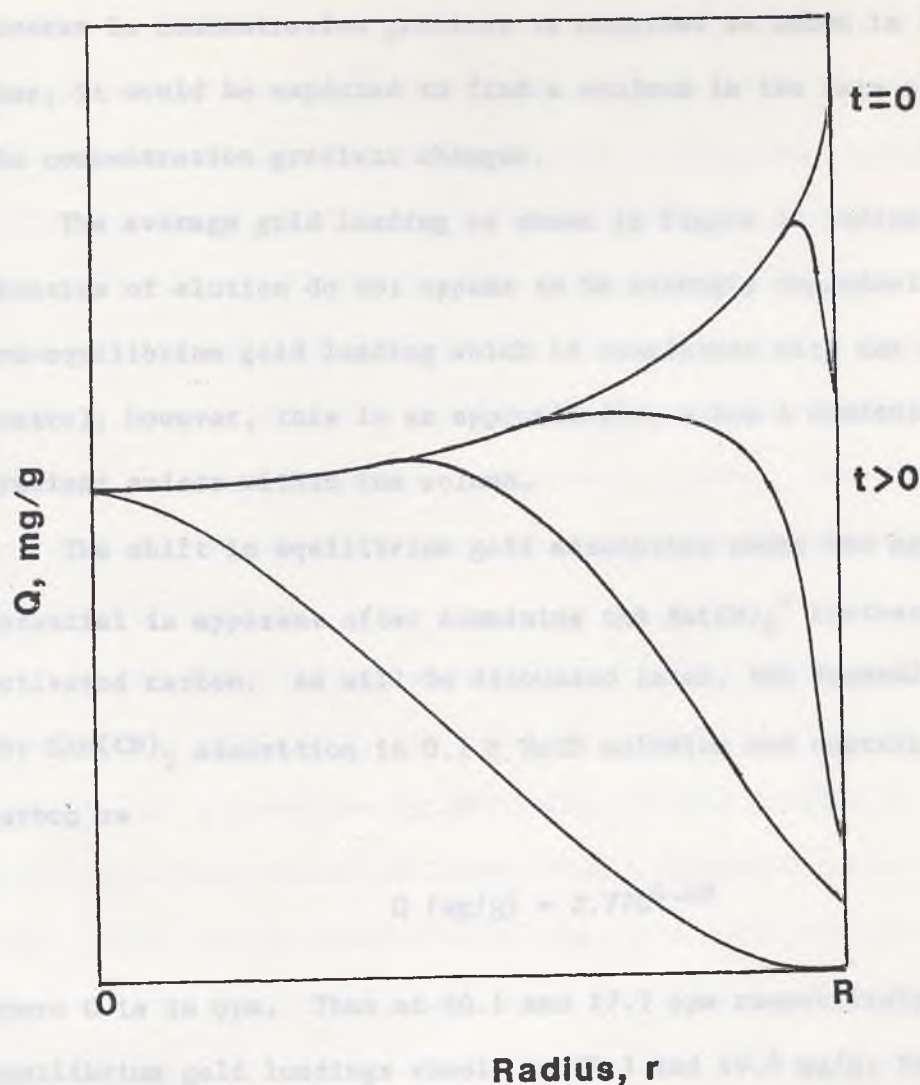


Figure 18. Proposed intraparticle gold loading as a function of position within the particle; t designates time of elution.

macropores to the surface. In the same way, as the concentration of gold in the macropores decreases, the rate of diffusion from the micropores to the macropores becomes rate limiting and eventually an inverse in concentration gradient is obtained as shown in figure 18. Thus, it would be expected to find a maximum in the rate of elution as the concentration gradient changes.

The average gold loading as shown in figure 17 indicates that the kinetics of elution do not appear to be strongly dependent on the non-equilibrium gold loading which is consistent with the diffusion control; however, this is an approximation since a concentration gradient exists within the column.

The shift in equilibrium gold adsorption under the applied potential is apparent after examining the $\text{Au}(\text{CN})_2^-$ isotherm for the activated carbon. As will be discussed later, the Freundlich expression for $\text{KAu}(\text{CN})_2$ adsorption in 0.1 M NaCN solution was correlated for this carbon as

$$Q \text{ (mg/g)} = 2.77C^{0.68} \quad [70]$$

where C is in ppm. Thus at 40.1 and 17.7 ppm respectively, the equilibrium gold loadings should be 34.1 and 19.5 mg/g; these values are significantly higher than those calculated to exist in the experiments. If the Freundlich expression is correlated to the experimental solution concentrations and carbon loading, the expression obtained is as follows:

$$Q = 1.25C^{0.76} \quad [71]$$

Thus, the capacity constant is 2.2 times less at -0.6 V vs Ag/AgCl.

Using this expression for the final solution concentration (8.3) ppm of the non-recirculating experiment and comparing the resultant gold loading to that for the non-recirculating experiment (8.8 mg/g) indicates that the solution exiting the column was not in equilibrium with the carbon bed; the predicted gold loading from equation [71] is 6.2 mg/g. These results are subject to some error owing to the nonequilibrium conditions for the recirculating elutions and their 0.1 M NaOH composition which should decrease slightly the equilibrium gold loading. Since the error resulting from the nonequilibrium condition is predictably greater than the hydroxide ion effect, the true decrease in the carbon's capacity for gold cyanide is probably greater than that shown numerically.

It was found through experiment, that the gold elution rate was dramatically affected by the ionic character of the electroeluting solution as is found in the desorption of gold cyanide by high-temperature distilled water after a caustic-cyanide pretreatment (46). Thus, at the conclusion of the above mentioned non-recirculating caustic cyanide electroelution where the final outlet gold concentration was 8.30 ppm, deionized distilled water followed by four other solutions on hand were used as the eluents. The procedure used was that after passing the old solution from the system, the new eluent to be used was passed through the column and for 2 to 5 minutes, the outlet gold concentration was monitored via the FIA-AAS system. The concentration behavior is shown in figure 19; the time scale represents time after application of the particular eluent. It is seen that with the water

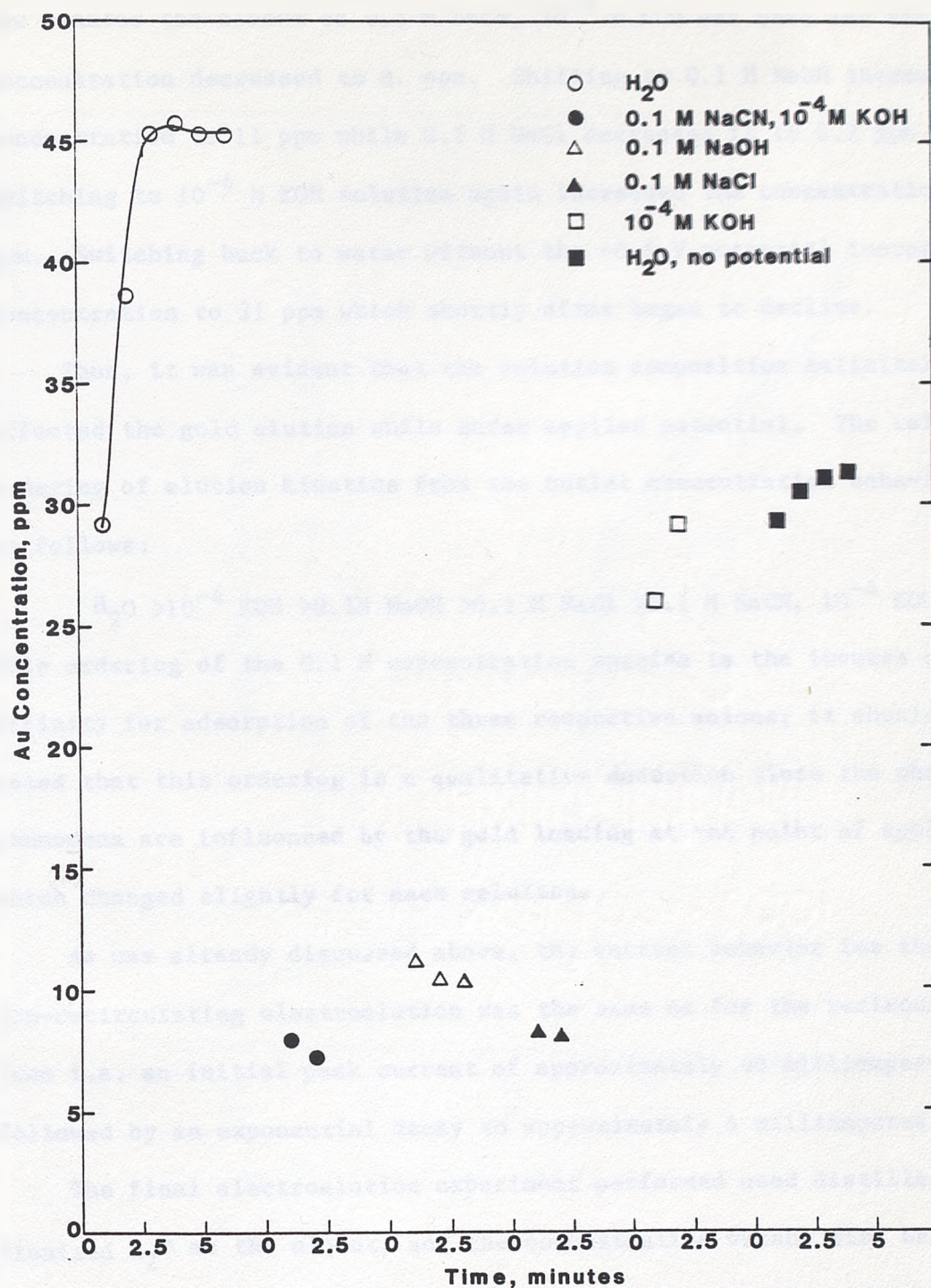


Figure 19. Effect of different eluting solutions on the outlet gold concentration in the nonrecirculating electroelution (-0.6 V) of gold from an aurocyanide-loaded activated carbon.

eluent, the outlet concentration quickly goes up to 45.3 ppm. After a few minutes the eluent of 0.1 M NaCN, 10^{-4} M KOH was used and the concentration decreased to 8. ppm. Shifting to 0.1 M NaOH increased the concentration to 11 ppm while 0.1 M NaCl decreased it to 8.2 ppm. Switching to 10^{-4} M KOH solution again increased the concentration to 30 ppm. Switching back to water without the -0.6 V potential increased the concentration to 31 ppm which shortly after began to decline.

Thus, it was evident that the solution composition definitely affected the gold elution while under applied potential. The relative ordering of elution kinetics from the outlet concentration behavior is as follows:



This ordering of the 0.1 M concentration species is the inverse of the affinity for adsorption of the three respective anions; it should be noted that this ordering is a qualitative deduction since the observed phenomena are influenced by the gold loading at the point of application which changed slightly for each solution.

As was already discussed above, the current behavior for the non-recirculating electroelution was the same as for the recirculating case i.e. an initial peak current of approximately 40 milliamperes followed by an exponential decay to approximately 4 milliamperes.

The final electroelution experiment performed used distilled dionized H_2O as the eluent, and the concentration versus time behavior is displayed in figure 20. The conditions here were non-recirculating operation and a gold loading of 8.83 mg/g. Initially, no potential was applied to observe simple water elution. As can be seen the

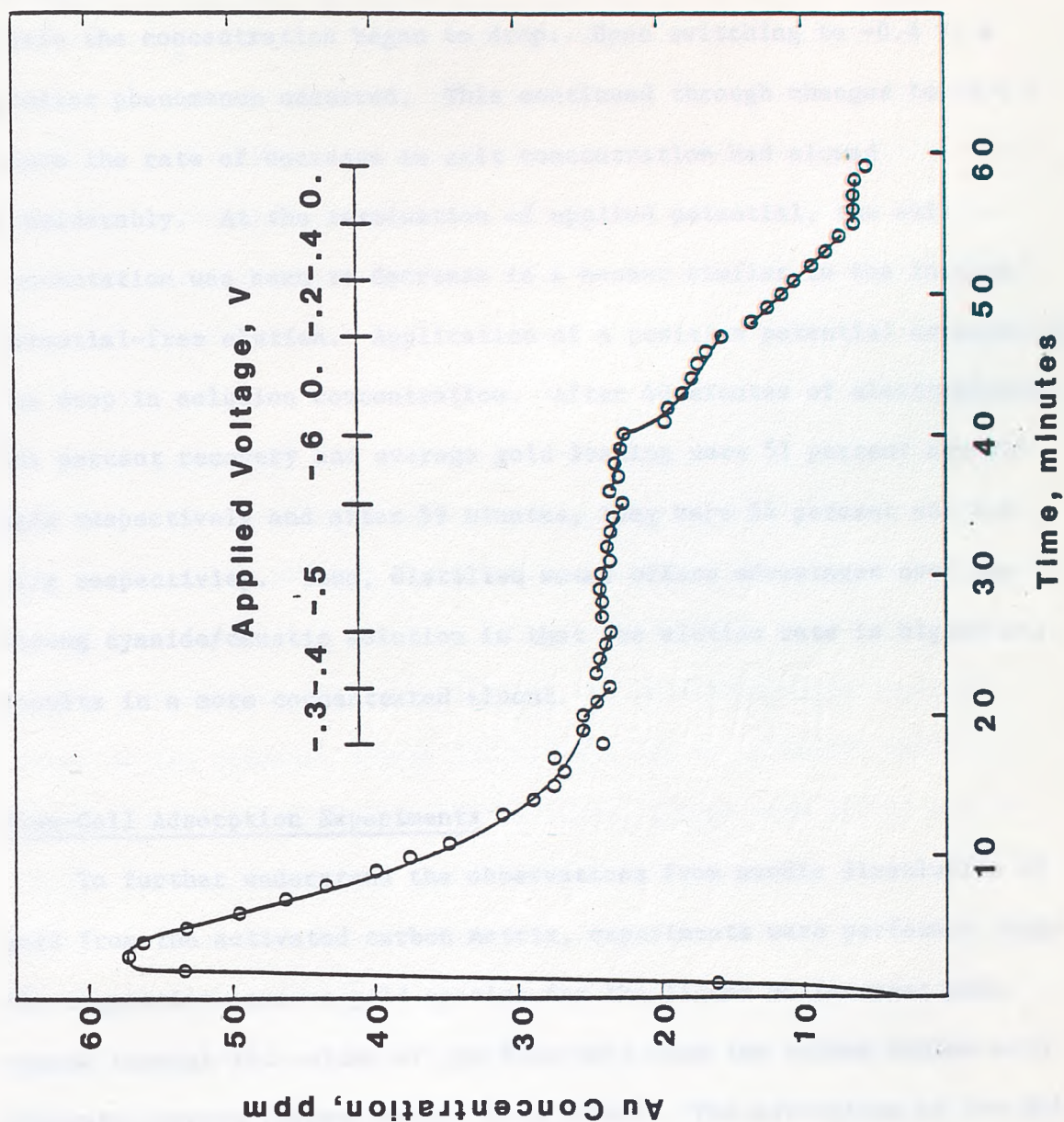


Figure 20. Eluent gold concentration profile for the nonrecirculating electroelution (deionized water, variable potential) of gold from an aurocyanide-loaded activated carbon having an initial loading of 8.83 mg/g.

concentration peaked rapidly at almost 58 ppm. The rate of elution however, rapidly dropped off and after 18 minutes a potential of -0.3 V vs Ag/AgCl was applied. This sustained the rate of elution slightly but again the concentration began to drop. Upon switching to -0.4 V, a similar phenomenon occurred. This continued through changes to -0.6 V where the rate of decrease in exit concentration had slowed considerably. At the termination of applied potential, the exit concentration was seen to decrease in a manner similar to the initial potential-free elution. Application of a positive potential accelerated the drop in solution concentration. After 40 minutes of electroelution, the percent recovery and average gold loading were 51 percent and 4.9 mg/g respectively and after 59 minutes, they were 54 percent and 4.1 mg/g respectively. Thus, distilled water offers advantages over the strong cyanide/caustic solution in that the elution rate is higher and results in a more concentrated eluent.

Flow-Cell Adsorption Experiments

To further understand the observations from anodic dissolution of gold from the activated carbon matrix, experiments were performed where the respective aqueous gold species for the ligand of interest were passed through the column of the flow cell with the column filled with activated carbon (approximately 0.73 grams). The adsorption of the gold complex was characterized by its concentration change in the solution reservoir as a function of time. Experiments of this type were done for the gold complexes $\text{Au}(\text{CN})_2^-$, $\text{Au}(\text{S}_2\text{O}_3)_2^{3-}$, $[\text{Au}(\text{SC}(\text{NH}_2)_2)_2]^+$, $\text{Au}(\text{SCN})_2^-$, and AuCl_4^- .

Figure 21 displays the concentration versus time profiles for the gold complexes $\text{Au}(\text{S}_2\text{O}_3)_2^{-3}$, $[\text{Au}(\text{SC}(\text{NH}_2)_2)_2]^+$, $\text{Au}(\text{SCN})_2^-$, and AuCl_4^- . Plotted along with the experimental data is equation [60] with the parameters $C_0 = 38 \text{ ppm}$ and $\tau = 83.3 \text{ minutes}$. This expression represents the concentration behavior of the reservoir acting as a perfectly back-mixed reactor and the column outlet concentration being zero. From the agreement between the experimental data and the solid curve, this was true and was verified by analyzing the exit stream for the gold cyanide complex adsorption experiment; it was zero for at least the initial portion of the experiment.

Only $\text{Au}(\text{S}_2\text{O}_3)_2^{-3}$ was different with respect to its adsorption behavior with equilibrium adsorption approached within 20 minutes at a gold loading of 0.27 mg/g. The reasons for the low gold loading in the thiosulfate system has not been fully elucidated at this point but various possibilities exist including the relatively high negative charge on the complex, steric limitations due to molecular structure, and or specific interactions of the ligand groups with carbon active sites. The rapid approach to saturation along with the finite adsorption indicate that possibly the charge on the thiosulfate complex limits the number of sites capable of dispersing the negative charge and accomodate the thiosulfate ligands. This behavior parallels that observed for copper(I) cyanide species with the anionic species adsorbed less with increasing charge.

The rapid approach to saturation observed might point to steric limitations with respect to the pore size in the carbon. Since some

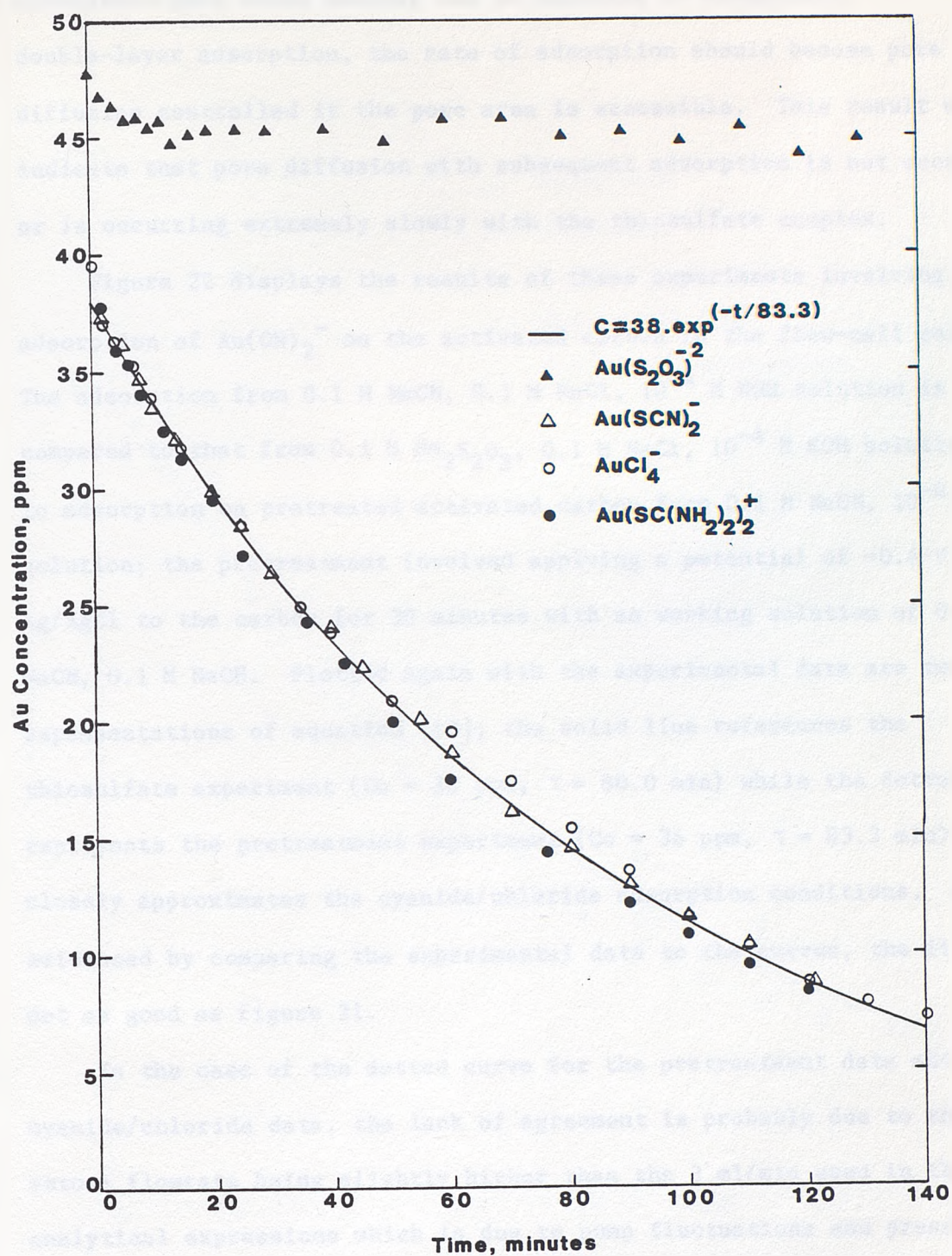


Figure 21. Concentration profiles for the recirculating flow-cell adsorption of gold thiourea, thiocyanate, chloride, and thiosulfate complexes on activated carbon.

adsorption does occur whether due to specific or nonspecific double-layer adsorption, the rate of adsorption should become pore diffusion controlled if the pore area is accessible. This result would indicate that pore diffusion with subsequent adsorption is not occurring or is occurring extremely slowly with the thiosulfate complex.

Figure 22 displays the results of three experiments involving the adsorption of $\text{Au}(\text{CN})_2^-$ on the activated carbon in the flow-cell column. The adsorption from 0.1 M NaCN, 0.1 M NaCl, 10^{-4} M KOH solution is compared to that from 0.1 M $\text{Na}_2\text{S}_2\text{O}_3$, 0.1 M NaCl, 10^{-4} M KOH solution and to adsorption on pretreated activated carbon from 0.1 M NaCN, 10^{-4} M KOH solution; the pretreatment involved applying a potential of -0.6 V vs Ag/AgCl to the carbon for 30 minutes with an working solution of 0.1 M NaCN, 0.1 M NaOH. Plotted again with the experimental data are two representations of equation [60]; the solid line references the thiosulfate experiment ($C_0 = 38$ ppm, $\tau = 80.0$ min) while the dotted line represents the pretreatment experiment ($C_0 = 36$ ppm, $\tau = 83.3$ min) and closely approximates the cyanide/chloride adsorption conditions. As evidenced by comparing the experimental data to the curves, the fit is not as good as figure 21.

In the case of the dotted curve for the pretreatment data and cyanide/chloride data, the lack of agreement is probably due to the actual flowrate being slightly higher than the 3 ml/min used in the analytical expressions which is due to pump fluctuations and pressure drop in the system. The lack of agreement in the thiosulfate experiment is due to the exit concentration being non-zero and thus equation [60] is not valid.

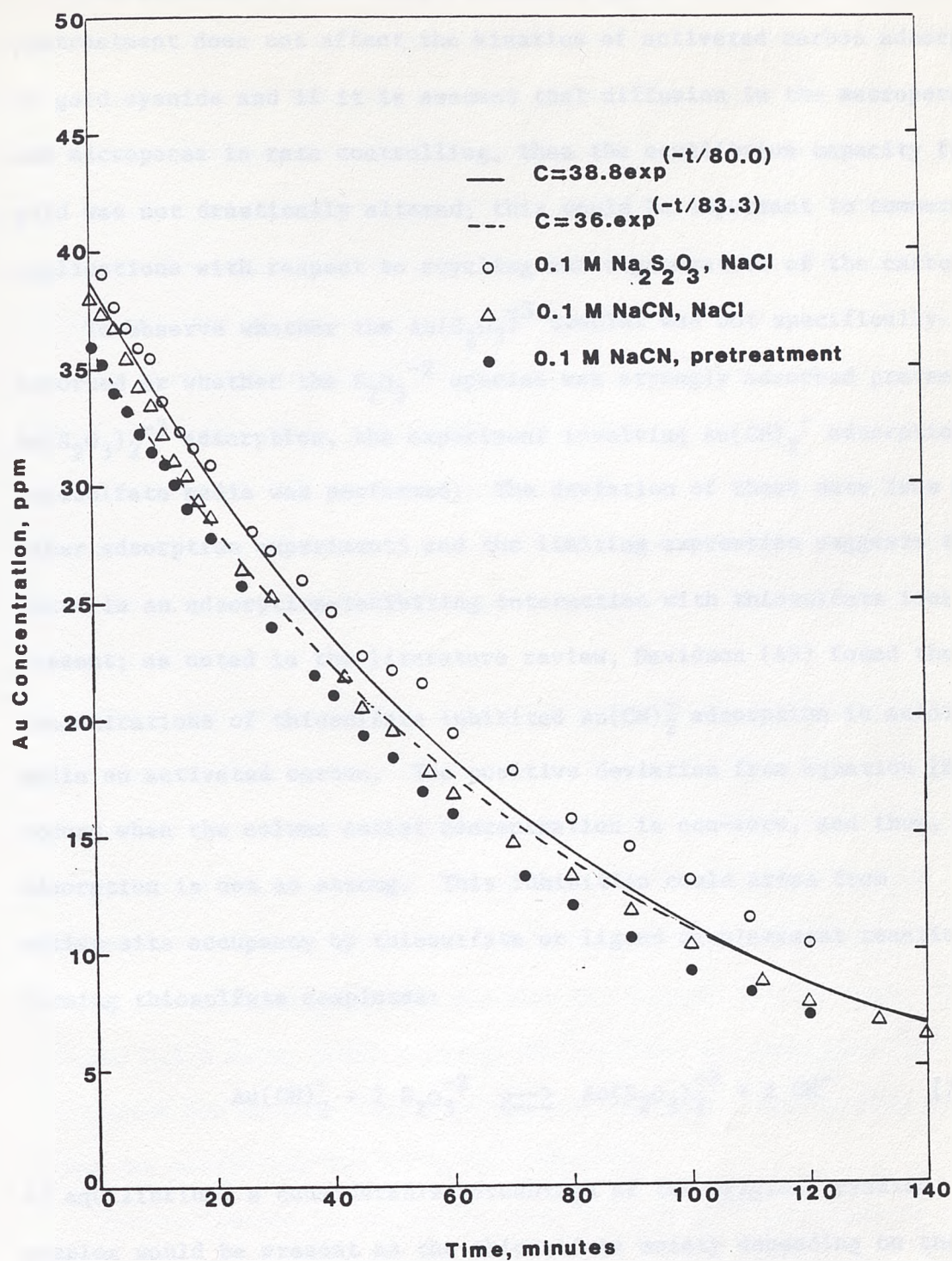
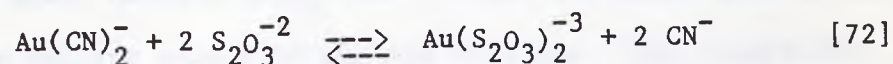


Figure 22. Concentration profiles for the recirculating flow-cell adsorption of aurocyanide on activated carbon.

The conclusion from the pretreatment experiments is that the pretreatment does not affect the kinetics of activated carbon adsorption of gold cyanide and if it is assumed that diffusion in the macropores and micropores is rate controlling, then the equilibrium capacity for gold was not drastically altered; this would be important to commercial applications with respect to recycling and regeneration of the carbon.

To observe whether the $\text{Au}(\text{S}_2\text{O}_3)_2^{3-}$ complex was not specifically adsorbed or whether the $\text{S}_2\text{O}_3^{2-}$ species was strongly adsorbed preventing $\text{Au}(\text{S}_2\text{O}_3)_2^{3-}$ adsorption, the experiment involving $\text{Au}(\text{CN})_2^-$ adsorption in thiosulfate media was performed. The deviation of these data from the other adsorption experiments and the limiting expression suggests that there is an adsorption-inhibiting interaction with thiosulfate ions present; as noted in the literature review, Davidson (49) found that low concentrations of thiosulfate inhibited $\text{Au}(\text{CN})_2^-$ adsorption in acidic media on activated carbon. The positive deviation from equation [60] occurs when the column outlet concentration is non-zero, and thus, the adsorption is not as strong. This inhibition could arise from active-site occupancy by thiosulfate or ligand displacement reactions forming thiosulfate complexes:



At equilibrium, a considerable percentage of the original cyanide complex would be present as the thiosulfate moiety depending on the kinetics of the exchange reaction.

To determine whether adsorption observed in the flow cell would

reveal any useful information with respect to adsorption of the gold cyanide complexes on carbonaceous gold ore, a couple of experiments were conducted with the Freeport gold ore. The first couple of experiments involved recirculation adsorption of $\text{Au}(\text{CN})_2^-$ from a 0.1 M NaCN, 10^{-4} M KOH solution at concentrations of 37.5 and 10.0 ppm gold. The reservoir concentration was monitored as a function of time for a preliminary period and then measured at a terminal time of either 13 or 17.5 hours.

As displayed in figure 23, the results revealed a limited adsorption under these conditions. The 38.0 ppm initial solution gave a final loading of 2.21 mg Au/g organic carbon at a final solution concentration of 37.0 ppm Au, and the 10.0 ppm initial solution gave a final loading of 1.46 mg Au/g organic carbon at a final solution concentration of 9.30 ppm.

Since the recirculating mode of adsorption was not sensitive to the small amount of gold adsorbed on the carbonaceous material, a couple of experiments were performed with the adsorption carried out in the non-recirculating mode where the column outlet concentration was monitored directly by the FIA-AAS system. The two conditions for adsorption of $\text{Au}(\text{CN})_2^-$ on the ore were 0.1 M NaCN, 0.05 M NaCl, 10^{-4} M KOH and 0.1 M NaCN, 0.025 M CaCl_2 , 10^{-4} M KOH; the respective ppm levels for sodium and calcium were 1150 ppm and 1000 ppm. The results for these two conditions are shown in figure 24.

The difference in adsorption from Na^+ and Ca^{+2} solutions is evident in the kinetics of each system; the NaCl solution rapidly approached equilibrium, whereas the calcium system approached equilibrium more slowly and reached a steady state condition after approximately 12

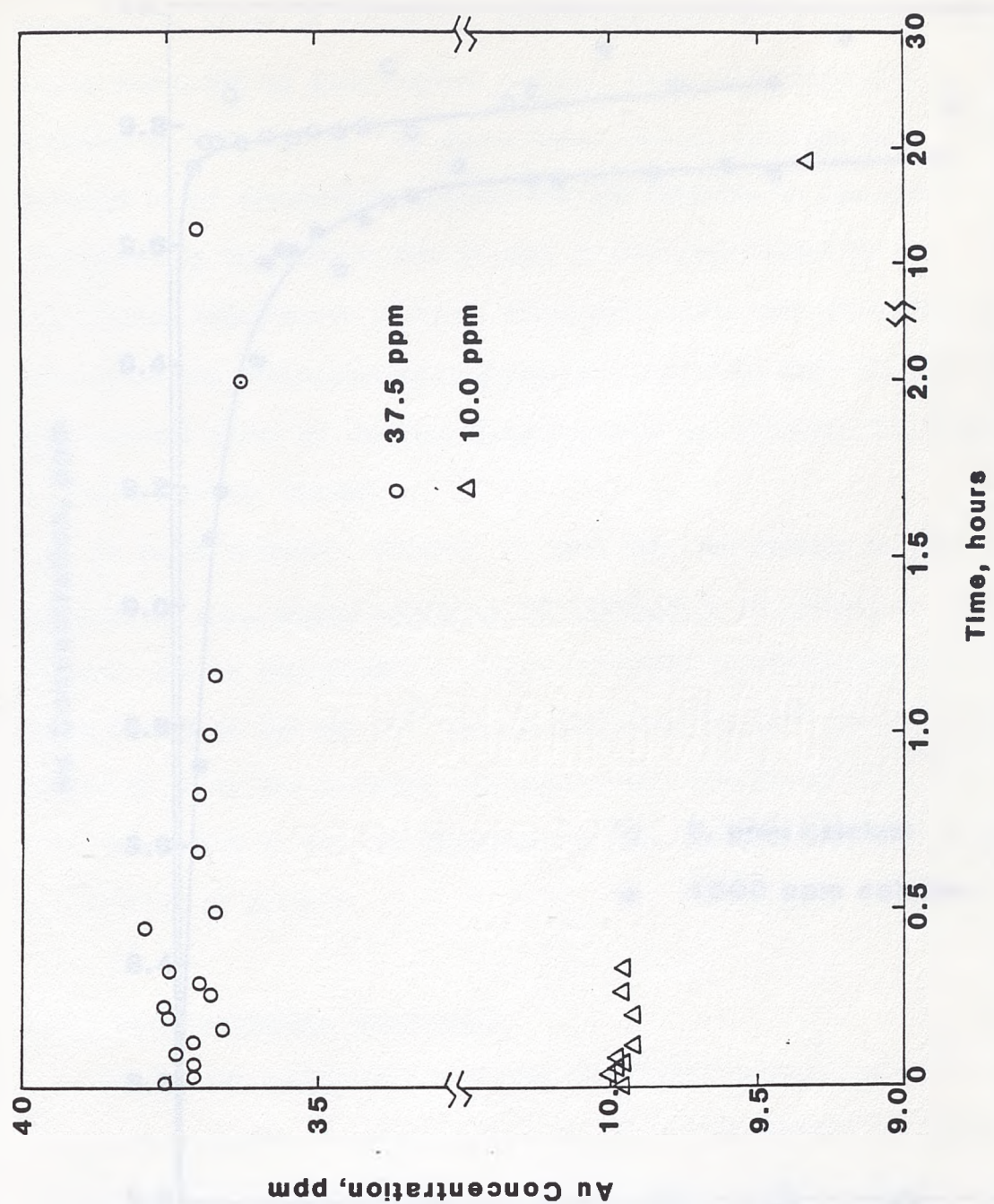


Figure 23. Concentration as a function of time for the recirculating flow-cell adsorption of aurocyanide on the Freeport carbonaceous gold ore.

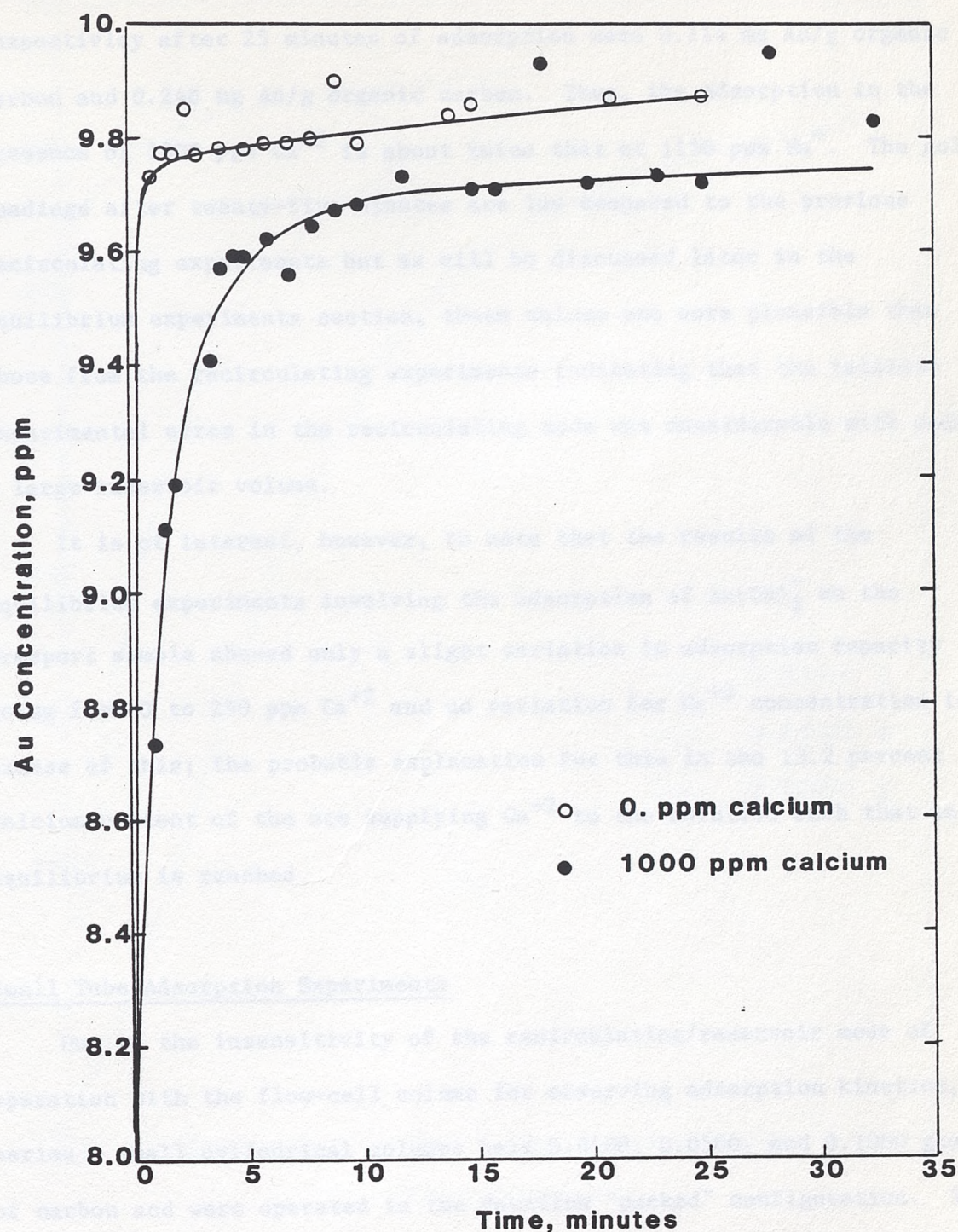


Figure 24. Concentration as a function of time for the nonrecirculating adsorption of aurocyanide on the Freeport carbonaceous gold ore in the presence of sodium and calcium ions.

minutes. The final gold loading for the sodium and calcium systems respectively after 25 minutes of adsorption were 0.114 mg Au/g organic carbon and 0.248 mg Au/g organic carbon. Thus, the adsorption in the presence of 1000 ppm Ca^{+2} is about twice that at 1150 ppm Na^{+} . The gold loadings after twenty-five minutes are low compared to the previous recirculating experiments but as will be discussed later in the equilibrium experiments section, these values are more plausible than those from the recirculating experiments indicating that the relative experimental error in the recirculating mode was considerable with such a large reservoir volume.

It is of interest, however, to note that the results of the equilibrium experiments involving the adsorption of $\text{Au}(\text{CN})_2^-$ on the Freeport sample showed only a slight variation in adsorption capacity going from 0 to 250 ppm Ca^{+2} and no variation for Ca^{+2} concentration in excess of this; the probable explanation for this is the 13.2 percent Calcium content of the ore supplying Ca^{+2} to the solution such that an equilibrium is reached.

Small Tube Adsorption Experiments

Due to the insensitivity of the recirculating/reservoir mode of operation with the flow-cell column for observing adsorption kinetics, a series of small cylindrical columns held 0.0100, 0.0500, and 0.1000 grams of carbon and were operated in the downflow "packed" configuration. The concentration profiles for each complex are displayed in figures 25 through 28.

The kinetics of adsorption parallel the capacity of the activated

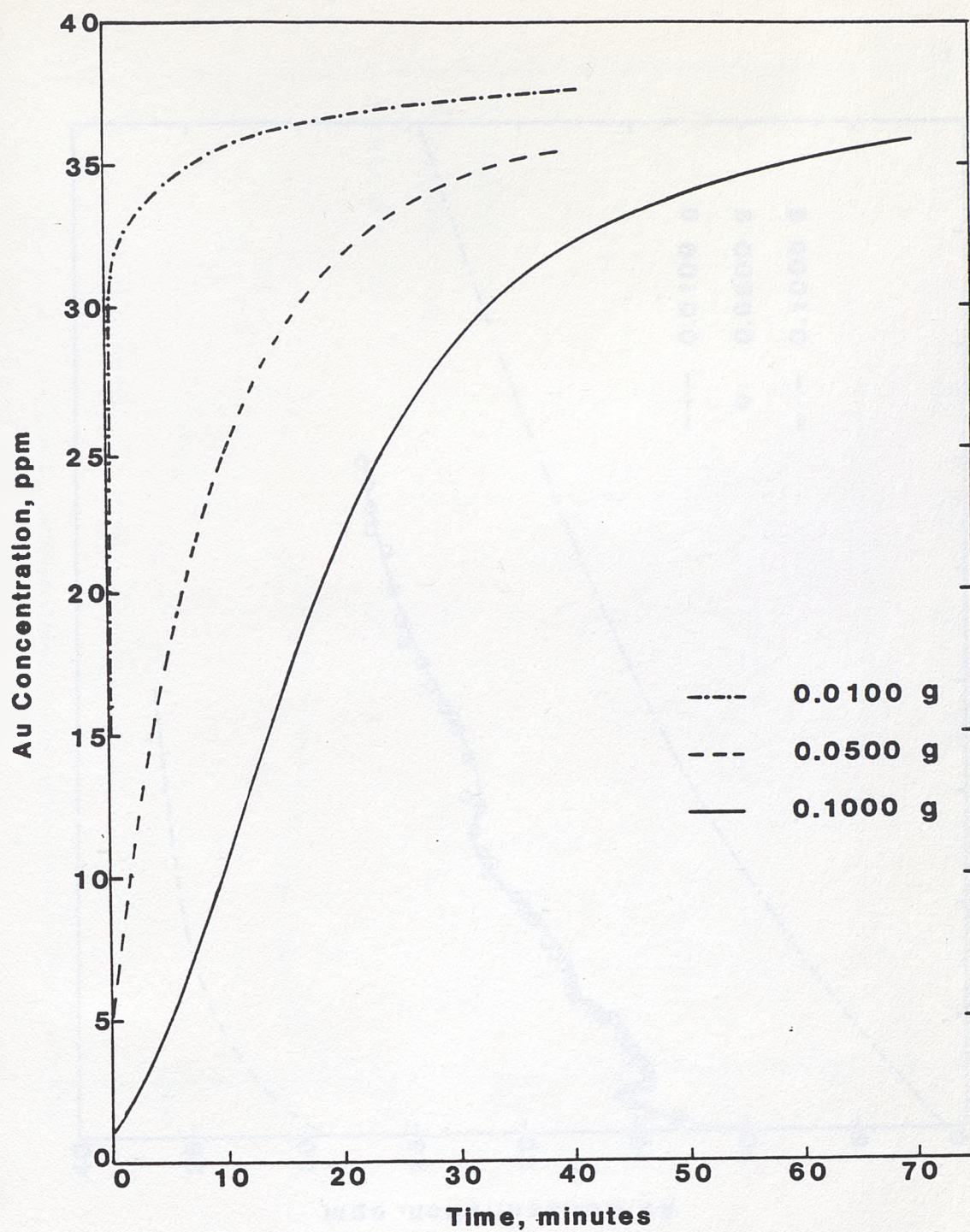


Figure 25. Concentration profiles for the nonrecirculating small-column adsorption of aurocyanide on activated carbon.

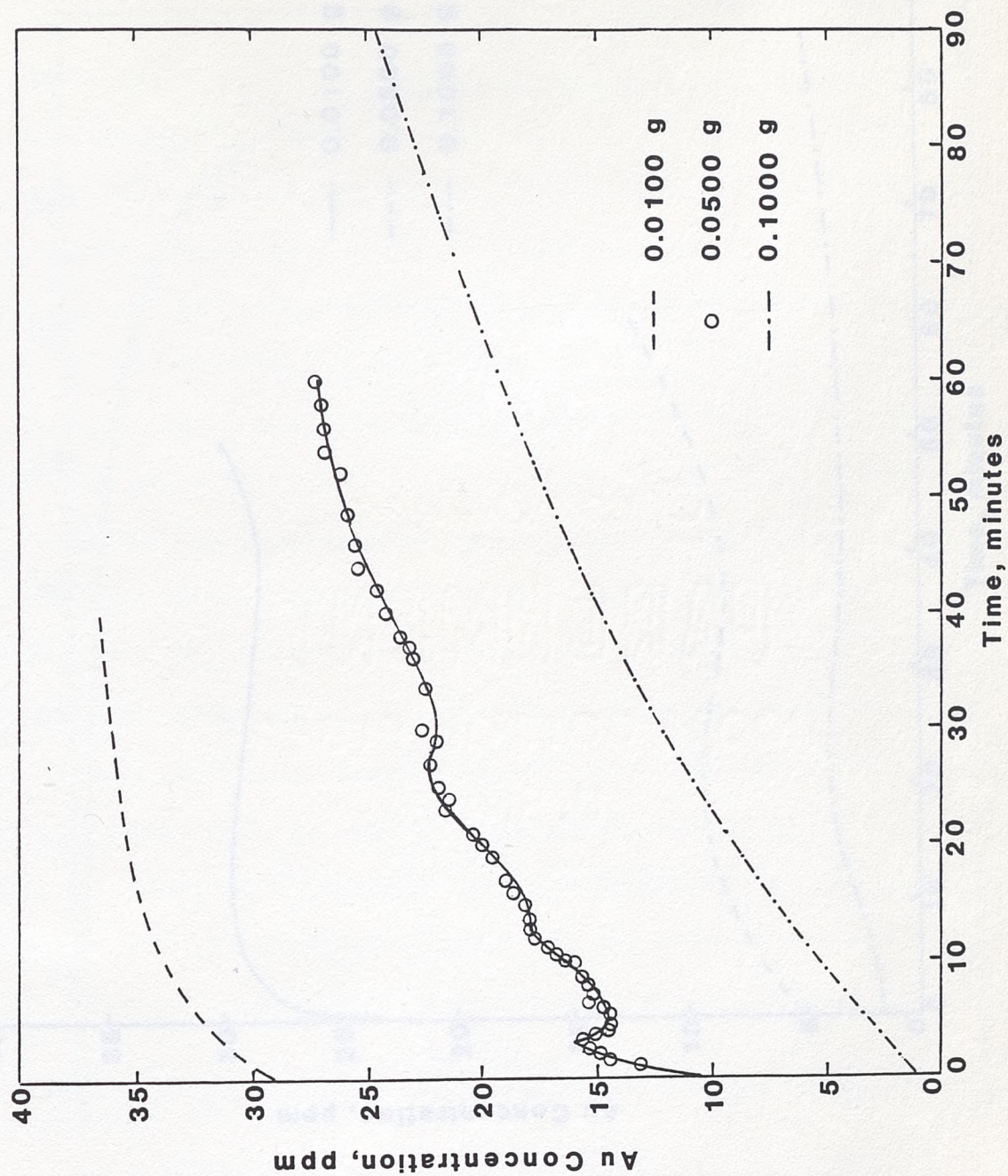


Figure 26. Concentration profiles for the nonrecirculating small-column adsorption of aurothiurea on activated carbon.

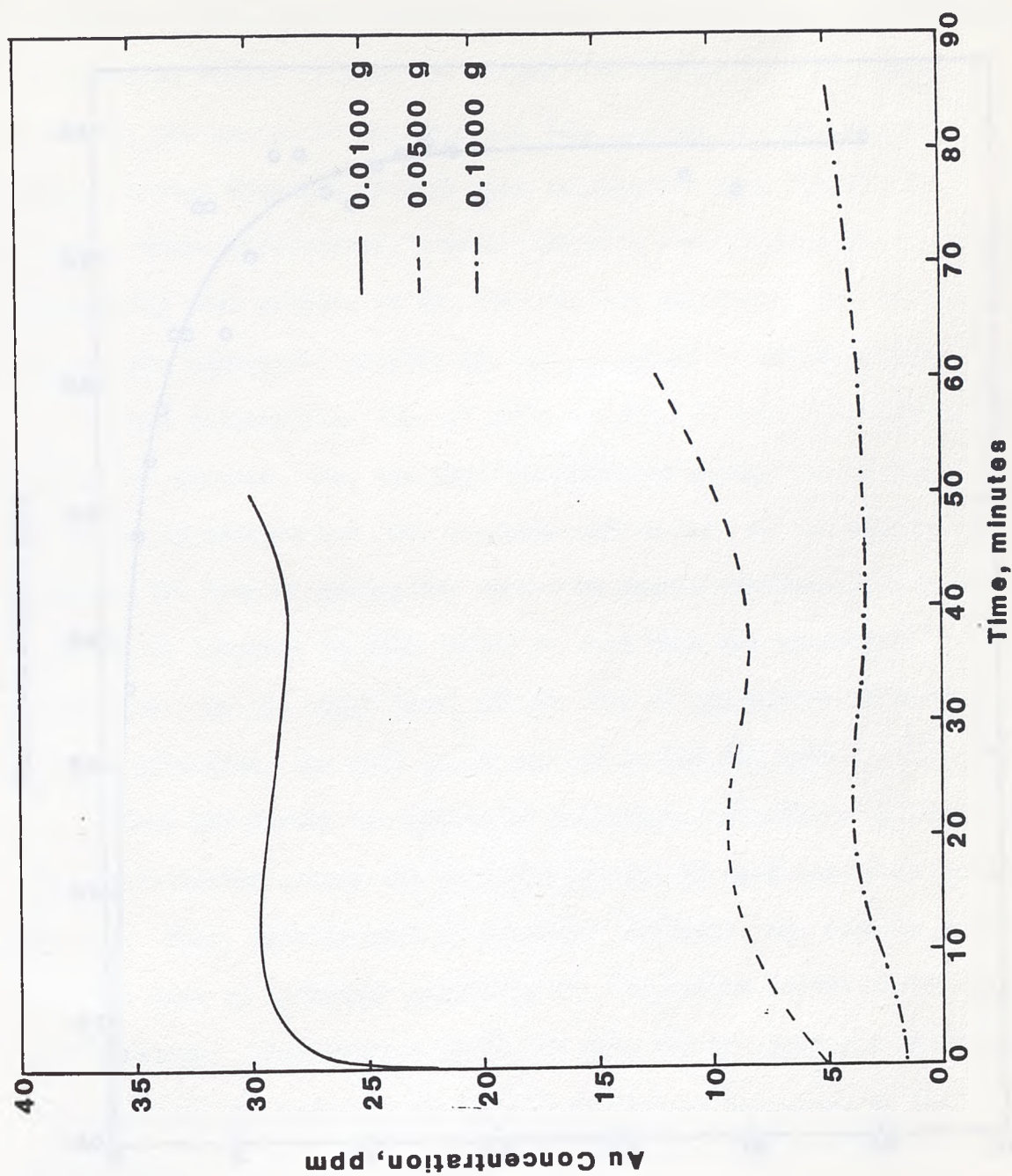


Figure 27. Concentration profiles for the nonrecirculating small-column adsorption of aurothiocyanate on activated carbon.

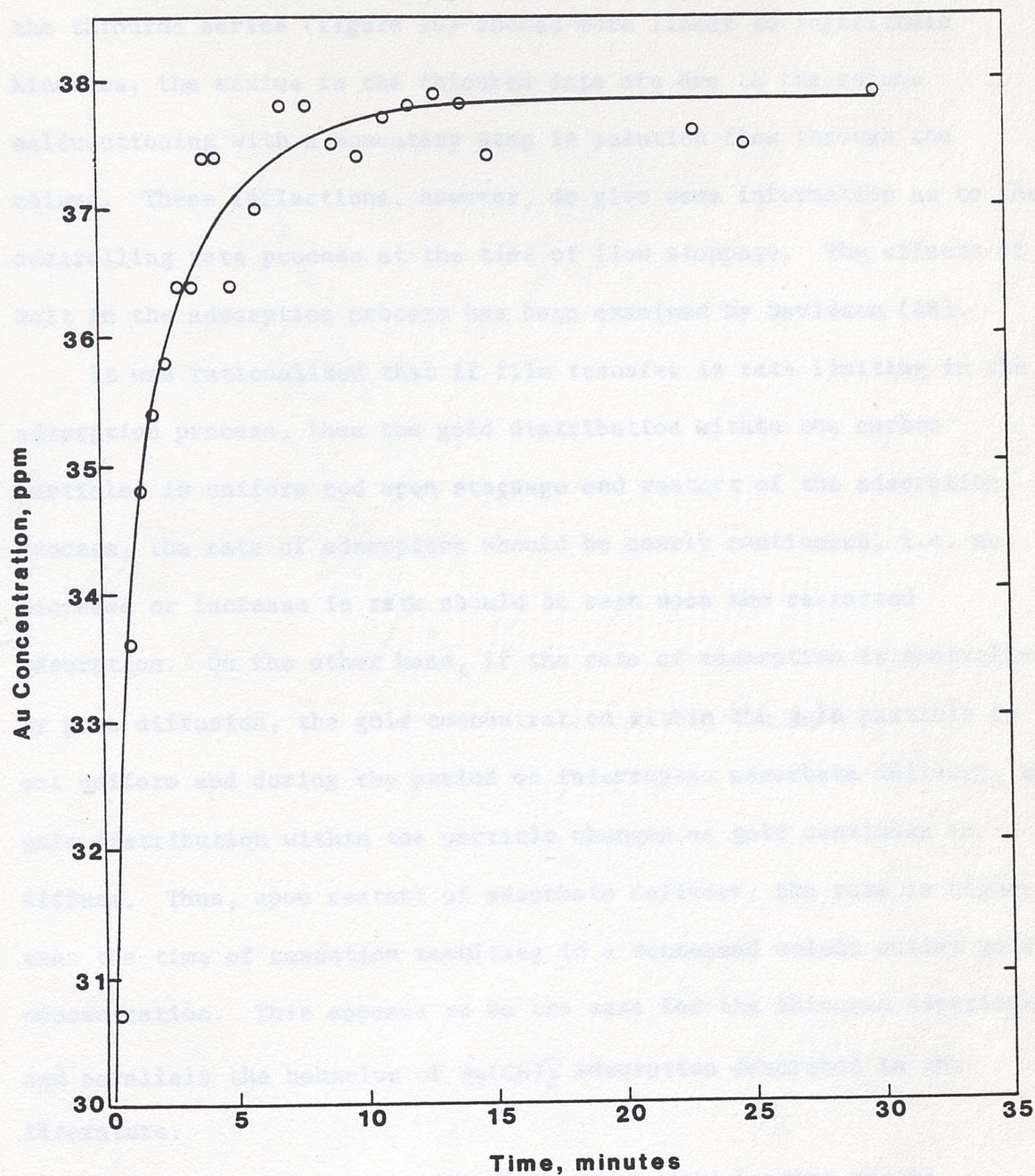


Figure 28. Concentration profiles for the nonrecirculating small-column adsorption of aurothiosulfate on activated carbon (0.0100 g activated carbon).

carbon for the different complexes. The gold cyanide complex (figure 25) showed a second order behavior for all three masses of carbon while the thiourea series (figure 26) showed more linear to logarithmic kinetics; the maxima in the thiourea data are due to the column malfunctioning with a momentary stop in solution flow through the column. These inflections, however, do give some information as to the controlling rate process at the time of flow stoppage. The effects of a halt in the adsorption process has been examined by Davidson (48).

It was rationalized that if film transfer is rate limiting in the adsorption process, then the gold distribution within the carbon particles is uniform and upon stoppage and restart of the adsorption process, the rate of adsorption should be nearly continuous, i.e. no decrease or increase in rate should be seen upon the restarted adsorption. On the other hand, if the rate of adsorption is controlled by pore diffusion, the gold concentration within the gold particle is not uniform and during the period of interrupted adsorbate delivery, the gold distribution within the particle changes as gold continues to diffuse. Thus, upon restart of adsorbate delivery, the rate is higher than the time of cessation resulting in a decreased column outlet gold concentration. This appears to be the case for the thiourea experiment and parallels the behavior of $\text{Au}(\text{CN})_2^-$ adsorption described in the literature.

The results of calculating the average gold loading on the activated carbon for the small column adsorption of $[\text{Au}(\text{SC}(\text{NH}_2)_2)_2]^+$ and $\text{Au}(\text{CN})_2^-$ are displayed in figures 29 and 30. A couple of features are common to these two figures. Firstly, the initial rate of adsorption

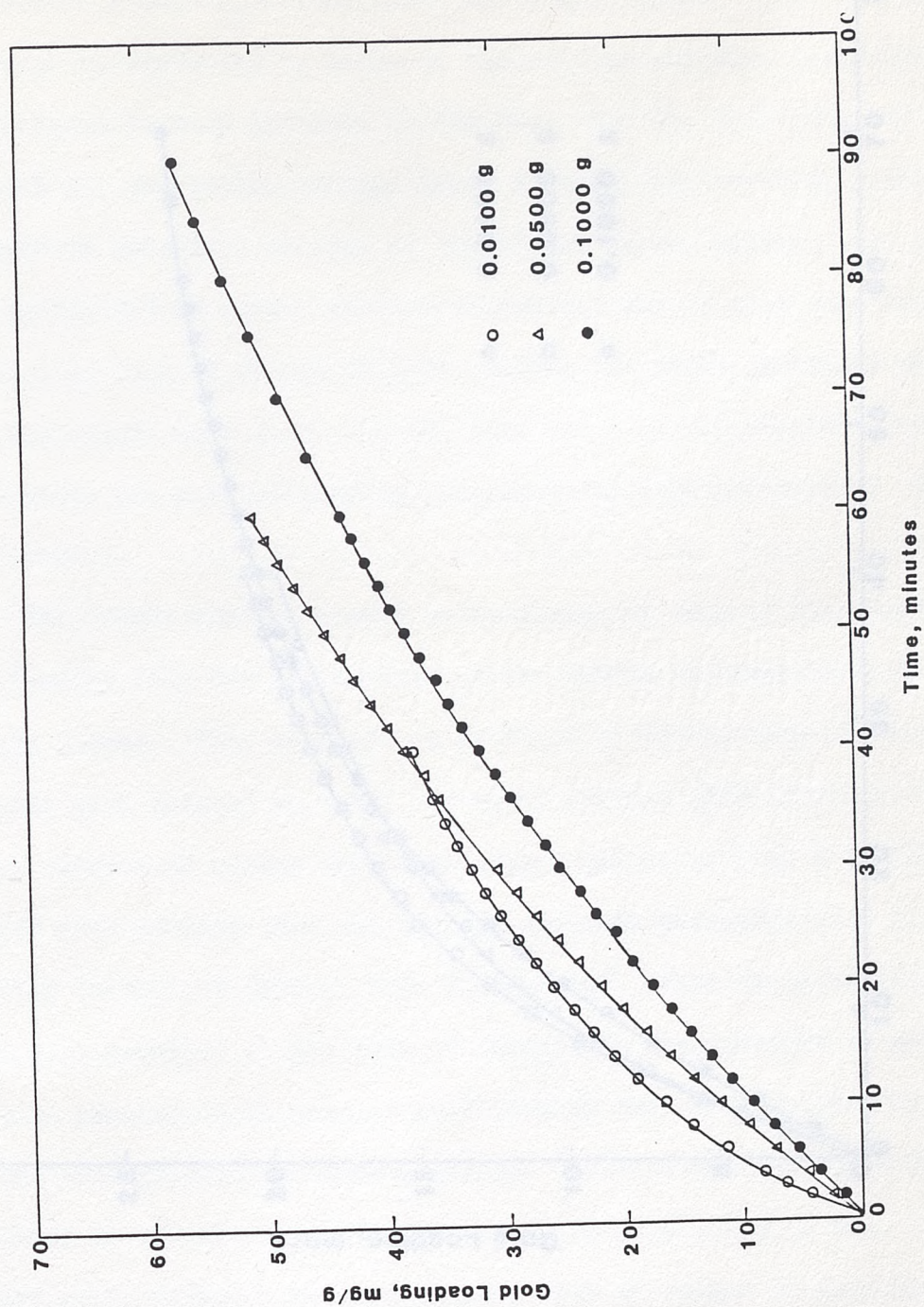


Figure 29. Average gold loading as a function of time for the nonrecirculating small-column adsorption of aurothiurea on activated carbon.

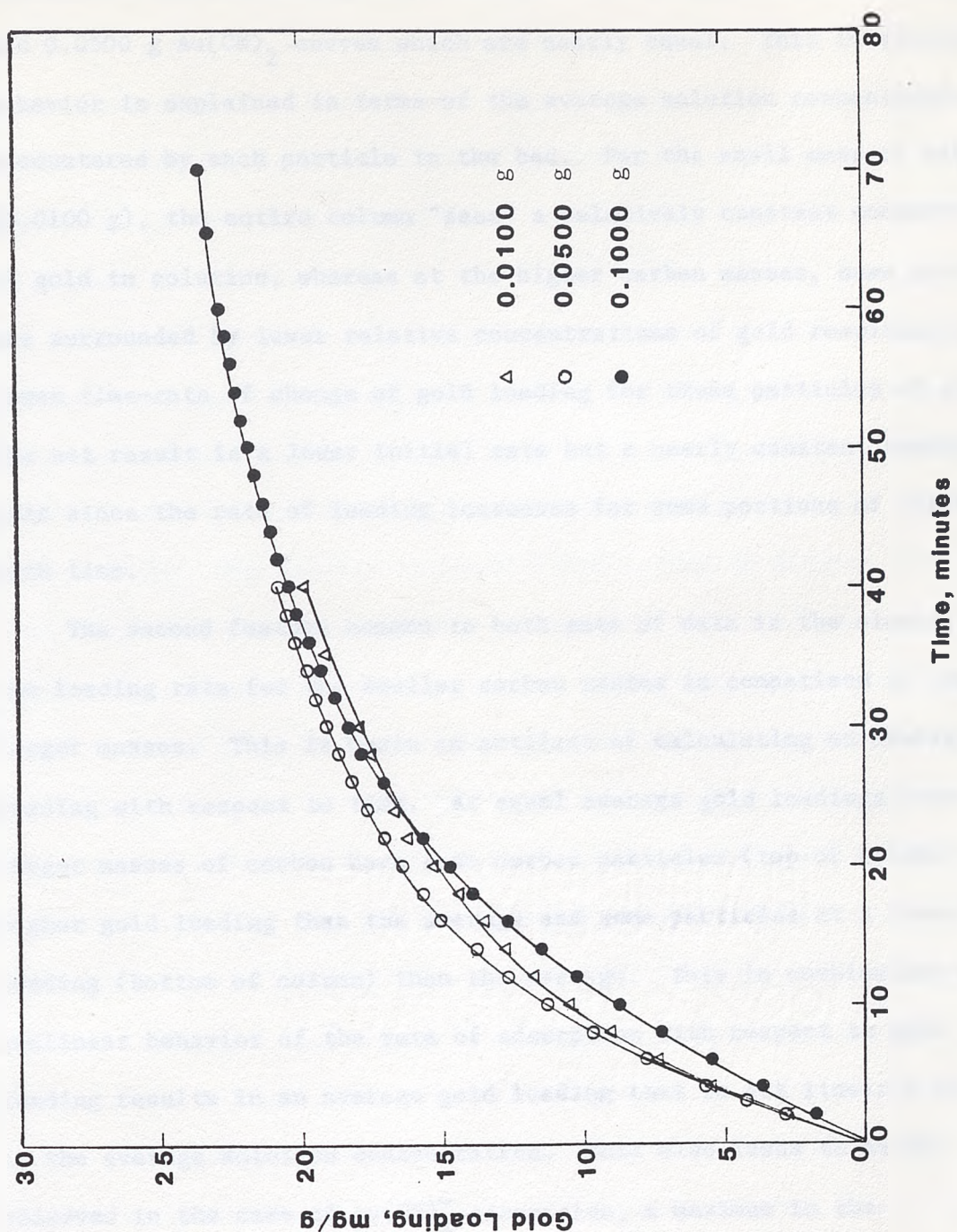


Figure 30. Average gold loading as a function of time for the nonrecirculating small column adsorption of aurocyanide on activated carbon.

decreases with increasing carbon mass with the exception of the 0.0100 and 0.0500 g $\text{Au}(\text{CN})_2^-$ curves which are nearly equal. This initial rate behavior is explained in terms of the average solution concentration encountered by each particle in the bed. For the small mass of carbon (0.0100 g), the entire column "sees" a relatively constant concentration of gold in solution, whereas at the higher carbon masses, some particles are surrounded by lower relative concentrations of gold resulting in a lower time-rate of change of gold loading for these particles of carbon. The net result is a lower initial rate but a nearly constant average rate since the rate of loading increases for some portions of the bed with time.

The second feature common to both sets of data is the slowing of the loading rate for the smaller carbon masses in comparison to the larger masses. This is again an artifact of calculating an average gold loading with respect to time. At equal average gold loadings, the larger masses of carbon have some carbon particles (top of column) at a higher gold loading than the average and some particles at a lower gold loading (bottom of column) than the average. This in combination with a nonlinear behavior of the rate of adsorption with respect to gold loading results in an average gold loading that is not linearly related to the average solution concentration. This also leads to as is observed in the case of $\text{Au}(\text{CN})_2^-$ adsorption, a maximum in the relationship between the initial time-rate of change of gold loading and carbon mass (or length). This would probably be observed with $[\text{Au}(\text{SC}(\text{NH}_2)_2)_2]^+$ adsorption at carbon masses less than 0.0100 g.

As was mentioned in the experimental procedure section, the eluting

behavior of the gold complexes from the activated carbon could be observed by passing deionized water through the small column adsorption cells following cessation of adsorbate delivery; this procedure was performed for the 0.0100 and 0.0500 g adsorption experiments. The gold concentration of the column effluent as a function of time is depicted in figures 31 and 32.

Figure 31 displays the outlet concentration for both complexes and percent recovery for $\text{Au}(\text{CN})_2^-$ as a result of eluting the gold complexes from the 0.0100 g masses of carbon; the terminal $[\text{Au}(\text{SC}(\text{NH}_2)_2)_2]^+$ and $\text{Au}(\text{CN})_2^-$ adsorbate concentrations were 37.6 ppm and 36.7 ppm respectively. The results indicate a rapid decay in elution rate for both complexes with no detectable increase in solution concentration upon elution above that for adsorption; the elution of $[\text{Au}(\text{SC}(\text{NH}_2)_2)_2]^+$ would indicate that it is strongly adsorbed even in deionized water.

Comparing this to the 0.0500 g adsorptions shown in figure 32 where the terminal adsorbate concentrations for the cyanide and thiourea complexes were 35.7 ppm and 27.3 ppm respectively reveals a substantial difference in elution kinetics. For 0.0500 g carbon and a similar $\text{Au}(\text{CN})_2^-$ loading, a much higher concentration of gold is obtained upon elution; the initial data point is an approximate value in figure 32 due to its magnitude relative to the standards used and is estimated to be plus or minus 20 ppm. Comparing the percent recovery curves for $\text{Au}(\text{CN})_2^-$ for both figures reveals that the relative rate of elution is nearly equal in each case. Thus, the peak concentration obtainable in solution is limited by the initial mass of carbon present (column length) which is consistent with a mathematical model of solution concentration

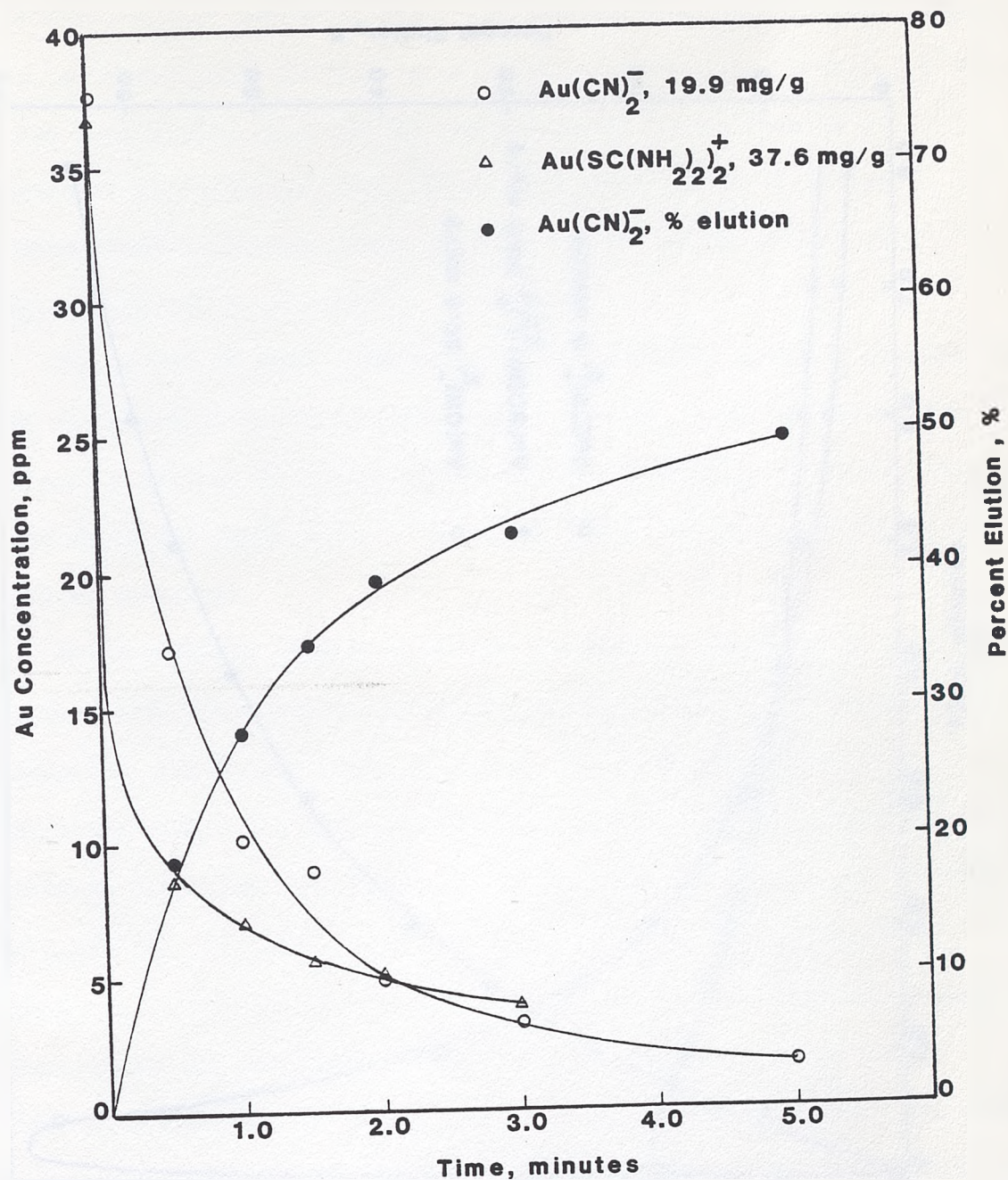


Figure 31. Gold concentration and percent elution profiles for the deionized water elution of gold immediately after loading from aurocyanide and aurothiourea solutions onto 0.0100 g activated carbon.

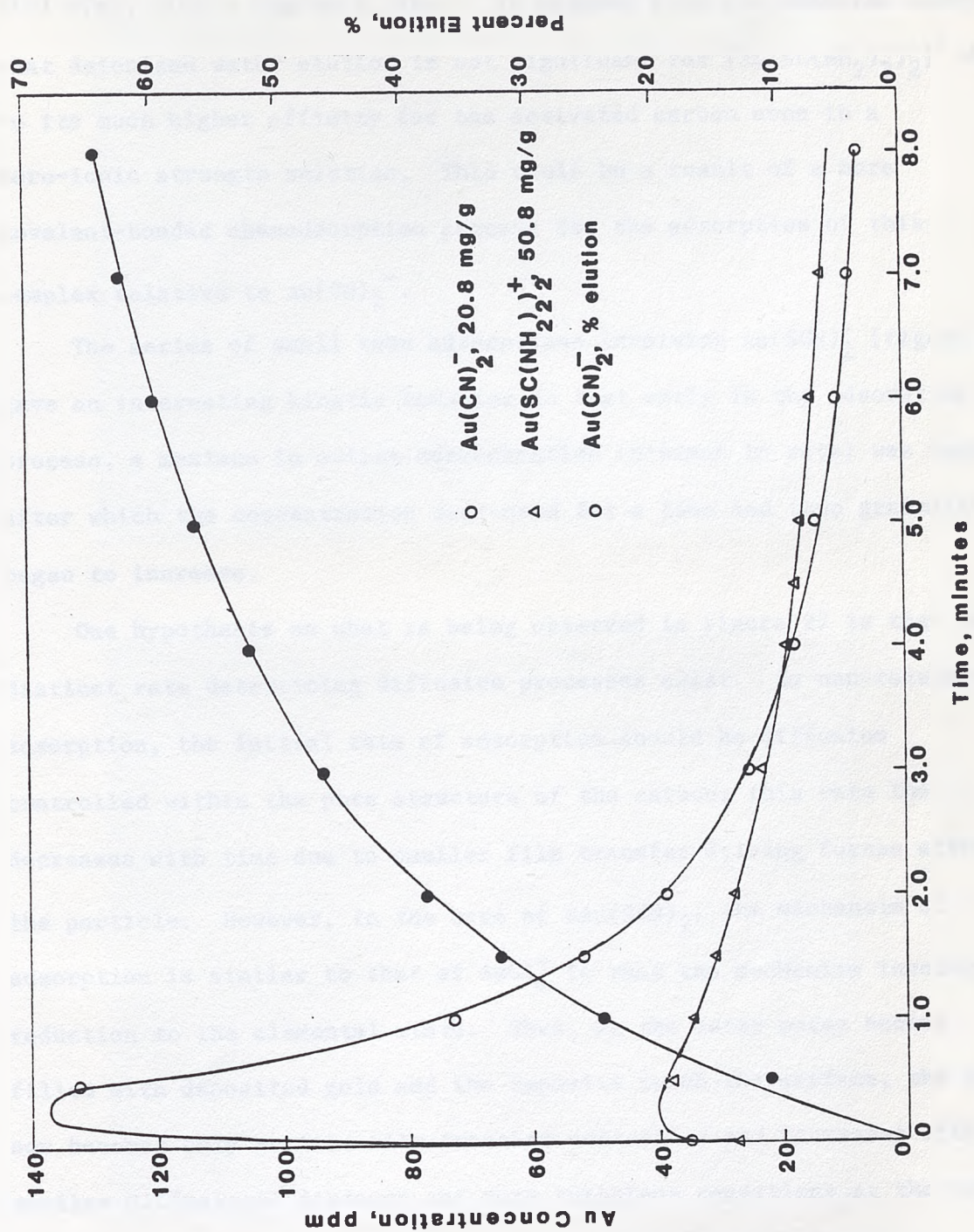
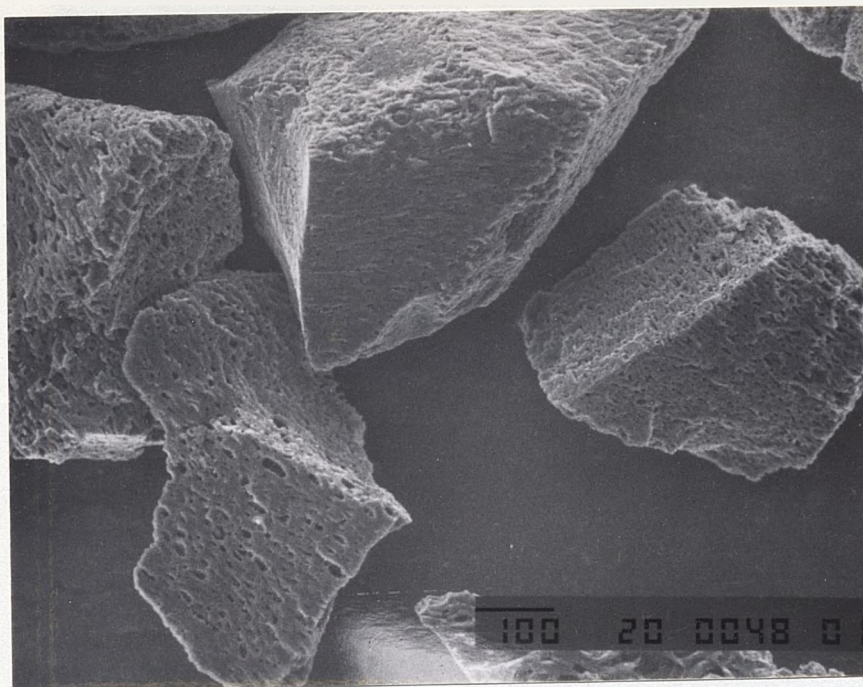


Figure 32. Gold concentration and percent elution profiles for the deionized water elution of gold immediately after loading from aurocyanide and aurothiourea solutions onto 0.0500 g activated carbon

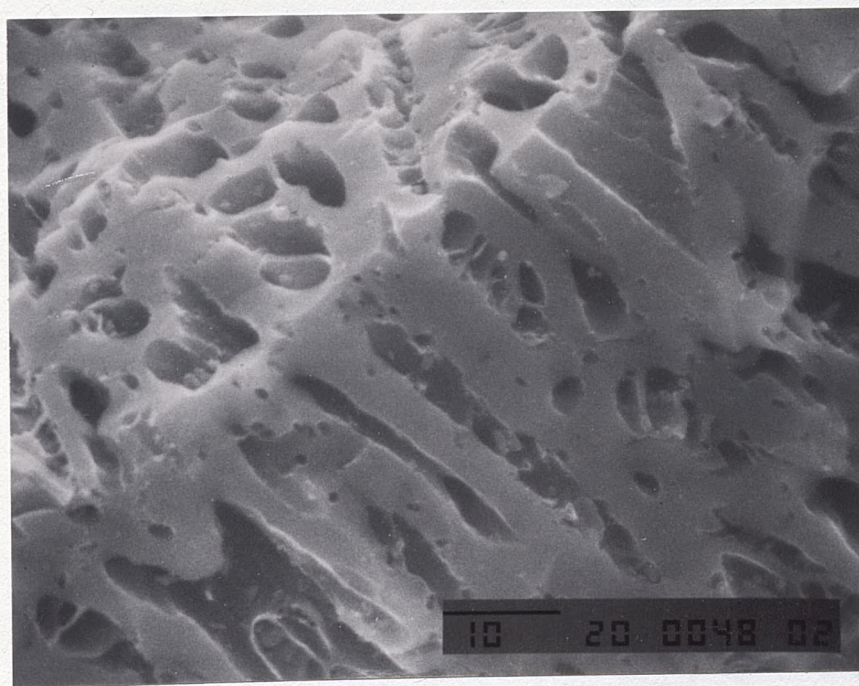
(solution of equation [33]) having a spatially dependent term i.e. $C = f(t) \cdot f(x)$, $f(x) = \exp(x/L)$, etc. It appears from the thiourea curves that deionized water elution is not significant for $[\text{Au}(\text{SC}(\text{NH}_2)_2)_2]^+$ due to its much higher affinity for the activated carbon even in a zero-ionic strength solution. This could be a result of a more covalent-bonded chemadsorption process for the adsorption of this complex relative to $\text{Au}(\text{CN})_2^-$.

The series of small tube adsorptions involving $\text{Au}(\text{SCN})_2^-$ (figure 27) gave an interesting kinetic behavior in that early in the adsorption process, a maximum in outlet concentration (minimum in rate) was reached after which the concentration decreased for a time and then gradually began to increase.

One hypothesis on what is being observed in figure 27 is that two distinct rate determining diffusion processes exist. In non-reductive adsorption, the initial rate of adsorption should be diffusion controlled within the pore structure of the carbon; this rate then decreases with time due to smaller film transfer driving forces within the particle. However, in the case of $\text{KAu}(\text{SCN})_2$, the mechanism of adsorption is similar to that of AuCl_4^- in that the mechanism involves reduction to the elemental state. Thus, as the outer pores become filled with deposited gold and the deposits reach the surface, the rate now becomes only surface film transfer controlled and increases with the smaller diffusional distance and more turbulent conditions at the outer surface. The basis for this model stems from scanning electron micrographs of the carbon surface after adsorption with $\text{Au}(\text{SCN})_2^-$. These micrographs are displayed in figures 33 to 36.

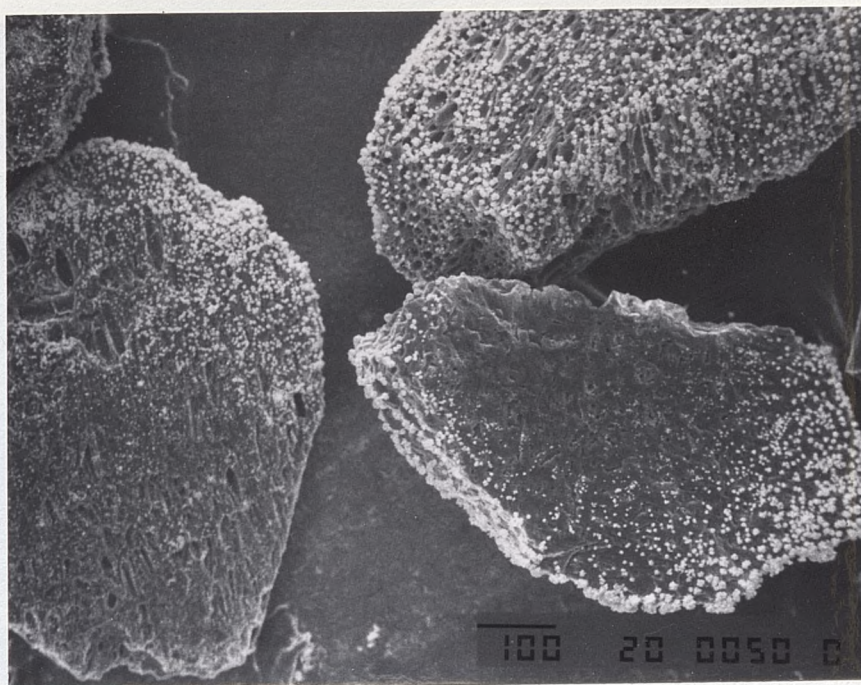


(a)

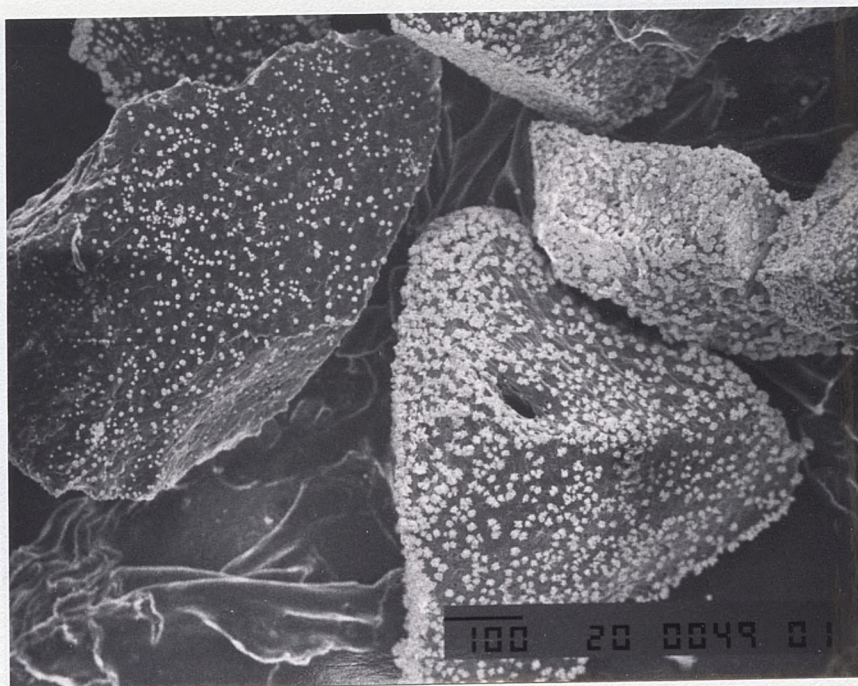


(b)

Figure 33. Scanning electron micrographs of activated carbon particles prior to adsorption: (a) 100X, (b) 1500X.

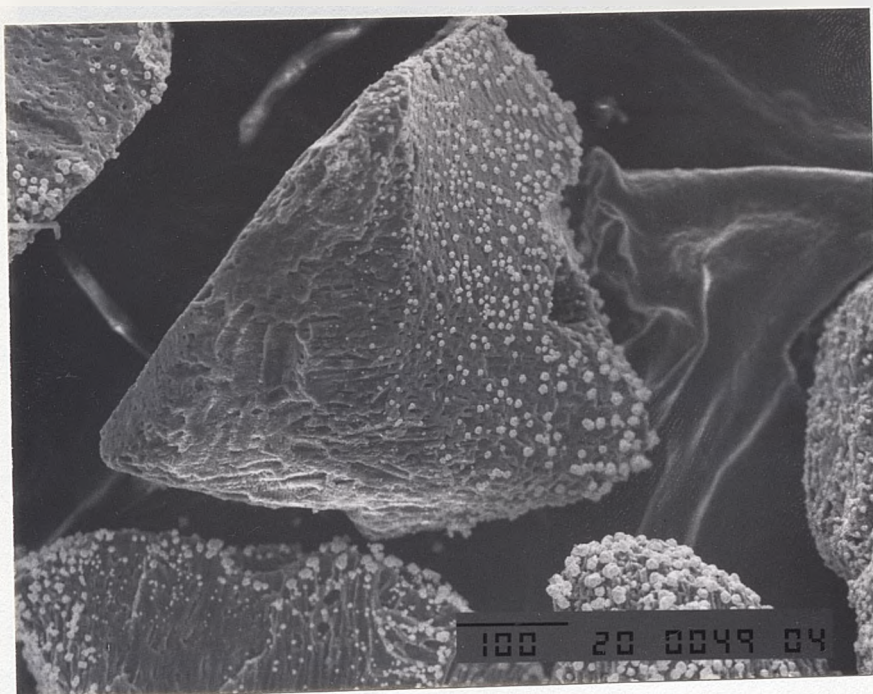


(a)

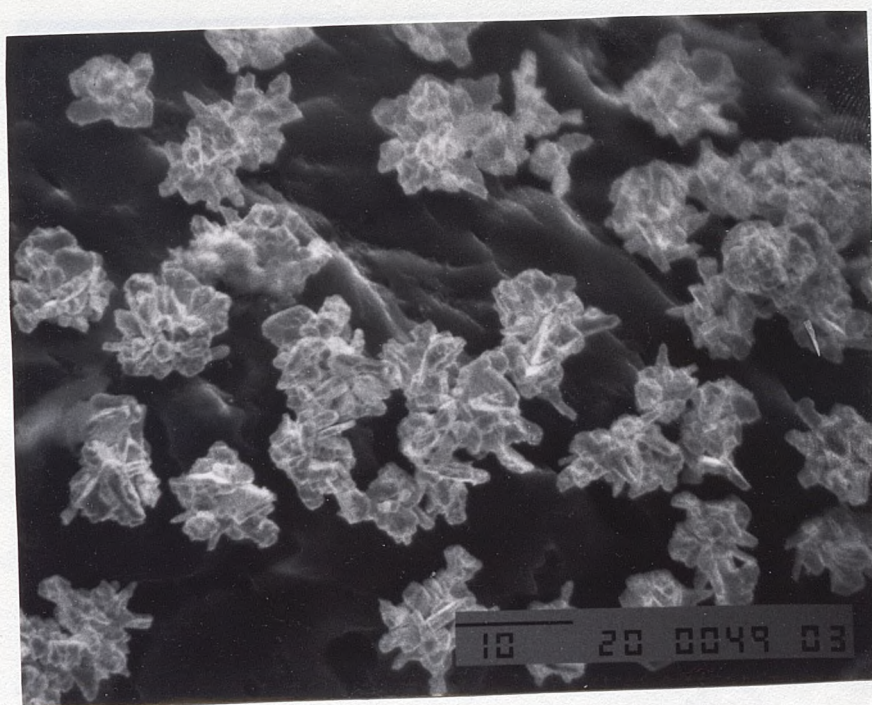


(b)

Figure 34. Scanning electron micrographs of activated carbon particles after adsorption of $\text{Au}(\text{SCN})_2^-$: (a) 100X, 226 mg/g; (b) 100X, 331 mg/g.

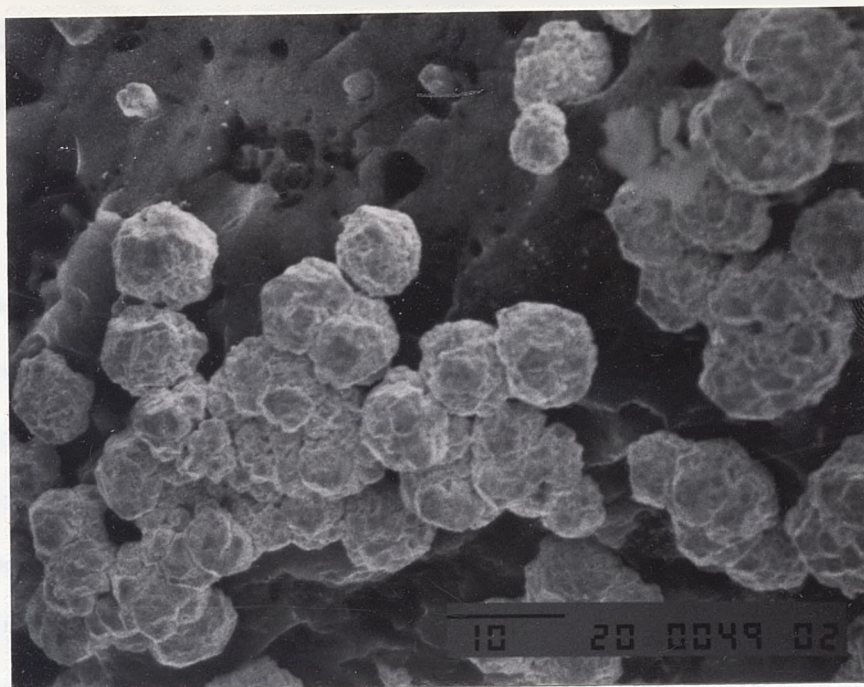


(a)

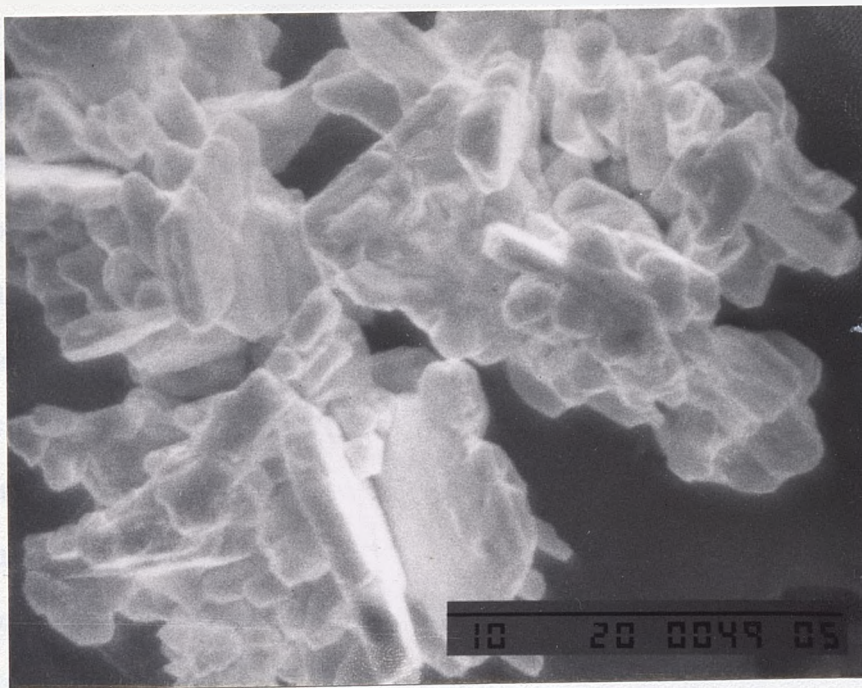


(b)

Figure 35. Scanning electron micrographs of activated carbon particles after adsorption of $\text{Au}(\text{SCN})_2^-$ to a 331 mg/g loading: (a) 150X micrograph of general structure; (b) 1500X micrograph of platelet-type crystal aggregates.



(a)



(b)

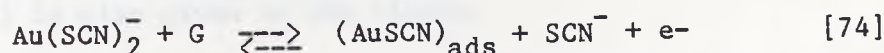
Figure 36. Scanning electron micrographs of activated carbon particles after adsorption of $\text{Au}(\text{SCN})_2^-$ to a 331 mg/g loading: (a) 1500X micrograph of spherule formation; (b) 5000X micrograph of platelet formation.

Figure 33 shows the activated carbon before adsorption at 100X and 1500X magnification; this high magnification reveals the porous nature of the carbon material. Figure 34 compares the observed gold deposits at two different gold loadings showing the increased coverage in the 331 mg/g case. It should be noted how heterogeneous the gold loading is from surface to surface. It appears as was reported for AuCl_4^- adsorption that higher loadings are found on particles with higher porosity and thus higher concentrations of surface functional groups capable of being oxidized.

Figure 35 displays two more micrographs at higher magnification of the 331 mg/g Au loaded carbon. Figure 35(b) is a 1500X magnification of the platelet-type crystals seen in figure 34(b). As can be seen from 34(b), two types of aggregates are found; the platelet type where rectangular crystals protrude from a nucleated center or the spherule type where the crystal aggregate has grown as a ball and appear in colonies. Figure 36 displays a 1500X micrograph of the spherule-type crystals and a 5000X micrograph of the platelet crystals; the fragmentation of platelets or growth of small platelets might produce the spherule crystal. The overall placement or concentration of gold deposits was at the end of the pore sites indicating selective nucleation either in the pore or at the pore edge on the solid surface. It is obvious, however, that electron transfer is readily accomplished at both the carbon/aqueous interface and gold/aqueous interface.

This leads to the possibility and postulation that diffusion is not controlling the rate of adsorption for $\text{Au}(\text{SCN})_2^-$, but the electron

transfer reaction at the surface is rate controlling. Writing this in equation form,



where C and G represent the carbon and gold surface sites respectively. Hence, it is likely that electron transfer to the delocalized pi orbitals of the aromatic carbon structure is not as favorable as transfer to the band structure of the gold metal. Thus, initially the rate is slower with reaction [73] dominating, but as gold deposits form, reaction [74] predominates with a more rapid rate. If both reactions are rapid such that the adsorption step in the electrochemical process is rate controlling, then the increased sites for adsorption with gold deposition could account for a rate that increases with gold loading.

Only one small tube adsorption experiment was conducted for $\text{Au}(\text{S}_2\text{O}_3)_2^{3-}$ due to its poorly adsorbing nature. This was done with 0.1000 gram of activated carbon with the concentration behavior shown in figure 28. Obviously only a few sites are capable of adsorbing this complex with the rate of adsorption essentially zero after 30 minutes at a gold loading of 0.718 mg/g.

Equilibrium Adsorption Experiments

To observe the relative adsorption of the different gold complexes on activated carbon, preliminary equilibrium tests were performed in a shaker bath at 25.0°C; The equilibrating period was 48 hours and the solution conditions were 0.1 M in the respective ligand and 10^{-4} M KOH

and 0.1 M HCl for cyanide and thiourea complexes respectively. The graphical display of the adsorption is shown in figure 37 where the logarithm of gold loading is plotted as a function of the logarithm of solution concentration; the correlation with the Freundlich expression (equation [26]) is also given in the figure.

The data indicate that the thiocyanate and thiourea complexes have much higher gold loadings than the cyanide complex and also have less scatter in the data. The n -values for the Freundlich correlation reveal an interesting trend. The n -values for gold thiourea and gold thiocyanate are indicative of a chemisorption process (reduction for $\text{Au}(\text{SCN})_2^-$), whereas, the high value obtained for gold cyanide is characteristic of physical adsorption of neutral molecules; this is also atypical for $\text{Au}(\text{CN})_2^-$ adsorption on activated carbon where n -values are generally less than 0.5. The capacity constant of this carbon for $\text{Au}(\text{CN})_2^-$ under these conditions is also slightly low; however, this could be due to the solution being 0.1 M in NaCN and the wide variation in the active properties of commercial carbons. The initial rate for the 0.0100 gram experiments is correlated to the respective B constant (capacity constant) in the Freundlich isotherm with a correlation coefficient of 0.99999. This is indicative of the diffusion kinetics with the driving force for adsorption being proportional to the gold capacity.

The adsorption of gold thiocyanate which has been determined to be adsorbed by a reduction mechanism to elemental gold by necessity causes the oxidation of a surface functional group. This might be proposed to be the reverse of that proposed by Tsuchida and Muir (65):

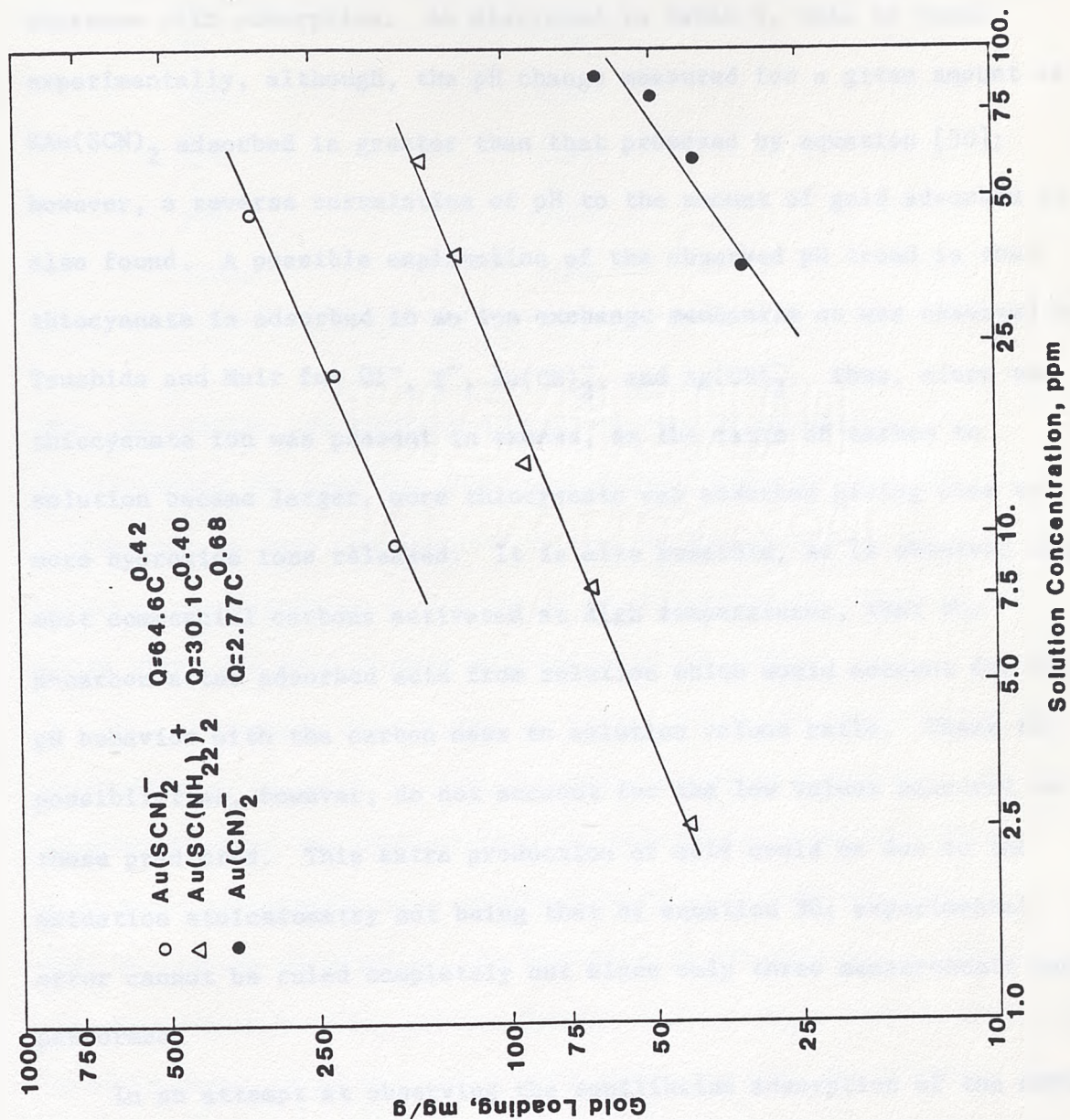
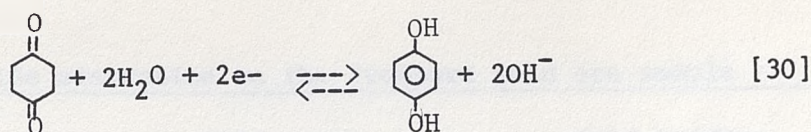


Figure 37. Log-Log plot of gold loading as a function of solution concentration for correlation of equilibrium adsorption data to the Freundlich isotherm.



Thus, if the reverse reaction is considered, the solution pH should decrease with adsorption. As displayed in table 3, this is found experimentally, although, the pH change measured for a given amount of $\text{KAu}(\text{SCN})_2$ adsorbed is greater than that proposed by equation [30]; however, a reverse correlation of pH to the amount of gold adsorbed is also found. A possible explanation of the observed pH trend is that thiocyanate is adsorbed in an ion exchange mechanism as was observed by Tsuchida and Muir for Cl^- , I^- , $\text{Au}(\text{CN})_2^-$, and $\text{Ag}(\text{CN})_2^-$. Thus, since the thiocyanate ion was present in excess, as the ratio of carbon to solution became larger, more thiocyanate was adsorbed giving rise to more hydroxide ions released. It is also possible, as is observed with most commercial carbons activated at high temperatures, that the H-carbon sites adsorbed acid from solution which would account for the pH behavior with the carbon mass to solution volume ratio. These two possibilities, however, do not account for the low values measured to those predicted. This extra production of acid could be due to the oxidation stoichiometry not being that of equation 30; experimental error cannot be ruled completely out since only three measurements were performed.

In an attempt at observing the equilibrium adsorption of the above mentioned complexes on the carbonaceous gold ore sample, an equilibrium experiment was performed at 25.0°C . The first series shown in table 4 is for adsorption of $\text{Au}(\text{CN})_2^-$ from a $0.1\text{M NaCN}/10^{-4}\text{ KOH}$ solution containing specified concentrations of calcium ions. These results show

Table 3. Gold cyanide adsorption on the Freeport gold ore sample

Ca^{+2} , conc. ppm	Gold, conc. ppm	Gold loading mg/g
0.	3.12	0.353
100.	2.81	0.412
250.	2.89	0.397
500.	2.81	0.412
1000.	2.81	0.412

that the calcium ion enhances adsorption but the adsorption is significantly the same for calcium concentrations over 100 ppm; it is interesting to note the capacity of the ore for adsorbing $\text{Au}(\text{CN})_2^-$ at a solution concentration of 2.8 ppm is approximately 12 oz/ton or about forty times the gold present originally in the ore.

The adsorption results for $\text{Au}[\text{SC}(\text{NH}_2)_2]^+$ on the carbonaceous ore are presented in table 5. The thiourea complex is moderately adsorbed in comparison to the limited data for the cyanide complex. These adsorption experiments were conducted with an initial solution of 0.1 M HCl, but it was observed at the beginning of the experiment that the HCl was reacting with CaCO_3 present forming gaseous CO_2 . This also resulted in an increase in pH as noted in the table for each data point. The poor correlation with the Freundlich isotherm of all four data points indicates that the solution pH possibly affects the $\text{Au}[\text{SC}(\text{NH}_2)_2]^+$ adsorption on the ore as it does for $\text{Au}(\text{CN})_2^-$ adsorption on activated carbon. The first three data points correlate with a 0.978 correlation

Table 4. Gold thiourea adsorption on the Freeport gold ore sample

Solution, conc. ppm	Gold loading mg/g	pH
21.0	2.88	5.97
25.5	3.46	5.71
30.6	5.00	5.06
32.2	10.4	6.45

Table 5. Results for gold thiocyanate adsorption on activated carbon

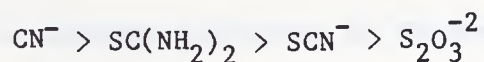
mmole Au adsorbed	Gold loading mg/g	mg carbon/ ml solution	measured pH	predicted pH
1.68×10^{-2}	331	0.2	3.99	4.76
2.30×10^{-2}	226	0.4	4.22	4.63
2.60×10^{-2}	171	0.6	4.48	4.58

coefficient to the isotherm expression with the 10. mg/g data point indicated to be high. The note above comparing the carbonaceous ore's capacity for gold thiourea to that for gold cyanide was based on calculating the equivalent gold loading of gold thiourea at 3.0 ppm from the Freundlich isotherm correlation of the first 3 data points in table 3; the calculated loading of gold thiourea at a 3.0 ppm solution concentration is 0.164 mg/g. Thus, even though the data presented shows significant gold thiourea adsorption, it is still less than that of $\text{Au}(\text{CN})_2^-$; data covering a broader concentration range for each species are needed to properly assess the gold ores capacity for adsorbing each species.

Data obtained for the adsorption of $\text{Au}(\text{SCN})_2^-$ proved to be erroneous due to the instability of $\text{Au}(\text{SCN})_2^-$ at the alkaline pH values (>7.5) encountered with the ore; thus, when the solution was equilibrated, the CaCO_3 in the ore raised the pH enough to precipitate $\text{Au}(\text{SCN})_2^-$ as AuOH . However, the extremely low values of gold found in solution (1 to 3 ppm) indicated that reductive or other adsorption had also taken place.

CONCLUSIONS

The anodic dissolution of disseminated gold in a conducting nonadsorbing matrix was found to be most favorable in cyanide solution with an observed rate of dissolution decreasing for the respective ligands in the order:



This relative ordering of anodic dissolution kinetics does not parallel the reported chemical dissolution kinetics for thiourea and cyanide media while it does parallel the chemical kinetics for thiosulfate and thiocyanate solutions. The chemical dissolution of gold in thiourea media is reportedly faster than in cyanide media while thiocyanate ion dissolution is reportedly faster than thiosulfate dissolution (5). The reason for the change in kinetic ordering is the effect of potential on ion migration, adsorption, and surface passivation resulting in different rate determining steps for the anodic dissolution.

For all the ligands, except possibly thiocyanate, the applied potential of 1.2 V vs Ag/AgCl is sufficient to bring the electrochemical step in the reaction mechanisms to be at a steady-state condition. Thus, the kinetics of dissolution are controlled by species diffusion to

or from the gold surface or through a passivating surface film. If in the case of cyanide ion, the rate of dissolution is controlled by transport of cyanide ion to the surface, the diffusive transport is enhanced by ion migration driven by the potential gradient in the diffuse-double layer.

In comparing this to thiourea, the ion migration contribution to the mass transport is absent and since the diffusion coefficients of thiourea and cyanide should be similar in magnitude, the net flux of cyanide ions to the surface is greater than the thiourea flux. The similarity in diffusion coefficients is postulated based on both cyanide and thiourea being weakly hydrated in solution. The weak hydration of aurocyanide also enhances its ability to migrate in a potential field. A further hindrance to thiourea diffusion is the passivating layer of sulfur suspected of forming on the gold surface which further slows the rate of dissolution. If the dissolution in cyanide media is controlled by the desorption step in the dissolution mechanism (equation [19]), then it may be concluded that the rate of cyanide ion transport to the surface is substantially higher than for thiourea.

Thiosulfate dissolution appeared to occur under severely passivating conditions. The initial maximum in the rate of dissolution followed by a subsequent rate increase gives support to this conclusion. This also parallels the chemical dissolution of gold in thiosulfate media where the dominant problem is excessive thiosulfate oxidation and subsequent surface passivation.

It was not conclusive for thiocyanate dissolution whether or not passivation was occurring. A small inflection in the data shown by the

reservoir concentration monitored with the flow-injection system cannot be attributed to passivation with confidence since the atomic absorption detector did not always operate flawlessly. It is possible that the dissolution was under chemical reaction control at the surface by either the electrochemical step or desorption step if the mechanism of dissolution parallels that in chloride solution (equations [7]-[9]).

Thus, it may be concluded from the anodic results in spectroscopic carbon, that cyanide solution is the most efficient media for anodically dissolving disseminated gold. Conclusions as to the optimum potentials to be used cannot generally be made from these data, but a couple of specific ones can be made.

In cyanide media it was observed that a solution saturated with air gave nearly as rapid dissolution kinetics as 1.2 V vs Ag/AgCl. The oxidation potential at the gold surface based on Nernstian behavior for the oxygen/water couple, an oxygen activity equal to its mole fraction in air (0.21), and a solution pH of eleven yields an approximate oxidation potential of +0.57 V vs Ag/AgCl; this figure is probably higher than that under active dissolution conditions, but it may be concluded that even at this low potential cyanide dissolution kinetics will be more rapid than in thiourea solution. This is postulated on comparing the thiourea rate at 0.5 V (figure 7) and the chemical dissolution rate in cyanide solution (figure 9).

It may be further concluded that there is no increase in the rate of gold dissolution in thiourea solution above 0.5 V vs Ag/AgCl irrespective of the solution acidity and that from experimental observations, appreciable dissolution in thiocyanate media does not

occur below 1.2 V vs Ag/AgCl. It cannot be concluded from this data that the anodic dissolution of gold in thiosulfate media would not be improved upon by using lower applied potentials possibly avoiding surface passivation.

With respect to anodic dissolution of disseminated gold from an activated carbon matrix, it can be concluded that chloride, thiocyanate, and thiourea are of little use since adsorption under positive potentials is quite strong. It is possible that at high positive potentials greater than 1.5 V vs Ag/AgCl, gold thiourea would be desorbed from the activated carbon like it is from cation exchange resins; however, the anodic dissolution in activated carbon is prohibited at these high potentials due to excessive oxidation of thiourea. And thus, with the extremely slow rate of recovery observed at potentials approaching 0.8 V, it can be concluded that anodic dissolution of gold from an activated carbon matrix with thiourea is not significant.

The anodic dissolution of disseminated gold was found to be possible in an activated carbon matrix at -0.6 V vs Ag/AgCl in 0.1 M NaCN solution. This was concluded to be possible by the effect of electrical potential on the adsorbing properties of the activated carbon.

The results of the electroelution experiments proved that the electrical potential of the activated carbon with respect to the aqueous phase can be manipulated to change the adsorbing capacity of the carbon for Au(CN)_2^- with lower gold loadings possible at more negative potentials. It was also shown that the ionic character of the eluting

solution significantly affected the recovery of gold cyanide under applied potential as is found in elution without applied potential; deionized water gave the highest elution rates.

The physical explanation for this phenomenon is not known but is proposed to be due to the shift in redox equilibria such as equation [30] coupled with an oxidative adsorption mechanism. Another description of this postulation is that the carbon normally acts as a reversible electrode; it is capable of reducing $\text{Au}(\text{SCN})_2^-$ and AuCl_4^- and can also oxidatively adsorb $\text{Au}(\text{CN})_2^-$ as shown by Tsuchida and Muir. Thus, by simply adjusting this reversible potential, the gold adsorption shifts accordingly to bring about a new equilibrium.

A further conclusion to be drawn, however, is that even though the potential of the carbon was made considerably positive (2.0 V vs Ag/AgCl), AuCl_4^- was not removed from the carbon which would be a reversal of the reduction mechanism. This was proposed to be due to another adsorption mechanism promoted by positive potentials possibly involving electrostatic attraction.

The conclusions from the adsorption experiments are that the rate of adsorption for gold complexes in a column adsorption situation increases with the equilibrium capacity of the carbon for the complex. The shapes of the small column curves indicated that pore diffusion was the rate controlling process for the adsorption of gold cyanide and gold thiourea on activated carbon. The consistent maximum in the rate of adsorption of gold thiocyanate indicated a change with gold loading in either the diffusive process or electron-transfer reaction leading to adsorption.

The conclusion on the effect of thiosulfate ions on the capacity of activated carbon to adsorb $\text{Au}(\text{CN})_2^-$ is limited to the statement that a 0.1 M thiosulfate concentration does hinder the adsorption of $\text{Au}(\text{CN})_2^-$ to a significant extent. The adsorption of gold thiosulfate was observed to be practically zero in comparison to the other gold(I) complexes and is postulated to be due to its high negative charge but is also possibly due to its ligand groups being more spatially restrictive; the tetrahedral thiosulfate group with a significant electron density should limit the surface orientations possible where the metal center can still coordinate.

With respect to carbonaceous gold ore, the adsorption of $\text{Au}(\text{CN})_2^-$ was observed to be kinetically enhanced by the presence of calcium ions in solution. This adsorption also was concluded to be a rapid surface transport controlled process. Significant gold thiourea adsorption was possible on the carbonaceous gold ore but the ore's capacity for gold thiourea is still less than that for gold cyanide.

The use of the on-line flow injection analysis was found to be invaluable with respect to the speed and precision of analysis of the gold concentration in solution. This speed and precision makes detectable small changes in rate processes that may occur in the duration of an experiment. It also allows the scale-down of experiments to a more manageable level in a practical sense. This was shown in the small column adsorption experiments where the bulk of the adsorption breakthrough curve was generated for the adsorption of $\text{Au}(\text{CN})_2^-$.

RECOMMENDATIONS

It is recommended that further work be done in the investigation of the effects of electrical potential on the adsorbing properties of activated carbon. These studies should evaluate the effect of applied potential coupled with different solution compositions, elution temperatures, and carbon materials. This work has the potential of leading to the profitable use of applied potential in the adsorbing and desorbing processes for recovering gold from pregnant cyanide solutions.

The flow system to be used was found to be important relative to the significance of the measured quantities. This was observed in the case of the recirculating adsorption experiments where the adsorption was so great that the experiment was insensitive to the differences in the activated carbon's capacity for the various gold complexes. Thus, the choice of the flow-system to be used should reflect this consideration; the use of a recycling reservoir system also couples two dynamic elements that need to be mathematically extricated to follow the kinetic behavior of either element.

The optimum choice of parameters to be investigated with column adsorption experiments may also be recommended based on the information from the small-tube experiments. The use of different carbon masses was not the best choice in parameters to vary since the adsorption was still quite significant and resulted in the adsorbing properties of the carbon being both a function of position and time; this makes conclusions based on a per mass or surface area of carbon basis an approximation without extensive mathematical modelling. In essence, the increase in carbon mass made the carbon bed length increase and to appreciate the effect of

changing this variable requires a mathematical model of the system since its effect is undoubtedly found in the argument of a spatially dependent exponential function.

A more practical choice of a parameter to vary would be the solution concentration or solution flow rate. A concentration change may allow assumptions about the initial rate to be determined while the effects of solution flow rate would expound on any surface mass transport dependence of the adsorption rate.

With respect to electrode preparation, the method of using specifically-mixed gold/carbon mechanical mixtures is advocated over the use of a stock mixture. With the stock mixture, the relative difference in specific gravities for gold and carbon causes a separation and composition disparity to occur when preparing the porous electrode; even the use of known masses of gold for each electrode does not insure that the gold will be evenly distributed throughout the bed. Although not investigated in this work, the use of carbon with an electroplated gold coating might prove to be a more precise method of experimentation for anodically dissolving gold in a disseminated state.

BIBLIOGRAPHY

- 1 Hausen, D.M. and Bucknom, C.H., Study of preg robbing in the cyanidation of carbonaceous gold ores from Carlin, Nevada, in: Park, W.C., Hausen, D.M. and Hagni, R.D. (Eds), Applied Mineralogy, AIME, Warrendale, 1984, pp.833-856
- 2 Osseo-Asare, K., et al, Carbonaceous matter in gold ores; isolation, characterization and adsorption behavior in aurocyanide solutions, in: Kudryk, V., Corrigan, D.A. and Liang, W.W. (Eds), Precious Metals: Metallurgy, Extraction, and Mining, AIME, Warrendale, 1984, pp. 125-144
- 3 Osseo-Asare, K., Interfacial phenomena in leaching systems, in: Bautista, R. (Ed), Hydrometallurgical Process Fundamentals, Plenum Press, New York, 1984, pp. 227-269
- 4 Finkelstein, N.P. and Hancock, R.D., A new approach to the chemistry of gold, Gold Bulletin, 7(3)(1974)72-77
- 5 Avraamides, J., Prospects for alternative leaching systems for gold: a review, in: Carbon-In-Pulp Technology for the Extraction of Gold, Australas. Inst. Min. Metall., Melbourne, 1982, pp. 369-391
- 6 Filmer, A.O., Lawrence, P.R. and Hoffman, W., A comparison of cyanide, thiourea, and chlorine as lixivients for gold, in: Perth and Kalgoorlie Branches, Regional Conference on "Gold-Mining, Metallurgy and Geology," Australas. Inst. Min. Metall., 1984, pp. 1-9
- 7 Nicol, M.J., The anodic behavior of gold, part I-oxidation in acidic solutions, Gold Bulletin, 13(1980)46-55
- 8 Nicol, M.J., The anodic behavior of gold, part II-oxidation in alkaline solutions, Gold Bulletin, 13(1980)105-111
- 9 Pletcher, D., Industrial Electrochemistry, Chapman and Hall, London, 1982, pp. 65-87
- 10 Kissinger, P.T. and Heineman, W.R. (Eds), Laboratory Techniques in Electroanalytical Chemistry, Marcel Dekker, New York, 1984, pp. 624-627
- 11 Bard, A.J. and Faulkner, L.R., Electrochemical Methods, Fundamentals and Applications, John Wiley and Sons, New York, 1980, pp. 398-404

- 12 Wang, Y.Y., Principles of packed-bed electrochemical reactors, in: Cheremisinoff, N.P. (Ed), Handbook of Heat & Mass Transfer and Reactor Design, Gulf Publishing, Houston, 1986, 1287-1305
- 13 Rousar, I., Micka, K. and Kimla, A., Electrochemical Engineering II. Parts D-F, Elsevier, New York, 1986, pp. 109-213
- 14 Kissinger, P.T. and Heineman, W.R. (Ed), Laboratory Techniques in Electroanalytical Chemistry, Marcel Dekker, New York, 1984, pp. 163-170
- 15 Nicol, M.J., An Electrochemical and Kinetic Investigation of the Behavior of Gold in Chloride Solutions II. The Anodic Dissolution of Gold, Report No. NIM-1844, Natl. Inst. Metall., Randburg, 1981, 24p
- 16 Nicol, M.J., An Electrochemical and Kinetic Investigation of the Behavior of Gold in Chloride Solutions III. The Gold(III)-Gold(I) Reaction on Platinum and the Disproportionation of Gold(I), Report No. NIM-1846, Natl. Inst. Metall., Randburg, 1981 24p
- 17 Lovrecek, B., Moslavac, K. and Matic, D.J., Anodic dissolution and passivation of gold particularly in the presence of chloride, Electrochimica Acta, 26(8)(1981)1087-1098
- 18 Podesta, J.J., Piatti, R.C. and Arvia, A.J., Periodic current oscillations at the gold/acid aqueous interface induced by HCl additions, Electrochimica Acta, 24(1979)633-638
- 19 Frankenthal, R.P. and Siconolfi, D.S., The anodic corrosion of gold in concentrated chloride solutions, J. Electrochem. Soc., 129(1982)1192-1196
- 20 Horikoski, T., et al., The anodic dissolution behavior of gold in surfuric acid solution containing chloride ions, Nippon Kagakie Kaishi, 8(1983)1118-83
- 22 Benari, M.D., Hefter, G.T. and Karker, A.J., Anodic dissolution of silver, copper, palladium and gold in dimethylsulfoxide-halide solutions, Hydrometallurgy, 10(1983)367-389
- 23 Byerley, J.J. and Enns, K., Electrochemical regeneration of cyanide from waste thiocyanate for cyanidation, Can. Min. Metall. Bull., 77(861)(1984)87-93
- 24 Nicholson, M.M., Voltommetry of thiocyanate ion at the stationary platinum electrode, Analytical Chemistry, 31(1)(1959)138-132
- 25 Groenewald, T., The dissolution of gold in acidic solutions of thiourea, Hydrometallurgy, 1(1976)277-290

- 26 Groenewald, T., Potential applications of thiourea in the processing of gold, J. S. Afr. Inst. Min. Metall., 77(11)(1977)217-223
- 27 Chen, C.K., Lung, T.N. and Wan, C.C., A study of the leaching of gold and silver by acidothioureation, Hydrometallurgy, 5(1980)207-275
- 28 Becker, E., Knothe, M. and Lobel, J., Gold recovery from nonmetallic secondary raw materials by leaching with thiourea and adsorption on ion exchangers, Hydrometallurgy, 11(1983)265-275
- 29 Schulze, R.G., New aspects in thiourea leaching of precious metals, J. Metals, (1984)62-65
- 30 Groenewald, T., Electrochemical studies on gold electrodes in acidic solutions of thiourea containing gold(I) thiourea complex ions, J. Appl. Electrochem., 5(1975)71-78
- 31 Habashi, F., Kinetics and Mechanism of Gold and Silver Dissolution in Cyanide Solution, Bulletin No. 59, Mont. Bur. Mines and Geol., 1959, 42p.
- 32 Pan, T.P. and Wan, C.C., A study of the anodic dissolution of gold in concentrated KCN solution, J. Chem. Tech. Biotechnol., 29(1979)427-432
- 33 Kirk, D.W., Foulkes, F.R. and Graydon, W.F., A study of the anodic dissolution of gold in aqueous alkaline cyanide, J. Electrochem. Soc., 125(9)(1978)1436-1443
- 34 Kirk, D.W., Foulkes, F.R. and Graydon, W.F., The electrochemical formation of Au(I) hydroxide on gold in aqueous potassium hydroxide, J. Electrochem. Soc., 127(5)(1980)1069-1075
- 35 Kirk, D.W., Foulkes, F.R. and Graydon, W.F., Gold passivation in aqueous alkaline cyanide, J. Electrochem. Soc., 127(9)(1980)1962-69
- 36 Kirk, D.W., Foulkes, F.R. and Graydon, W.F., Anodic dissolution of gold in aqueous alkaline cyanide solution at low over potentials, J. Electrochem. Soc., 127(9)(1980)1993-1997
- 37 Osseo-Asare, K., Xue, T. and Ciminelli, V.S., Solution chemistry of cyanide leaching systems, in: Kudryk, V., Corrigan, D.A. and Liang, W.W. (Eds), Precious Metals: Metallurgy, Extraction, and Mining, AIME, Warrendale, 1984, pp. 173-198
- 38 Flett, D.S., Derry, R. and Wilson, J.C., Chemical study of thiosulfate leaching, Trans. Inst. Min. Metall. Sect. C, 92(1983)C216-C223

- 39 Ten-Ara Kelyon, K.A., Bagdasaryon, K.A. and Dgonyon, A.G., On the technological expediency of sodium thiosulfate usage for gold extraction from raw material, *Isv. V.U.Z. Tsvetn. Metall.*, (5)(1984)72-76
- 40 Nickless, G. (Ed), *Inorganic Sulfur Chemistry*, Elsevier, New York, 1968, pp. 85-103
- 41 Mattson, J.S. and Mark, H.B., *Activated Carbon: Surface Chemistry and Adsorption from Solution*, Marcel Dekker, New York, 1971
- 42 Zadra, J.B., A process for the recovery of gold from activated carbon by leaching and electrolysis, Report No. RI4672, U.S. Bur. Mines, 1950
- 43 Kyffin, D., Charles, W.D. and Wilson, D., Gold recovery using activated carbon, in: Reese, D.A. (Ed), *Precious Metals 1983*, Pergamon Press, Toronto, 1984, pp.117-136
- 44 Davidson, R.J., The mechanism of gold adsorption on activated charcoal, *J. S. Afr. Inst. Min. Metall.*, 74(1974)67-76
- 45 Davidson, R.J. and Duncanson, D., The elution of gold from activated carbon using deionized water, *J. S. Afr. Inst. Min. Metall.*, 77(1977)254-261
- 46 Davidson, R.J. and Veronese, V., Further studies on the elution of gold from activated carbon using water as the eluant., *J. S. Afr. Inst. Min. Metall.*, 79(1979) 437-445
- 47 Davidson, R.J., and Strong, B., The recovery of gold from plant effluent by the use of activated carbon, *J. S. Afr. Inst. Min. Metall.*, 83(1983)131-188
- 48 Davidson, R.J., Veronese, V. and Nkosi, M.V., The use of activated carbon for the recovery of gold and silver from gold plant solutions, *J. S. Afr. Inst. Min. Metall.*, 79(1979)281-297
- 49 Dixon, S., Cho, E.H. and Pitt, C.H., The interaction between gold cyanide, silver cyanide and high surface area charcoal, *AICHE Symposium Series*, 1976, pp. 75-83
- 50 Cho, E.H. and Pitt, C.H., The adsorption of silver cyanide on activated charcoal, *Metall. Trans. B*, 10B(1979)159-164
- 51 Cho, E.H. and Pitt, C.H., Kinetics and thermodynamics of silver cyanide adsorption on activated charcoal, *Ibid*, 165-169
- 52 Cho, E.H., Dixon, S. and Pitt, C.H., The kinetics of gold cyanide adsorption on activated charcoal, *Ibid*, 185-189

- 53 McDougall, G.J. and Hancock, R.D., Activated carbons and gold-A literature survey, Minerals Sci. Engng., 12(2)(1980)85-93
- 54 McDougall, G.J., Hancock, R.D., Nicol, M.J., Wellington, D.L. and Copperthwaite, R.G., The mechanism of the adsorption of gold cyanide on activated carbon, J. S. Afr. Inst. Min. Metall., 80(1980)344-356
- 55 McDougall, G.J. and Hancock, R.D., Gold complexes and activated Carbon: A literature review, Gold Bulletin, 14(4)(1981)138-153
- 56 Muir, D.M., Recovery of gold from activated carbon: A review, Carbon-In-Pulp Technology for the Extraction of Gold, Australas. Inst. Min. Metall. 1982, pp. 7-22
- 57 Davidson, R.J., The recovery of gold from plant effluents by the use of activated carbon, J. S. Afr. Inst. Min. Metall., 83(1983)181-188
- 58 Nicol, M.J., Fleming, C.A. and Cromberge, G., The adsorption of gold cyanide onto activated carbon I. The kinetics of adsorption from pulps, J. S. Afr. Inst. Min. Metall., 84(2)(1984)50-54
- 59 Gupta, A. and Ofori-Ansah, K., A study of the electrokinetic properties of activated carbon in relation to gold adsorption, Proc. Australas. Inst. Metall., 289(1984)239-245
- 60 Williams, D.F. and Glasser, D., The modelling and simulation of processes for the adsorption of gold by activated carbon, J. S. Afr. Inst. Min. Metall. 85(9)(1985)237-243
- 61 Van Rensburg, D.J. and Van Deventer, J.S., Simulation of adsorption of metal cyanides in packed beds of activated carbon, in: Extraction Metallurgy '85, Int. Inst. Min. Metall., London, 1985, pp. 289-308
- 62 Muir, D.M., Hinchcliffe, W., Tsuchida, N. and Ruane, M., Solvent elution of gold from CIP carbon, Hydrometallurgy, 14(1985)47-65
- 63 Muir, D.M., Hinchcliffe, W.D. and Griffin, A., Elution of gold from carbon by the Micron Solvent Distillation Procedure, Hydrometallurgy, 14(1985)151-169
- 64 Tsuchida, N. and Muir, D.M., Potentiometric studies in the adsorption of $\text{Au}(\text{CN})_2^-$ and $\text{Ag}(\text{CN})_2^-$ onto activated carbon, Metall. Trans. B, 17B(1986)523-528
- 65 Tsuchida, N. and Muir, D.M., Studies on the role of oxygen in the adsorption of $\text{Au}(\text{CN})_2^-$ and $\text{Ag}(\text{CN})_2^-$ onto activated carbon, Metall. Trans. B, 17B(1986)529-533

- 66 House, C.I. and Shergold, H.L., Adsorption of polyvalent metal species on activated carbon, Trans. Inst. Min. Metall. Sect. C, 93(1984)C19-C22
- 67 De Siegel, E.A. and Soto, A.M., Microscopic observations on the adsorption of metallic gold on activated carbon, Trans, Inst. Min. Metall. Sect. C, 93(1984)C90-C92
- 68 Fleming, C.A. and Nicol, M.J., The adsorption of gold cyanide onto activated carbon. III. Factors influencing the rate of loading and the equilibrium capacity, J. S. Afr. Inst. Min. Metall., 84(4)(1984)85-93
- 69 Deschenes, G., Literature survey on the recovery of gold from thiourea solutions and comparison to cyanidation, CIM Bull., 79(895)(1986)76-83
- 70 Pesic, B., Adsorption of gold on activated carbon from thiourea solutions, Presented at the 1986 National meeting, AIME, Denver, 1986
- 71 Huyhwa, J.C. and Gundiler, I.H., Kinetics of recovery of gold and silver from acidic thiourea solutions by carbon adsorption, Presented at the 1986 National Meeting, AIME, Denver, 1986
- 72 Lie., K.P., Eisele, J.A. and McClelland, G.E., Electrolytic Production of Precious Metals, U.S. Patent No. 4,554,058, 1985
- 73 Walker, A.T.S. and Wragg, A.A., The modelling of concentration-time relationships in recirculating electrochemical reactor systems, Electrochimica Acta, 2(1977)1192-1134
- 74 Nicol, M.J., Fleming, C.A. and Cromberge, G., The adsorption of gold cyanide onto activated carbon. II. Application of the kinetic model to multistage adsorption operations, J. S. Afr. Inst. Min. Metall., 84(3)(1984)70-78
- 75 Taylor, P.D., Clay, S.E. and Martins, G.P., The mathematical modelling of continuous activated carbon precious metal circuits, in: Gaskell, D.R., Hager, J.P., Hoffman, J.E. and Mackey, P.J. (Eds), The Reinhardt Schuhmann International symposium on Innovative Technology and Reactor Design in Extraction Metallurgy, AIME, 1986, pp. 273-292
- 76 Grabovskii, A.I., and Ivanova, L.S., Sorption separation of gold by activated carbon from polycomponent cyanide solutions, Tsvetn. Met., 11(1982)98-100
- 77 Ivanova, L.S., Grabchak, S.L., Alekseevo, R.K. and Grabovskii, A.I., The selectivity of sorption of complex ions of heavy metals on activated carbon, Ukr. Khim. Zh., 50(6)(1984)588-592

- 78 Murrey, C., Progress Report, p.12, communicated from Dr. John Nelson, October, 1985
- 79 Kazakov, V.P., Lapsmin, A.L. and Peshchevitskii, B.I., Redox potential of the gold(I) thiourea complex, Russ. J. Inorg. Chem., 9(5)(1964)708-709
- 80 Brown, H., Sodium aurothiosulfate. A simple method for its preparation, J. Am. Chem. Soc. 49(1927)958-959
- 81 Bjerrum, N. and Kirschner, P., Danske Selsk. Skr. 8(5)(1918)22
- 82 Barry, W.L., Bureau of Mines Practices in Fire Assaying, U.S. Dept. Int., 1982

APPENDIX A

Table 1. Atomic Absorption Data and Results for Experiment # 5

Time Minutes	Sample Absorbance	10 ug/ml Absorbance	Solution Conc. ug/ml	Percent Dissolution
5.	0.103	0.248	20.8	59.2
10.	0.115	0.248	23.2	65.8
15.	0.139	0.248	28.0	79.0
20.	0.142	0.248	28.6	80.2
25.	0.124	0.248	25.0	69.8
30.	0.146	0.248	29.4	81.7
40.	0.142	0.248	28.6	79.0
50.	0.149	0.248	30.9	82.5
60.	0.147	0.248	29.6	80.9
80.	0.150	0.248	30.2	82.1
100.	0.148	0.248	29.8	80.6
120.	0.150	0.248	30.2	81.3

Table 2. Atomic Absorption Data and Results for Experiment # 6

Time Minutes	Sample Absorbance	10 ug/ml Absorbance	Solution Conc. ug/ml	Percent Dissolution
5.	0.003	0.281	0.55	9.4
10.	0.004	0.281	0.70	12
15.	0.004	0.281	0.70	12
21.	0.006	0.281	1.0	17
25.	0.006	0.280	1.0	17
30.	0.005	0.280	0.9	15
40.	0.007	0.280	1.2	20
50.	0.010	0.280	1.8	30.
60.	0.012	0.280	2.0	33.
80.	0.014	0.280	2.5	41.
100.	0.015	0.280	2.7	44.
120.	0.020	0.280	3.5	46.
Final Solution	0.080	0.280	2.8	46.

Table 3. Atomic Absorption Data and Results for Experiment # 8

Time Minutes	Sample Absorbance	10 ug/ml Absorbance	Solution Conc. ug/ml	Percent Dissolution
2.5	0.080	0.271	15	61
5.	0.101	0.271	18.6	77.1
10.	0.112	0.271	20.5	84.6
15.	0.110	0.271	20.2	82.9
20.	0.111	0.270	20.5	83.7
25.	0.114	0.270	21.1	85.7
30.	0.117	0.270	21.6	87.3
40.	0.130	0.270	24.1	96.9
50.	0.116	0.270	21.6	86.4
60.	0.129	0.270	23.9	95.1
90.	0.130	0.270	24.2	95.8
120.	0.119	0.270	22.0	86.6
Final Solution	0.126	0.270	23.3	91.2

Table 4. Atomic Absorption Data and Results for Experiment # 9

Time Minutes	Sample Absorbance	10 ug/ml Absorbance	Solution Conc. ug/ml	Percent Dissolution
2.5	0.028	0.258	5.4	13.
5.0	0.043	0.258	8.4	19.
10.	0.058	0.258	11.	26.
15.	0.078	0.258	15.	35.
20.	0.088	0.256	17.	39.
25.	0.120	0.258	23.2	52.2
30.	0.116	0.256	22.6	50.6
40.	0.180	0.256	35.0	78.0
50.	0.172	0.253	34.0	75.4
60.	0.208	0.253	41.1	90.6
90.	0.223	0.253	44.0	96.5
120.	0.203	0.253	40.1	87.5
Final Solution	0.880	0.253	34.8	75.5

Table 5. Atomic Absorption Data and Results for Experiment # 10

Time Minutes	Sample Absorbance	10 ug/ml Absorbance	Solution Conc. ug/ml	Percent Dissolution
2.5	0.016	0.254	3.1	5.1
5.	0.026	0.254	5.1	8.3
10.5	0.060	0.254	12.	20.
15.	0.077	0.254	14.	23.
20.	0.100	0.253	19.9	32.0
25.	0.103	0.250	20.6	32.9
30.	0.118	0.250	23.5	37.4
40.	0.162	0.250	32.4	51.2
50.	0.166	0.250	33.2	52.2
60.	0.176	0.250	35.3	55.3
80.	0.217	0.250	43.4	67.6
100.	0.237	0.250	47.4	73.4
120.	0.292	0.250	58.3	89.8

APPENDIX B

Table 1. Fire-assay data

Experiment Number	Sample Mass Grams	Gold Mass Grams	Gold Fraction
5	0.50102	6.6×10^{-4}	1.3×10^{-3}
6	0.94608	5.8×10^{-4}	6.1×10^{-4}
7	0.59001	3.8×10^{-4}	6.4×10^{-4}
8	0.51839	$9. \times 10^{-5}$	$2. \times 10^{-4}$
9	0.92426	3.0×10^{-4}	3.2×10^{-4}
10	0.93750	1.21×10^{-3}	1.29×10^{-3}

Table 2. Initial Gold Mass Determinations.

Experiment #	Ligand	Supporting Electrolyte	Initial Au Mass (mg)
5	CN^-	ClO_4^-	7.02
6	$\text{S}_2\text{O}_3^{2-}$	ClO_4^-	1.17
8	CN^-	Cl^-	4.80
9	$\text{SC}(\text{NH}_2)_2$	ClO_4^-	8.66
10	SCN^-	ClO_4^-	12.2

APPENDIX C

Table 1. Anodic Dissolution of Gold at 1.2 V from Spectroscopic Carbon in Cyanide Solution (0.1M).

Time Minutes	Peak Height cm	Au Concentration ppm	Percent Dissolution
1.	0.29	1.1	2.5
2.	1.7	6.64	15.1
3.	2.90	11.5	26.2
4.	3.82	15.5	35.3
5.	4.60	18.9	43.0
6.	5.12	21.1	48.1
7.	5.63	23.1	52.7
8.	5.98	24.5	55.9
9.	6.40	26.2	59.8
10.	6.70	27.4	62.6
11.	6.83	27.9	63.8
12.	7.21	29.5	67.5
13.	7.48	30.6	70.0
14.	7.59	31.0	71.0
15.	2.90	32.3	74.0
20.	8.77	35.8	82.0
25.	9.62	39.3	90.0
30.	10.20	41.7	95.6
35.	10.55	43.1	98.8
43.	12.11	45.14	103.5
50.	12.21	45.55	104.6
60.	12.09	45.16	103.8
70.	12.18	45.43	104.5
80.	12.47	46.61	107.2
90.	12.38	46.24	106.5
100.	12.59	47.10	108.5
110.	12.61	47.18	108.8
120.	12.77	47.84	110.4

Table 2. Chemical Dissolution of Au from Spectroscopic Carbon in Cyanide Solution (0.1M) with the Solution Exposed to Air.

Time Minutes	Peak Height cm	Au Concentration ppm	Percent Dissolution
1.	0.47	1.6	3.6
2.	0.95	3.34	7.60
3.	1.43	5.04	11.5
4.	1.85	6.51	14.8
5.	2.28	8.03	18.3
6.	2.68	9.44	21.5
8.	3.41	12.0	27.4
9.	3.82	13.4	30.6
10.	4.20	14.7	33.5
11.	4.58	16.0	36.5
12.	4.97	17.4	39.7
13.	5.27	18.4	42.0
14.	5.68	19.8	45.3
15.	5.95	20.6	47.1
22.	8.20	29.0	66.3
24.	9.00	31.8	72.7
25.	9.31	32.9	75.2
28.	10.12	35.70	81.7
30.	10.55	37.18	85.1
35.	11.46	40.30	92.3
37.	11.59	40.78	93.4
40.	11.70	41.17	94.3
42.5	11.90	41.88	96.0
45.	12.05	42.41	97.3
50.	12.24	43.08	98.9
55.	12.25	43.12	99.1
60.	12.36	43.51	100.
70.	12.37	43.54	100.
80.	12.38	43.58	100.
90.	12.16	42.80	98.6
100.	12.25	43.12	99.4
110.	12.60	44.36	102.
120.	12.25	43.12	99.6

Table 3. Chemical Dissolution of Au from Spectroscopic Carbon in Cyanide Solution (0.1 M) with the Solution Sparged With Nitrogen

Time Minutes	Peak Height cm	Au Concentration ppm	Percent Dissolution
1.	0.37	1.4	3.2
2.	0.64	2.3	5.2
3.	0.83	3.0	6.8
4.	0.92	3.4	7.7
5.	1.01	3.70	8.43
7.	1.17	4.28	9.76
8.	1.22	4.46	10.2
10.	1.45	5.30	12.1
15.	1.69	6.16	14.1
20.	1.83	6.63	15.2
25.	2.00	7.22	16.5
31.	2.21	7.92	18.1
37.	2.45	8.74	20.0
40.	2.47	8.80	20.1
50.	2.80	9.95	22.8
61.	3.08	10.9	25.0
70.	3.36	12.0	27.5
80.	3.61	12.9	29.5
90.	3.87	13.7	31.4
100.	4.13	14.6	33.5
112.	4.40	15.6	35.8
120.	4.57	16.2	37.2
130.	4.86	17.3	39.7

Table 4. Chemical Dissolution of Au from Activated Carbon in Cyanide Solution (0.1M) Saturated with Air: 0.7300 g Carbon

Time Minutes	Peak Height cm	Au Concentration ppm	Percent Dissolution
1.	0.00	0.0	0.0
2.	0.08	0.4	0.9
3.	0.14	0.64	0.9
4.	0.38	0.85	1.9
5.	0.50	1.1	2.5
6.	0.58	1.3	3.0
7.	0.69	1.5	3.4
8.	0.71	1.6	3.6
9.	0.80	1.8	4.1
10.	0.88	2.0	4.5
11.	0.95	2.1	4.7
12.	1.02	2.28	5.15
13.	1.03	2.30	5.19
14.	1.11	2.48	5.58
15.	1.12	2.50	5.62
20.	1.33	2.97	6.68
22.5	1.41	3.15	7.08
25.	1.48	3.30	7.42
30.	1.59	3.55	7.95
35.	1.71	3.81	8.54
40.	1.80	4.00	8.96
50.	1.84	4.08	9.14
60.	1.90	4.20	9.41
70.	1.85	4.07	9.09
80.	1.89	4.15	9.27
90.	1.85	4.04	9.02
100.	1.86	4.05	9.05

Table 5. Anodic Dissolution of Au from Spectroscopic Carbon in 0.1 M HCl, Thiourea Solution at 0.5 V.

Time Minutes	Peak Height cm	Au Concentration ppm	Percent Dissolution
1.	0.10	0.51	1.2
2.	0.29	1.48	3.36
3.	0.66	3.38	7.68
4.	1.00	5.13	11.7
5.	1.29	6.62	15.1
6.	1.48	7.60	17.3
7.	1.64	8.43	19.2
8.	1.86	9.56	21.8
9.	1.98	10.2	23.2
10.	2.12	10.9	24.9
12.	2.37	12.2	27.9
14.	2.56	13.2	30.2
16.	2.62	13.5	30.9
18.	2.79	14.4	33.0
20.	3.00	15.5	35.6
22.	3.21	16.6	38.1
24.	3.49	18.1	41.6
26.	3.96	20.1	46.2
28.	4.10	21.4	49.2
30.	4.47	23.3	53.6
32.	4.76	24.8	57.1
34.	5.02	26.2	60.3
36.	5.29	27.7	63.8
38.	5.49	28.8	66.3
40.	5.70	29.9	68.9
42.	5.69	29.9	68.9
46.	6.07	32.0	73.8
50.	6.19	32.8	75.7
55.	6.46	34.3	79.1
63.	6.69	35.5	81.9
65.	6.60	35.0	80.9
70.	6.60	35.0	80.9
100.	6.91	36.5	84.4
110.	6.97	36.5	84.4
120.	7.03	37.2	86.1

Table 6. Anodic Dissolution of Au from Spectroscopic Carbon in Neutral Thiocyanate Solution (0.1 M) at 1.2 V.

Time Minutes	Peak Height cm	Au Concentration ppm	Percent Dissolution
1.	0.08	0.4	0.9
2.	0.09	0.4	0.9
5.	0.09	0.4	0.9
7.	0.15	0.76	1.7
8.	0.16	0.81	1.8
9.	0.21	1.1	2.5
10.	0.35	1.8	4.1
12.	0.44	2.2	5.0
14.	0.57	2.9	6.6
16.	0.72	3.7	8.4
20.	1.01	5.22	11.9
22.	1.14	5.90	13.5
24.	1.28	6.65	15.2
26.	1.40	7.29	16.6
28.	1.38	7.20	16.4
30.	1.56	8.16	18.6
35.	1.90	9.99	22.8
40.	2.20	11.6	26.5
45.	2.62	13.4	30.6
50.	2.83	15.1	34.5
55.5	3.06	16.4	37.5
60.	3.22	17.3	39.6
70.	3.69	19.9	45.5
80.	4.09	22.0	50.3
90.	4.50	24.2	55.4
100.	4.79	25.6	58.6
110.	5.12	27.3	62.5
120.	5.49	29.2	66.9

Table 7. Anodic Dissolution of Au from Activated Carbon in Thiourea Solution (0.1 M): 0.7250 g Activated Carbon.

Time Minutes	Peak Height cm	Au Concentration ppm	Percent Dissolution
5.	0.06	0.3	0.7
6.	0.08	0.4	0.9
7.	0.09	0.4	0.9
8.	0.14	0.66	1.5
9.	0.15	0.71	1.6
10.	0.15	0.71	1.6
11.	0.15	0.71	1.6
13.	0.21	0.99	2.2
15.	0.21	0.99	2.3
17.	0.29	0.99	2.3
30.	0.29	1.4	3.2
22.	0.31	1.4	3.2
25.	0.36	1.7	3.9
35.	0.47	2.2	5.0
38.	0.57	2.6	5.9
52.	0.61	2.8	6.4
55.	0.69	3.1	7.1
60.	0.70	3.2	7.3
70.	0.78	3.5	8.0
75.	0.70	3.2	7.3
85.	0.80	3.6	8.3
90.	0.78	3.5	8.0
92.	0.78	3.5	8.0
95.	0.77	3.5	8.0
100.5	0.78	3.5	8.1
103.	0.78	3.5	8.1

Table 8. Anodic Dissolution of Au from Activated Carbon in Cyanide Solution (0.1 M) at -0.6 V: 0.7257 g Activated Carbon

Time Minutes	Peak Height cm	Au Concentration ppm	Percent Dissolution
1.	0.0	0.0	0.0
2.	0.37	0.29	0.26
3.	0.72	0.56	0.51
4.	0.71	0.56	0.51
5.	1.43	1.12	1.02
6.	1.41	1.11	1.02
7.	1.78	1.40	1.28
8.	2.16	1.70	1.56
10.	2.85	2.24	2.05
12.	3.57	2.80	2.57
14.	4.59	3.60	3.30
16.	5.67	4.45	4.08
18.	6.77	5.31	4.87
20.	7.81	6.13	5.63
22.	9.25	7.26	6.67
24.	11.01	8.74	7.94
26.	12.06	9.47	8.71
32.	3.70*	14.7	13.5
34.	4.01	15.9	14.6
36.	4.40	17.6	16.2
38.	4.76	19.0	17.5
40.	5.15	20.6	19.0
42.5	5.57	22.4	20.7
45.	5.80	23.3	21.5
52.	6.64	27.5	25.3
55.	6.98	29.4	27.1
60.	7.27	30.9	28.5
67.	7.79	33.3	30.8
70.	7.82	33.4	30.9
75.5	7.88	33.7	31.3
80.	8.00	34.3	31.9
85.	8.18	34.2	32.8
90.	8.32	35.9	33.4
100.	8.61	37.4	34.9
110.	8.56	37.1	34.7
120.	8.65	37.6	35.2

* switched from 1 mV to 5 mV recorder Span

Table 9. Anodic Dissolution of Au from Activated Carbon in Thiosulfate Solution (0.1 M) at Various Potentials: 0.7257 g Activated Carbon

Potential Volts	Time Minutes	Peak Height cm	Au Concentration ppm	Percent Dissolution
0.11	1.	0.0	0.0	0.0
"	2.	0.09	0.4	0.9
"	3.	0.09	0.4	0.9
0.30	5.	0.10	0.49	1.1
"	6.	0.12	0.49	1.3
"	7.	0.14	0.69	1.6
"	8.	0.11	0.54	1.2
"	9.	0.16	0.78	1.8
0.50	10.	0.10	0.49	1.1
"	11.	0.10	0.49	1.1
"	12.	0.14	0.69	1.6
"	14.	0.17	0.83	1.9
0.70	15.	0.13	0.63	1.4
"	16.	0.18	0.88	2.0
"	17.	0.20	0.97	2.2
"	18.	0.21	1.0	2.3
"	19.	0.20	0.92	2.1
0.80	20.	0.22	0.97	2.2
"	22.	0.27	1.3	2.9
"	24.	0.20	0.92	2.2
0.90	26.	0.29	1.4	3.2
"	28.	0.28	1.4	3.2
"	30.	0.30	1.4	3.2
"	35.	0.30	1.4	3.2
1.00	40.	0.36	1.7	3.9
"	45.	0.39	1.9	4.4
1.20	50.	0.40	1.9	4.4
"	52.	0.41	2.0	4.6
"	54.	0.41	2.0	4.6
1.50	56.	0.49	2.4	5.5
"	58.	0.49	2.4	5.5
1.70	60.	0.49	2.4	5.6
"	62.	0.41	2.5	5.8

Table 9. (Cont.) Anodic Dissolution of Au from Activated Carbon in Thiosulfate Solution (0.1 M) at Various Potentials: 0.7257 g Activated Carbon

Potential Volts	Time Minutes	Peak Height cm	Au Concentration ppm	Percent Dissolution
1.20*	80.	0.60	2.9	6.7
"	85.	0.65	3.1	7.6
"	86.	0.66	3.2	7.8
"	88.	0.79	3.8	9.3
"	90.	0.96	4.3	10.5
"	92.	1.00	4.84	11.7
"	95.	1.04	5.08	12.4
"	100.	1.30	6.29	15.4
"	105.	1.53	7.41	18.1
"	110.	1.77	8.57	20.9
"	115.	1.99	9.64	23.5
"	120.	2.12	10.3	25.1
"	125.	2.34	11.3	27.5
"	130.	2.52	12.2	29.7
"	135.	2.67	12.9	31.4
"	140.	2.78	13.5	32.9
"	145.	2.87	13.9	33.9
"	155.	3.15	15.3	37.3

* added thiosulfate to give 0.5 M concentration

APPENDIX D

Table 1. Recirculating 0.1 M NaCN, NaOH electroelution of 27.7 mg/g loaded carbon at -0.6 V: 0.7429 g loaded carbon.

Time Minutes	Peak Height cm	Au Concentration ppm	Percent Elution
0.	0.05	0.2	0.2
1.	0.09	0.3	0.4
2.	0.12	0.48	0.60
3.	0.12	0.48	0.60
4.	0.16	0.64	0.80
5.	0.17	0.68	0.84
6.	0.55	2.2	2.74
7.	1.08	4.31	5.39
8.	1.57	6.27	7.85
9.	1.99	7.65	9.96
10.	2.35	9.41	11.8
12.	3.13	12.7	15.9
14.	3.69	15.2	19.1
16.	4.21	17.4	21.8
18.	4.63	19.3	24.3
20.	5.07	21.2	26.7
23.	5.61	23.5	29.6
25.5	5.97	25.1	31.6
27.	6.15	25.9	32.6
30.	6.52	27.6	34.8
38.5	7.38	31.4	39.6
40.	7.38	31.4	39.6
45.	7.79	33.2	41.9
50.5	8.06	34.4	43.4
55.	8.21	35.1	44.3
61.5	8.48	36.3	45.9
70.	8.59	36.8	46.5
80.	8.87	38.1	48.2
100.	9.17	39.1	49.5
121.5	9.86	41.7	52.8
130.	9.46	40.0	50.7
2.*	0.07	0.3	51.2
3.	0.09	0.4	51.3
4.	0.09	0.4	51.3
5.	0.13	0.52	51.5
6.	0.15	0.60	51.6
7.	0.22	0.88	51.9
8.	0.21	9.84	51.9
9.	0.29	1.2	52.3
10.	0.30	1.2	52.3
15.	0.43	1.7	53.0
20.	0.58	2.3	53.7
30.	0.99	3.9	55.7
60.	1.98	7.70	60.5

* switched to second solution of initial composition

Table 2. Recirculating 0.1 M NaCN, NaOH Electroelution of 13.3 mg/g Loaded Carbon at -0.6 V: 0.7542 g Loaded Carbon.

Time Minutes	Peak Height cm	Au Concentration ppm	Percent Elution
1.	0.02	0.08	0.2
2.	0.02	0.08	0.2
3.	0.02	0.08	0.2
4.	0.02	0.08	0.2
5.	0.02	0.08	0.2
6.	0.05	0.2	0.5
7.	0.10	0.40	1.0
8.	0.20	0.80	2.0
9.	0.15	0.59	1.5
10.	0.15	0.59	1.5
12.	0.30	1.2	3.0
14.	0.37	1.4	3.6
16.	0.50	2.0	5.1
18.	0.55	2.2	5.6
20.	0.68	2.7	6.9
25.	1.00	3.91	9.95
30.	1.28	4.99	12.7
35.	1.70	6.62	16.8
40.	1.98	7.72	19.6
45.	2.30	8.98	22.8
50.	2.58	10.1	25.7
55.	2.85	11.2	28.5
60.	3.08	12.2	31.1
70.	3.48	13.9	35.4
80.	3.85	15.4	39.3
90.	4.05	16.3	41.6
100.	4.20	16.8	42.9
110.	4.39	17.5	44.7
120.	4.45	17.6	45.0
130.*	4.49	17.7	45.3
135.	4.49	17.7	45.3
140.	4.55	18.0	46.1
150.	4.69	18.6	47.7
160.	4.88	19.3	49.5
170.	4.90	19.5	50.0
180.	5.01	20.0	51.3
190.	5.00	20.0	51.4

* switched to -0.7 V

Table 3. Nonrecirculating 0.1 M NaCN, NaOH, -0.6 V Electroelution of 25.6 mg/g Loaded Carbon: 0.6798 g Loaded Carbon.

Time Minutes	Peak Height cm	Au Concentration ppm	Percent Elution	Gold Loading mg/g
1.	2.25	8.45	0.07	25.3
2.	2.10	7.88	0.20	25.3
3.	2.06	7.72	0.88	25.3
4.	2.08	7.76	0.46	25.2
5.	2.15	8.03	0.59	25.2
6.	2.91	10.9	0.74	25.2
7.	3.84	14.4	0.95	25.1
8.	4.61	17.3	1.21	25.0
9.	5.42	20.4	1.52	25.0
10.	5.99	22.5	1.87	24.9
12.	7.09	26.7	2.69	24.7
14.	7.39	27.8	3.60	24.4
16.	7.44	28.0	4.52	24.2
18.	7.31	27.5	5.42	24.0
20.	7.30	27.5	6.33	23.7
24.	7.30	27.5	8.15	23.3
28.	7.32	27.6	7.98	22.8
32.	7.48	28.2	11.8	22.3
36.	7.47	28.2	13.7	21.9
40.	7.49	28.3	15.5	21.4
45.	7.59	28.7	17.9	20.8
50.	7.81	29.6	20.3	20.2
55.	7.73	29.3	22.7	19.6
60.	7.98	29.9	26.1	19.0
70.	7.97	30.5	30.1	17.7
80.	8.20	31.4	35.2	16.4
90.	7.41	28.3	40.1	15.2
100.	6.80	25.5	44.5	14.1
110.	5.98	22.4	48.5	13.1
122.	4.61	16.7	54.8	11.4
140.	4.13	15.0	57.4	10.8
160.	3.35	12.0	61.9	9.66
180.	2.29	8.30	65.2	8.82

Table 4. Dionized Water Electroelution of 8.83 mg/g Loaded Carbon at Various Potentials.

Time Minutes	Peak Height cm	Au Concentration ppm	Percent Elution
1.	3.96	16.0	0.304
2.	12.59	53.4	1.62
3.	13.49	57.2	3.73
4.	13.29	56.3	5.89
5.	12.54	56.3	7.98
6.	11.68	53.2	9.93
7.	10.93	46.2	11.8
8.	10.29	43.3	13.4
9.	9.51	39.9	15.0
10.	8.99	37.6	16.5
13.	7.51	31.0	19.1
15.	6.68	27.4	21.4
17.	6.67	27.4	23.4
20.	6.18	25.3	26.3
25.	5.84	23.8	30.9
30.	5.90	24.0	35.4
35.	5.57	22.6	39.9
40.	5.61	22.7	43.4

APPENDIX E

Table 1. Flow-Cell Recycling Adsorption of Aurocyanide on Activated Carbon: 38.0 ppm Initial Concentration.

Time Minutes	Peak Height cm	Au Concentration ppm
1.	6.91	38.2
2.	6.78	37.4
3.	6.72	37.0
4.	6.70	36.8
5.	6.55	35.9
6.	6.49	35.5
7.	6.28	34.2
8.	6.29	34.3
9.	6.20	33.7
10.	6.17	33.5
12.	5.98	32.3
14.	5.78	31.1
16.	5.66	30.4
18.	5.49	29.4
20.	5.38	28.7
25.	4.99	26.4
30.	4.80	25.3
42.	4.20	21.8
45.	3.98	20.5
50.	3.80	19.5
56.	3.48	17.7
60.	3.31	16.8
70.	2.94	14.7
80.	2.69	13.3
90.	2.37	11.7
100.	2.09	10.2
112.	3.56 ¹	8.64
120.	3.18	7.73
130.	2.88	7.00
140.	12.66 ²	6.34

¹ recorder span changed from 10 mV to 5 mV

² recorder span changed from 5 mV to 1 mV

Table 2. Flow-Cell Recycling Adsorption of AuCl_4^- on Activated Carbon
39.0 ppm Initial Concentration.

Time Minutes	Peak Height cm	Au Concentration ppm
0.	11.07	39.5
2.	10.41	38.00
4.	10.22	36.28
5.	10.20	36.2
7.	9.93	36.2
9.	9.75	34.5
10.	9.57	33.9
15.	8.98	31.7
24.	8.10	28.5
26.	8.09	28.4
35.	7.10	24.9
40.	6.79	23.8
50.	6.01	20.9
60.	5.65	19.6
70.	4.80	17.4
80.	4.25	15.3
90.	3.77	13.5
100.	3.35	11.6
110.	2.98	10.3
120.	2.70	9.27
130.	2.31	7.91
140.	2.11	7.23
150.	1.90	6.51

Table 3. Flow-Cell Recycling Adsorption of Aurothiourea on Activated Carbon: 38.0 ppm Initial Concentration.

Time Minutes	Peak Height cm	Au Concentration ppm
1.	11.06	37.64
2.	10.95	37.74
3.	10.71	37.37
4.	10.48	35.98
5.	10.32	35.53
6.	10.23	35.33
7.	10.10	34.98
8.	9.79	34.0
9.	9.62	33.5
10.	9.59	33.5
12.	9.28	32.6
14.	8.95	31.7
15.	8.78	31.2
20.	8.30	29.6
25.	7.64	27.1
30.	7.44	26.3
36.	6.90	24.3
42.	6.40	22.5
50.	5.68	20.0
60	5.00	17.5
76.	4.12	14.4
80.	3.97	13.9
90.	3.49	12.2
100.	3.10	10.8
110.	2.72	9.53
120.	2.42	8.47

Table 4. Flow-Cell Recycling Adsorption of Aurothiosulfate on Activated Carbon: 47.0 ppm Initial Concentration.

Time Minutes	Peak Height cm	Au Concentration ppm
1.	9.18	47.0
2.	9.13	46.7
3.	9.13	46.7
4.	9.05	46.3
5.	8.97	45.7
6.	8.95	45.7
7.	9.96	45.7
8.	9.98	45.8
9.	8.96	45.7
10.	8.91	45.4
12.	8.97	45.6
14.	8.80	44.7
17.5	8.81	44.7
20	8.95	45.3
25.	8.99	45.4
30.	9.02	45.4
40.	9.05	45.3
50.	8.97	44.8
60.	9.20	45.7
70.	9.25	45.8
80.	9.07	45.0
80.	9.12	45.2
100.	9.04	44.8
110.	9.16	45.4
120.	8.93	44.2
130.	9.07	44.9

Table 5. Flow-Cell Adsorption of Aurothiocyanate on Activated Carbon: 38.0 ppm Initial concentration.

Time Minutes	Peak Height cm	Au Concentration ppm
0.0	7.97	38.0
2.0	7.90	37.7
3.0	7.67	36.6
4.	7.78	37.1
5.	7.60	36.2
6.	7.42	35.4
7.	7.39	35.2
8.	7.28	34.7
9.	7.17	34.2
10.	7.02	33.4
12.	6.89	32.8
14.	6.75	32.1
15.	6.69	31.8
20.	6.29	29.9
25.	5.98	28.4
30.	5.86	26.4
35.	5.28	25.0
40.	5.04	23.9
45.	4.70	22.3
50.	4.40	20.9
55.	4.23	20.1
60.	3.92	18.6
70.	3.41	16.1
80.	3.07	14.5
90.	2.78	13.0
100.	2.50	11.7
110.	2.21	10.3
121.	1.89	8.75

Table 6. Flow-Cell Recycling Adsorption of Aurocyanide on Activated Carbon in the presence of 0.1 M Thiosulfate.

Time Minutes	Peak Height cm	Au Concentration ppm
0.0	5.45	38.7
1.	5.62	40.0
2.	5.49	39.1
3.	5.24	37.3
5.	5.10	36.3
6.	5.18	36.8
7.	4.99	35.5
8.	5.05	36.9
9.	4.97	35.3
10.	5.00	35.5
12.	4.73	33.6
15.	4.57	32.4
20.	4.36	30.9
25.	3.94	28.1
30.	3.86	27.3
35.	3.67	26.0
40.	3.47	24.6
45.	3.22	22.8
50.	3.12	22.1
55.	2.89	20.5
60.	2.74	19.4
70.	2.51	17.8
80.	2.21	15.7
90.	2.03	14.5
100.	1.85	13.1
110.	1.63	11.4
120.	1.48	10.3

Table 7. Flow-Cell Recycling Adsorption of Aurocyanide on Activated Carbon Pretreated Electrolytically at -0.6 V.

Time Minutes	Peak Height cm	Au Concentration ppm
0.0	8.52	35.9
1.0	8.50	35.8
2.	8.35	35.2
4.	8.09	34.0
5.	8.00	33.7
6.	7.89	33.2
7.	7.99	33.6
8.	7.69	32.3
9.	7.69	32.3
10.	7.50	31.5
12.	7.38	30.9
14.	7.20	30.1
16.	6.97	29.1
18.	6.81	29.4
20.	6.66	27.8
25.	6.20	25.8
30.	5.80	24.0
37.	5.31	21.9
40.	5.12	21.1
50.	4.47	18.4
55.	4.12	16.9
60.	3.93	16.0
72.	3.29	13.3
80.	2.99	12.0
90.	2.64	10.6
100.5	2.29	9.12
110	2.06	8.21
120.	1.82	7.25

APPENDIX F

Table 1. Concentration Data for the Recirculating Flow-Cell Adsorption of Aurocyanide on the Freeport Gold Ore: 37.5 ppm Initial Concentration.

Time Minutes	Peak Height cm	Au Concentration ppm
0.0	8.90	37.6
1.	8.87	37.6
2.	8.76	37.1
3.	8.80	37.2
4.	8.78	37.1
5.	8.79	37.1
6.	8.86	37.4
7.	8.80	37.1
8.	8.80	37.1
9.	8.81	37.1
10.	8.70	36.6
12.	8.90	37.5
14.	8.94	37.6
16.	8.76	36.8
18.	8.83	37.0
20.	8.96	37.5
27.	9.06	37.9
30.	8.79	36.7
40.	8.89	37.0
50.	8.93	37.0
60.	8.89	36.8
70.	8.87	36.7
120.	8.66	36.3
13 hrs.	8.61	37.0

Table 2. Concentration Data for the Recirculating Flow-Cell Adsorption of Aurocyanide on the Freeport Gold ore: 10.0 ppm Initial Concentration.

Time Minutes	Peak Height cm	Au Concentration ppm
0.	2.41	9.96
2.	2.42	10.0
3.	2.37	9.79
4.	2.41	9.96
5.	2.37	9.79
7.	2.40	9.92
12.	2.40	9.92
16	2.41	9.96
20	2.30	9.50
17.5 hrs.	2.27	9.30

Table 3. Concentration Data for the Nonrecirculating Flow-Cell Adsorption of Aurocyanide on the Freeport Gold Ore in 0.05 M NaCl Solution: 10.0 ppm Initial Au Concentration.

Time Minutes	Peak Height cm	Au Concentration ppm
1.	12.74	9.73
2.	12.78	9.77
3.	12.77	9.77
4.	12.78	9.78
5.	12.78	9.78
6.	12.78	9.79
7.	12.77	9.79
8.	12.78	9.80
9.	12.75	9.79
10.	12.75	9.79
12.	12.65	9.73
14.	12.78	9.84
21.	12.79	9.87
25.	12.78	9.87

Table 4. Concentration Data for the Nonrecirculating flow-Cell Adsorption of Aurocyanide on the Freeport Gold Ore in 0.025 M CaCl_2 Solution.

Time Minutes	Peak Height cm	Au Concentration ppm
1.	11.69	8.73
2.	12.29	9.19
3.5	12.55	9.41
4.	12.76	9.57
5.	12.77	9.59
6.	12.78	9.61
7.	12.69	9.56
9.	12.78	9.66
10.	12.78	9.66
15.	12.78	9.71
18.	13.07	9.94
20.	12.78	9.72
25.	12.77	9.72
30.	12.90	9.83

APPENDIX G

Table 1. Concentration Data for the Small-Column Adsorption of Aurocyanide on Activated Carbon: 38.0 ppm Au, 0.1000 g Activated Carbon.

Time Minutes	Peak Height cm	Au Concentration ppm
1.0	0.41	1.5
2.0	0.62	2.2
3.0	0.85	3.1
4.0	1.11	3.99
5.0	1.52	5.11
6.0	1.70	6.12
7.0	1.98	7.12
8.0	2.29	8.24
9.0	2.57	9.24
10.	2.86	10.3
12.	3.47	12.9
14.	4.04	15.2
16.	4.66	17.8
18.	5.11	19.7
29.	5.61	21.8
22.	5.96	23.2
24.	6.39	25.0
26.	6.80	26.8
28.	6.91	27.2
30.	7.28	28.7
32.	7.31	28.9
34.	7.61	30.1
36.	7.81	31.0
38.	7.95	31.5
40.	7.99	31.7
45.	8.39	33.4
50.	8.42	33.5
60.	8.71	34.7
65.5	8.96	35.8
70.	8.96	35.8

Table 2. Concentration Data for the Small-Column Adsorption of Aurocyanide on Activated Carbon: 38.0 ppm Au, 0.0500 g Activated Carbon.

Time Minutes	Peak Height cm	Au Concentration ppm
1.0	2.00	8.63
2.0	2.69	11.6
3.0	3.18	13.7
4.0	3.62	15.6
5.0	4.11	17.7
6.0	4.41	19.0
7.0	4.85	20.9
8.0	5.06	21.8
9.0	5.41	23.2
10.	5.69	24.4
12.	6.28	27.0
14.	6.52	28.0
16.	6.98	29.9
18.	7.10	30.4
20.	7.39	31.6
22.	7.53	32.2
24.	7.67	32.8
26.	7.89	33.7
28.	7.96	34.0
30.	8.09	34.5
32.	8.10	34.5
34.	8.22	35.2
36.	8.23	35.0
38.	8.24	35.1
40.	8.41	35.7
1.0*	8.65	72.6
1.5	6.20	52.0
2.0	4.71	39.5
3.0	3.05	25.6
4.0	2.13	17.9
5.0	1.69	14.2
6.0	1.27	10.6
7.0	1.00	8.39
8.0	0.80	6.71

* started deionized water elution

Table 3. Concentration Data for the Small-Column Adsorption of Aurocyanide on Activated Carbon: 38.0 ppm Au, 0.0100 g Activated Carbon.

Time Minutes	Peak Height cm	Au Concentration ppm
1.0	7.99	32.4
2.0	8.10	32.8
3.0	8.25	33.4
4.0	8.34	33.8
5.0	8.39	34.0
6.0	8.50	34.4
7.0	8.68	34.2
8.0	8.56	34.7
9.0	8.67	35.1
10.	8.80	34.7
12.	8.90	36.1
14.	8.89	36.0
16.	9.00	36.5
18.	9.08	36.8
20.	8.86	36.9
22.	9.08	36.8
24.	9.25	37.5
26.	9.10	36.8
28.	9.27	37.5
30.0	9.19	37.2
35.2	9.16	37.1
40.	9.28	37.6
0.5*	4.26	17.2
1.0	2.49	10.1
1.5	2.20	8.90
2.0	1.21	4.90
3.0	0.79	4.90
5.0	0.42	1.70

* started deionized water elution

Table 4. Concentration Data for the Small-Column Adsorption of Aurothiourea on Activated Carbon: 38.0 ppm Au, 0.1000 g Activated Carbon.

Time Minutes	Peak Height cm	Au Concentration ppm
1.0	0.42	1.7
2.0	0.51	2.0
3.0	0.59	2.4
4.0	0.74	3.0
5.0	0.87	3.5
6.0	0.97	3.9
7.0	1.08	4.32
8.0	1.20	4.79
9.0	1.11	4.43
10.	1.25	4.98
12.	1.50	5.96
14.	1.68	6.67
16.	1.85	7.32
18.	2.00	7.90
20.	2.19	8.63
22.	2.43	9.56
24.4	2.64	10.4
26.	2.70	10.6
28.	2.96	11.6
30.	3.09	12.0
32.	3.28	12.8
34.	3.48	13.5
36.	3.56	13.8
38.	3.74	14.4
40.	3.86	14.9
42.	3.92	15.1
44.	4.13	15.8
46.	4.26	16.3
48.	4.38	16.7
50.	4.52	17.2
52.	4.65	17.7
54.	4.79	18.2
56.	4.85	18.4
58.	5.01	18.9
60.	5.15	19.4
65.	5.40	20.2
70.	5.61	21.1
75.2	5.82	21.9
80.	6.11	23.0
85.	6.39	24.2
90.	6.50	24.6

Table 5. Concentration Data for the Small-Column Adsorption of Aurothiourea on Activated Carbon: 38.0 ppm Au, 0.0500 g Activated Carbon.

Time Minutes	Peak Height cm	Au Concentration ppm
1.0	2.99	13.1
2.0	3.31	14.5
3.0	3.59	15.8
4.0	3.28	14.4
5.0	3.28	14.4
6.0	3.34	14.7
7.0	3.43	15.1
8.0	3.49	15.4
9.0	3.55	15.6
10.	3.61	15.9
12.	3.99	17.6
14.	4.11	18.2
16.	4.19	18.6
18.	4.39	19.5
20.	4.50	20.0
22.	4.77	21.2
24.	4.82	21.4
26.	4.99	22.2
28.	4.99	22.2
30.	5.06	22.6
36.	5.14	23.0
38.	5.28	23.6
40.	5.42	24.2
42.	5.50	24.6
44.	5.69	25.4
46.	5.73	25.6
48.	5.77	25.8
50.	5.85	26.1
52.	5.86	26.2
54.	5.86	26.2
56.	5.99	26.8
58.	6.05	27.0
60.	6.10	27.3
0.5*	8.51	38.0
1.0	7.65	34.2
2.0	6.25	27.9
2.5	5.62	25.1
3.0	5.12	22.9
4.0	4.25	19.0
5.0	3.70	16.5
6.0	3.27	14.6
7.0	2.86	12.8
8.0	2.60	11.6

* started deionized water elution

Table 6. Concentration Data for the Small-Column Adsorption of Aurothiurea on Activated Carbon: 38.0 ppm Au, 0.0100 g Activated Carbon.

Time Minutes	Peak Height cm	Au Concentration ppm
1.0	7.13	29.8
2.0	7.22	30.2
3.0	7.40	31.0
4.0	7.60	31.8
5.0	7.61	31.9
6.0	7.77	32.6
7.0	7.81	32.8
8.0	7.89	33.1
9.0	7.85	33.0
10.	8.05	33.8
12.	8.12	34.1
14.	8.27	34.8
16.	8.30	34.9
18.	8.34	35.1
20.	8.35	35.2
22.	8.37	35.3
24.	8.38	35.3
26.	8.39	35.4
28.	8.50	35.9
30.	8.49	35.8
32.	8.59	36.3
34.	8.57	36.2
36.	8.59	36.3
40.	8.68	36.7
0.5*	2.0	8.60
1.0	1.65	7.09
1.5	1.29	5.54
2.0	1.18	5.07
3.0	0.90	3.9
4.0	2.85	12.2
5.0	3.00	12.9
6.0	3.17	13.6
7.0	3.41	14.6
8.0	3.57	15.3
9.0	3.40	14.5
10.	3.70	15.8
11.	3.91	16.7

* started deionized water elution

Table 7. Concentration Data for the Small-Column Adsorption of Aurothiocyanate on Activated Carbon: 38.0 ppm Au, 0.1000 g Activated Carbon.

Time Minutes	Peak Height cm	Au Concentration ppm
1.0	0.41	1.8
2.0	0.43	1.9
3.0	0.41	1.8
4.0	0.40	1.8
5.0	0.47	2.1
6.0	0.41	1.8
7.0	0.49	2.2
8.0	0.58	2.6
9.0	0.55	2.4
10.	0.58	2.6
12.	0.69	3.1
14.	0.71	3.2
16.	0.73	3.3
18.	0.83	3.7
20.	0.79	3.5
22.	0.87	3.9
24.	0.87	3.9
26.	0.80	3.6
28.	0.86	3.8
30.	0.87	3.9
32.	0.80	3.6
34.	0.80	3.6
36.	0.79	3.5
38.	0.78	3.5
40.	0.71	3.2
45.2	0.74	3.3
50.	0.75	3.3
55.	0.85	3.8
60.	0.86	3.8
70.	0.92	4.0
80.	0.99	4.3
85.	0.92	4.9

Table 8. Concentration Data for the Small-column Adsorption of Aurothiocyanate on Activated Carbon: 38.0 ppm Au, 0.0500 g Activated Carbon.

Time Minutes	Peak Height cm	Au Concentration ppm
1.0	1.15	5.71
2.0	1.16	5.75
3.0	1.24	6.14
4.0	1.30	6.43
5.0	1.47	7.26
7.0	1.58	7.79
8.0	1.59	7.83
9.0	1.60	7.87
10.	1.62	7.96
12.2	1.70	8.33
14.	1.67	8.17
16.	1.84	8.98
18.	1.92	9.35
20.	1.98	9.62
22.	2.02	9.80
24.	1.85	8.95
26.	1.85	8.95
26.	1.85	8.93
28.	1.87	8.48
30.	1.80	8.66
35.	1.70	8.18
37.5	1.84	8.88
40.	1.71	8.27
42.5	1.76	8.54
45.	1.80	8.76
47.5	1.98	9.66
50.	2.01	9.83
52.5	2.11	10.4
57.5	2.39	11.8
60.	2.41	11.9

Table 9. Concentration Data for the Small-Column Adsorption of Aurothiocyanate on Activated Carbon: 38.0 ppm Au, 0.0100 g Activated Carbon.

Time Minutes	Peak Height cm	Au Concentration ppm
1.0	4.59	26.4
2.0	4.75	27.4
3.0	4.87	28.1
4.0	4.99	28.8
5.0	4.99	28.8
6.0	5.04	29.1
7.0	5.11	29.5
8.0	4.17	29.8
9.0	5.09	29.4
10.	5.17	29.8
12.	5.19	30.0
14.	5.12	29.6
16.	5.10	29.5
18.	5.16	29.8
20.	5.10	29.5
25.	5.08	29.4
30.	5.04	29.2
35.	4.90	28.4
40.	4.84	28.1
45.	4.99	29.0
50.	5.20	30.1

Table 10. Concentration Data for the Small-Column Adsorption of Aurothiosulfate on Activated Carbon: 38.0 ppm Au, 0.1000 g Activated Carbon.

Time Minutes	Peak Height cm	Au Concentration ppm
1.0	7.45	33.6
2.0	7.85	35.4
3.0	8.07	36.4
4.0	8.29	37.4
5.0	8.11	36.5
6.0	8.21	37.0
7.0	8.41	37.8
8.0	8.41	37.8
9.0	8.35	37.5
10.	8.21	36.9
11.	8.40	37.7
12.	8.43	37.8
14.	8.44	37.8
15.	8.25	36.9
23.	8.41	37.6
30.0	8.47	37.9